ELSEVIER

Coordination Chemistry Reviews
209 (2000) 333–386

COORDINATION CHEMISTRY REVIEWS

www.elsevier.com/locate/ccr

Annual survey of organometallic metal cluster chemistry for the year 1998

Michael G. Richmond *

Department of Chemistry, University of North Texas, Denton, TX 76203, USA

Received 27 August 1999; accepted 30 August 1999

Contents

Abstract

The synthetic, mechanistic and structural chemistry of organometallic metal cluster compounds is reviewed for the year 1998.

Keywords: Organometallic metal cluster compounds

* Tel.: +1-940-565-3548; fax: +1-940-565-4318.
E-mail address: cobalt@unt.edu (M.G. Richmond).

0010-8545/00/$ - see front matter
PII: S0010-8545(99)00228-3

1. Dissertations

The dinuclear complexes $(\eta\text{-}RC_5Me_4)_2Ta_2(\mu\text{-}Cl)_4$ (where R = Me, Et) give a number of species upon reduction with sodium amalgam. The trinuclear clusters $[(\eta\text{-}RC_5Me_4)_3Ta_3(\mu\text{-}Cl)_6]^+$ have been isolated and structurally characterized by X-ray crystallography [1]. Thermolysis of *cyclo*-$(MeAsS)_{3,4}$ with $Cp^*_2Cr_2(CO)_4$ and $CpCr(CO)_2NO$ gives the clusters $[Cp^*_3Cr_3S_4]_2(\mu_6\text{-}As)$ and $[(CpCr)_2\text{-}\mu_2,\eta^2\text{-}(SAsMeS)(\mu_3,\eta^3\text{-}S)(NO)_2]$, respectively. The use of *cyclo*-$(MeAsS)_{3,4}$ as a precursor to a wide variety of mixed organoarsenic–sulfur complexes is discussed [2]. The reactivity of the butterfly cluster $Cp_2Mo_2Co_2S_3(CO)_4$ in thiol desulfurization reactions has been investigated. Cyclopropylmethyl thiol and 5-hexenethiol were both stoichiometrically desulfurized to give $Cp_2Mo_2Co_2S_4(CO)_2$ and rearranged organic products via a 'radical clock' activation pathway [3]. A set of supported bimetallic catalysts has been prepared from $[Re_7IrC(CO)_{23}]^{2-}$ at 773 K under H_2. Reduction of $PtRu_5C(CO)_{16}$ has led to nanoparticles whose identity was established by common surface science techniques [4].

The kinetics of CO-substitution in $Ru_3(CO)_{11}L$ and $Ru_5C(CO)_{14}L$ (where L = various phosphine and phosphite ligands) have been studied. The trinuclear clusters react by both associative and dissociative pathways, whereas only an associative pathway was observed with the pentaruthenium clusters. The rate data have been successfully analyzed by quantitatively separating the steric and electronic contributions of the rate expression [5]. The protonation of the clusters $Os_3(CO)_9(\mu\text{-}H)_2(\mu_3,\eta^2\text{-}C_8H_7N)$ and $Os_3(CO)_9(\mu_3\text{-}H)_2(\mu_3,\eta^2\text{-}C_9H_9N)$, which exist in solution as tautomeric complexes, using CF_3SO_3H or TFA has been explored. The initial site of protonation and the reactivity of the cationic clusters were verified by spectroscopic methods. The reactivity of the latter cluster with H_2 (high pressure) was also studied. The decarbonylation chemistry of $Os_3(CO)_{10}(\mu,\eta^2\text{-}C_9H_7RR'N)(\mu\text{-}H)$ was found to give the electron deficient cluster $Os_3(CO)_9(\mu_3,\eta^2\text{-}C_9H_7RR'N)(\mu\text{-}H)$. Also reported in this dissertation are the absolute rate constants for hydrogen abstraction from $Os_3(\mu\text{-}H)_2(CO)_9(PPh_3)$ and $Os_3(\mu\text{-}H)(H)(CO)_{10}(PPh_3)$ [6]. The synthesis of P–P bonded cluster oligomers possessing redox-active capping ligands has appeared. The cluster building blocks include $Fe_3(CO)_9(\mu_3\text{-}PX)_2$ and $Fe_3(CO)_9(\mu_3\text{-}PMe)(\mu_3\text{-}PX)$ (where X = Cl, Br, $SnMe_3$). The redox chemistry of these new clusters reveals the existence of extended electronic communication between cluster units in several cases. The X-ray structures of three clusters are discussed [7]. New polynuclear fullerene complexes have been prepared and characterized. Treatment of $Ru_3(CO)_{12}$ with C_{60} and C_{70} affords $Ru_3(CO)_9(\mu_3\text{-}\eta^2,\eta^2,\eta^2\text{-}C_{60})$ and $Ru_3(CO)_9(\mu_3\text{-}\eta^2,\eta^2,\eta^2\text{-}C_{70})$, respectively. The carbide cluster $Ru_6C(CO)_{17}$ reacts with C_{60}, followed by CO substitution with dppm, to furnish $Ru_6C(CO)_{12}(dppm)(\mu_3\text{-}\eta^2,\eta^2,\eta^2\text{-}C_{60})$, while the related arene cluster $Ru_6C(CO)_{13}[PPh_2(\mu\text{-}\eta^6\text{-}C_6H_6)]$ was isolated from the thermolysis of $Ru_6C(CO)_{16}(PPh_3)$. The coordinated aryl group is reversibly released depending upon the reaction conditions [8]. The high-yield synthesis of $[Ru_{10}C_2(CO)_{24}]^{2-}$ from the reaction of $Ru_5C(CO)_{15}$ with sodium is reported. The reactivity of the Ru_{10} cluster with allene and nbd was explored and the resulting allene-substituted cluster

fully characterized. The thermal reaction of $Ru_{10}C_2(CO)_{23}$(alkyne) with added alkynes and $[Ru_{10}C_2(CO)_{24}]^{2-}$ with C_{60} is reported [9]. The synthesis and electrocatalytic behavior of (μ-dppm)[(benzene)$RuCl_2]_2$·[Pt(dppm)Cl_2] have been described [10]. The layer-segregated clusters $Pt_3Ru_6(CO)_{21}[Au(PEt_3)](\mu\text{-}H)_3$, $Pt_3Ru_6(CO)_{21}[Au(PEt_3)]_2(\mu_3\text{-}H)_2$, $Pt_3Ru_6(CO)_{21}(\mu_3\text{-Cp*Ir})(\mu_3\text{-}H)_2$ and $[Pt_3Ru_6(CO)_{21}(\mu_3\text{-HgI})(\mu_3\text{-}H)_2]^-$ have been synthesized from $Pt_3Ru_6(CO)_{21}(\mu_3\text{-}H)(\mu\text{-}H)_3$. All four of these new clusters were structurally characterized by X-ray crystallography. The ligand substitution chemistry and hydrosilation reactivity with these Pt_3Ru_6 clusters are discussed [11].

Single-crystal neutron diffraction data on $[Rh_{13}H_2(CO)_{24}]^{3-}$ reveal that both hydride ligands are located in square pyramidal cavities. X-ray data on $[Rh_{13}H_3(CO)_{24}]^{2-}$ show the same Rh_{13} cage and CO ligand pattern as found for $[Rh_{13}H_n(CO)_{24}]^{(5-n)-}$ (where $n = 1-3$). The ligand exchange reactivity of $[Rh_{13}H_3(CO)_{24}]^{2-}$ and the synthesis of $[Ni_9Pt_3H(CO)_{24}]^{3-}$ are presented and fully discussed [12]. The formation of $Ir_4(CO)_{12}$ from $Ir(CO)_2$(acac) inside zeolite NaY and the catalytic behavior of zeolite NaY-supported Ir catalysts are described. A series of carbon-supported Pt, Pt/Ru and Ru nanoparticles, obtained by the activation of $Pt_2Ru_4(CO)_{18}$, $PtRu_5C(CO)_{16}$ and $Ru_5C(CO)_{15}$, have been prepared and studied for their reactivity in methanol formation from *syn* gas. The catalytic behavior of these systems is discussed relative to electrooxidation catalysts in direct methanol oxidation fuel cells [13].

2. Homometallic clusters

2.1. Group 5 clusters

The synthesis and magnetic properties of $Cp^*_3V_3(\mu\text{-}Cl)_6$ have been published. The antiferromagnetic behavior exhibited by $Cp^*_3V_3(\mu\text{-}Cl)_6$ is discussed relative to the two crystalline forms found in the V_3 complex [14].

2.2. Group 6 clusters

Treatment of $[M(CO)_4(S_2CNEt_2)]^-$ with $[M'S_4]^{2-}$ and $M(CO)_6$ with $[M'S_4]^{2-}$ (where M = Mo, W; M′ = Mo, W) furnishes the trinuclear clusters $[(OC)_4MoS_2MoS_2Mo(CO)_4]^{2-}$, $[(OC)_4WS_2WS_2W(CO)_4]^{2-}$, $[(OC)_4MoS_2WS_2Mo(CO)_4]^{2-}$ and $[(OC)_4WS_2MoS_2W(CO)_4]^{2-}$. Two X-ray structures accompany this report. The solution spectroscopic and cyclic voltammetric data, in conjunction with the X-ray results, indicate that these clusters possess metal-separated oxidations and rich charge-transfer behavior [15]. Pyrolysis of $Cp^*H_3WB_4H_8$ gives the metalloborane cluster $Cp^*_3(\mu\text{-}H)W_3B_8H_8$, which has been characterized in solution and by X-ray crystallography. The solid-state structure (Fig. 1) consists of a $Cp^*_3W_3(\mu\text{-}H)$ triangle that is tethered by 8 BH fragments. The polyhedral shape of this 11-vertex cluster is contrasted with other known 11-atom metal clusters [16].

2.3. Group 7 clusters

A report on the structural and bonding trends in rhenium carbonyl clusters was published previously. Bond enthalpies for rhenium–rhenium bonds and the total rhenium–rhenium bond enthalpies have been calculated, and trends in ΣE as a function of the cluster nuclearity and ligand count are discussed [17]. The cyclic pentarhenium cluster $[Re_5(\mu\text{-}H)_4(CO)_{20}]^-$ has been isolated in high yield from the reaction between 1,2-*eq*,*eq*-$Re_2(CO)_8(THF)_2$ and $[Re_3H_2(\mu\text{-}H)_2(CO)_{12}]^-$. Protonation with CF_3SO_3H furnishes the corresponding neutral Re_5 cluster in quantitative yield. Both cluster frames, which have 80 valence electrons, exhibit an unusual cyclopentane-like geometry that is unprecedented among hydrido-carbonyl clusters [18]. The controlled acidolysis of $[Re_2(\mu\text{-}OMe)_3(CO)_6]^-$ under CO gives the trirhenium cluster complex $[Re_3(\mu\text{-}OMe)_3(\mu_3\text{-}OMe)(CO)_9]^-$, whose X-ray structure reveals the presence of a Re_3 triangle held together by one face-capping and three bridging methoxo groups. The synthetic relationship between this Re_3 complex and other rhenium-oxo species was unequivocally established [19]. Photolysis of $Re_2(CO)_{10}$ with tetramethylthiourea affords the cluster compounds $Re_5(CO)_{17}(\mu\text{-}R)(\mu_4\text{-}S)_2[C(NMe_2)_2]$ (where R = SH, OH). Both new compounds have been fully characterized in solution and their molecular structures determined by crystallographic methods. A distorted Re_3S_2R octahedral core is observed in each case [20]. A report describing the synthesis of chain clusters via the anionic oligomerization of $Re_2(\mu\text{-}H)_2(CO)_8$ was published previously. Treatment of $[Re(CO)_5Re(CO)_4(\mu\text{-}H)ReH(CO)_4]^-$, which is prepared from $[Re(CO)_5]^-$ and $Re_2(\mu\text{-}H)_2(CO)_8$, with $Re_2(\mu\text{-}H)_2(CO)_8$ gives the pentarhenium species $[Re_5H_4(CO)_{21}]^-$ and the heptarhenium complex $[Re_7H_6(CO)_{29}]^-$. The reactions using $[Re(CO)_5\{ReH(CO)_4\}_{2n}]^-$ as

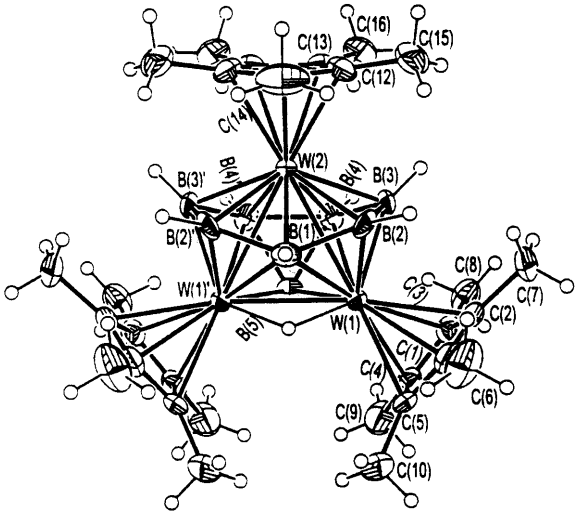

Fig. 1. X-ray structure of $Cp^*_3(\mu\text{-}H)W_3B_8H_8$. Reprinted with permission from Journal of American Chemical Society. Copyright 1998 American Chemical Society.

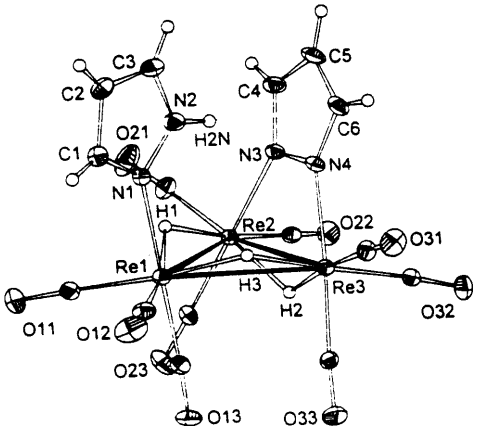

Fig. 2. X-ray structure of $[Re_3(\mu\text{-}H)_3(\mu\text{-}\eta^2\text{-}pz)(CO)_9(Hpz)]^-$. Reprinted with permission from Organometallics. Copyright 1998 American Chemical Society.

an oligomeric building block have been studied by using isotopically enriched ^{13}CO material in order to verify the stepwise growth of these chains. The chemistry exhibited by these 'alkene-like' substrates is briefly compared with that observed in conventional alkene polymerization systems [21]. Reaction of the nitrile-stabilized cluster $Re_3(\mu\text{-}H)_3(CO)_{11}(MeCN)$ and the unsaturated cluster $Re_4(\mu\text{-}H)_4(CO)_{12}$ with Hampy, Hmerpy and 2-hydroxy-6-methylpyridine has been investigated. The nitrile-stabilized cluster reacts slowly with Hampy and Hmerpy in refluxing toluene to give $Re_2(\mu\text{-ampy})_2(CO)_6$ and $Re_2(\mu\text{-merpy})_2(CO)_6$, whereas the latter ligand does not show any reaction under these conditions. The Re_4 cluster reacts with Hampy and Hmerpy to afford the anionic trinuclear clusters $[Re_3(\mu\text{-}H)_3(\mu_3\text{-ampy})(CO)_9]^-$ and $[Re_3(\mu\text{-}H)_3(\mu_3\text{-merpy})(CO)_9]^-$. The X-ray structures of these latter two clusters accompany this report [22]. The thermolysis reaction of $[Re_3(\mu\text{-}H)_4(CO)_{10}]^-$ with pyrazole proceeds in a stepwise fashion to initially give $[Re_3(\mu\text{-}H)_3(\mu\text{-}\eta^2\text{-}pz)(CO)_{10}]^-$ and H_2. Subsequent loss of CO and substitution by additional pyrazole furnishes $[Re_3(\mu\text{-}H)_3(\mu\text{-}\eta^2\text{-}pz)(CO)_9(Hpz)]^-$, which contains one pz ligand that bridges a cluster edge and a terminally bound pz ligand on the third vertex of the triangle (Fig. 2). The results of VT ^1H-NMR studies that show evidence for intramolecular hydrogen bonding between the pz ligands are discussed. The substitution chemistry of $[Re_3(\mu\text{-}H)_4(CO)_9(PMe_2Ph)]^-$ with pyrazole is also described [23].

2.4. Group 8 clusters

The homoleptic ruthenabenzene compound $Ru_3(CO)_6(C_7H_{11})_2$ was prepared from the 'open' ruthenocene complex $(C_7H_{11})_2Ru$ and $Ru_3(CO)_{12}$. The double insertion of two $Ru(CO)_3$ units into all four terminal C–H bonds in the *endo* position accounts for the formation of the ruthenabenzene cluster. The X-ray structure is presented and the redox chemistry is discussed relative to other classical metal-

locene complexes [24]. Silica-supported α-$[Os(CO)_3Cl_2]_2$ in the presence of alkali-metal carbonates can produce reactive surface osmium(II) species that have been shown to furnish $Os_3(CO)_{12}$, $H_4Os_4(CO)_{12}$, $[H_3Os_4(CO)_{12}]^-$ and $[Os_{10}C(CO)_{24}]^{2-}$ depending upon the reaction conditions. The effect of the alkali-metal carbonate, temperature and gas pressure on the nature of the product(s) is described [25].

$Ru_3(CO)_{12}$ reacts with 2,6-bis(bromomethyl)pyridine to give an insoluble oligomer having the formula $[Ru_2Br_2(CO)_4\{\mu\text{-}C_5H_3N\text{-}2\text{-}C(O)CH_2\text{-}6\text{-}CH_2\}]$ and a mononuclear ruthenium complex [26]. Electron-transfer catalysis using CpFe(I)arene complexes has been studied with the substrates $M_3(CO)_{12}$ (where M = Fe, Ru) and $MeCCo_3(CO)_9$. The ligands employed in these studies were several ferrocenyldiphenylphosphine ligands. The advantage of these electrocatalysts originates from the driving force associated with the initiation step, which is easily modulated by changing the number of methyl groups on the arene rings [27]. The reaction of $Ru_3(CO)_{12}$ with 1,6-bis(trimethylsilyl)hexa-1,3,5-triyne gives the butterfly cluster $Ru_4(CO)_{12}(\mu_4\text{-}\eta^1,\eta^1,\eta^2,\eta^2\text{-}Me_3SiC{\equiv}CC_2C{\equiv}CSiMe_3)$ and $Ru_2(CO)_6$-$[\mu\text{-}\eta^2,\eta^4\text{-}C(C{\equiv}CSiMe_3){=}C(C{\equiv}CSiMe_3)C(C{\equiv}CSiMe_3){=}C(C{\equiv}CSiMe_3)]$. The pendant ethynyl ligands in both complexes can be further functionalized with suitable reagents. The reaction between the Ru_4 cluster and $Ru_4(\mu_4\text{-}PPh)(CO)_{13}$ is discussed [28].

The cyclocarbonylation of yne-aldehydes to give bicyclic α,β-unsaturated γ-butyrolactones has been achieved using $Ru_3(CO)_{12}$ as a catalyst precursor. Two plausible mechanisms are presented for the formation of the observed products [29]. Site-selective carbonylations at a C–H bond in aza-heterocycles have been demonstrated with $Ru_3(CO)_{12}$. This work provides the first examples of a direct carbonylation at a C–H bond that is β to a directing nitrogen center [30]. A report describing the cross-carbonylation of alkynes and 2-norbornenes to give hydroquinones using $Ru_3(CO)_{12}$ has appeared. The reaction is believed to involve a maleoylruthenium species that is generated by the reaction of an alkyne and two molecules of CO [31]. C–H bond activation of *N*-benzyl-*N*-(3-methyl-2-pyridyl)amine in the presence of various alkenes is promoted by $Ru_3(CO)_{12}$. This reaction proceeds via the regiospecific activation of the benzylic sp^3 C–H bond [32]. Propargyl alcohols react with $Ru_3(CO)_{12}$ to give $HRu_3(CO)_9[C_2CR(OH)R']$ in hydrocarbon solution. When the same reactions are carried out in the presence of MeOH/KOH the corresponding allenylidene clusters $HRu_3(CO)_9[HC_2C(R)R']$ are formed as the major products. Reaction of the chiral cluster $HRu_3(CO)_9$-$[C_2CMe(OH)Ph]$ with dppm yields the bridged cluster $HRu_3(CO)_7(dppm)$-$[C_2CMe(OH)Ph]$, which has been shown to exist as a pair of diastereomers in both the solution and the solid state [33]. Five new polynuclear ruthenium complexes have been isolated from the reaction between $Ru_3(CO)_{12}$ and but-3-yn-2-ol. The solid-state structures of all five clusters were determined and the unique features present in each cluster are discussed [34]. The product formed from the reaction between $Ru_3(CO)_{12}$ and cyclododeca-1,5-9-triene, which was previously identified as $Ru_3(\mu\text{-}H)(\mu_3\text{-}C_{12}H_{15})(CO)_9$, has now been shown to contain a $\mu_3\text{-}C_{12}H_{17}$ ligand. The details associated with the diffraction data, electrospray mass spectra and NMR studies are presented [35]. The silaborate complex $[MeSiB_{10}H_{12}]^-$

reacts with $Ru_3(CO)_{12}$ in near quantitative yield to give $[Ru_3(CO)_8(\eta^5\text{-}MeSiB_{10}H_{10})]^-$. CO substitution by added PMe_2Ph gives the corresponding bisphosphine-substituted cluster [36].

A review describing the chemistry exhibited by triosmium alkylidyne clusters, ruthenium clusters containing a μ_4-nitrene ligand and mixed-metal clusters of osmium and palladium was published previously [37]. The synthetic methodologies and structures of $M_3(CO)_9$-[C_{60}]fullerene (where M = Ru, Os) have been reviewed [38]. The reactivity of $Ru_3(\mu\text{-}H)_2(CO)_9(\mu_3\text{-}\eta^2\text{-}C_8H_{12})$ and $Ru_3(\mu\text{-}H)(CO)_9(\mu_3\text{-}\eta^3\text{-}C_{12}H_{19})$ with CO and H_2 was investigated. Both clusters are converted to $Ru_3(CO)_{12}$ under low CO pressure and $H_4Ru_4(CO)_{12}$ is observed under low H_2 pressure. The homogeneous hydrogenation of 1-hexene was studied using these starting clusters as a function of temperature [39]. The hydrogenation of alkynes under homogeneous and solid-state conditions was explored by using the cluster compounds $Fe_3(CO)_9(\perp\text{-}RC_2R')$ (where R = R′ = Ph, Et; R = Me, R′ = Ph). Evidence supporting cluster catalysis is presented and the catalytic activity is discussed relative to the coordinating ability of the alkyne substrates. It is observed that competition occurs between hydrogenation and formation of metallacyclic by-products, which greatly lower the catalytic hydrogenation activity [40]. The hydrogenation of alkynes and 1,4-cyclohexadiene has been examined by using $HRu_3(CO)_9(\perp\text{-}C_2'Bu)$ as a catalyst precursor. While cluster catalysis seems likely, there is evidence for the partial fragmentation of the cluster. The formation of metallacyclic compounds leads to catalytically inactive species [41]. Thermolysis of $Ru_3(\mu_3\text{-}PhC_2C{\equiv}CPh)(\mu\text{-}CO)(CO)_9$ leads to dimerization and subsequent internal cyclization of the 1,3-diyne ligands to give $Ru_6(PhCHC_3C_6H_4)_2(CO)_{15}$. X-ray analysis reveals that the two newly formed methyleneindyne molecules are coordinated in η^2 and η^4 modes to the Ru_6 core [42]. The accuracy of different non-local density functional theory (NL-DFT) methods in computing the geometries and relative energies of $Fe_3(\mu_3\text{-}\eta^2\text{-}HC_2H\text{-}|)(\mu\text{-}CO)(CO)_9$ and $Fe_3(\mu_3\text{-}\eta^2\text{-}HC_2H)(\mu\text{-}CO)(CO)_9$ has been evaluated [43]. Treating $Fe_3(CO)_9(\mu_3\text{-}\eta^2\text{-}\perp\text{-}C_2Et_2)$ with the substituted propargylamine *N*-benzyl-*N*-methylpropargylamine affords the complexes $Fe_3(CO)_8[C_2Et_2C(H)\text{-}\{CH_2N(Me)CH_2Ph\}]$ and $Fe_2(CO)_6[C_2Et_2C\{CH_2N(Me)CH_2Ph\}CH]$. Both products were structurally characterized by X-ray analysis, with two different orientations for the insertion of the propargylamine between the iron core and alkyne ligand in the reactant being observed [44].

The reactivity of NH_3 with $Ru_3H(\mu\text{-}H)(\mu\text{-}CO)(CO)_{10}$ and $Os_3H(\mu\text{-}H)(CO)_{11}$ has been investigated by ^1H, ^{13}C and ^{15}N NMR spectroscopy. At room temperature the major product of the reaction is $[NH_4][M_3(\mu\text{-}H)(\mu\text{-}CO)(CO)_{11}]$. When the reaction is carried out at low temperature several kinetic products are observed, one of which contains a carbamoyl moiety [45]. H_2 reacts with $Ru_3(CO)_{11}(MeCN)$ to give $H_2Ru_3(CO)_{11}$. The dihydride cluster is relatively stable under H_2 and has been characterized in solution by ^1H- and ^{13}C-NMR spectroscopy. The stereochemical non-rigidity of the dihydride cluster was explored by VT ^{13}C-NMR spectroscopy, and an exchange sequence involving edge hopping of the μ-H group coupled with the concerted migration of the CO groups is discussed. Protonation of the dihydride with TFA at low temperature initially occurs by a reversible *O*-protonation at the

μ-CO site. Higher temperatures lead to the formation of $(\mu\text{-H})Ru_3(\mu\text{-}\eta^3\text{-}O_2CCF_3)(CO)_{10}$ [46]. Activation of a C–C bond in biphenylene occurs during the co-thermolysis of biphenylene with $Fe_3(CO)_{12}$. The major product isolated was characterized as $Fe_2(CO)_5(\mu\text{-CO})[\mu\text{-}\eta^2,\eta^4\text{-}(C_6H_4)_2]$. When the same reaction is carried out with $Ru_3(CO)_{12}$ both $Ru_2(CO)_5(\mu\text{-CO})[\mu\text{-}\eta^2,\eta^4\text{-}(C_6H_4)_2]$ and the known carbide cluster $Ru_6(CO)_{17}(\mu_6\text{-C})$ are obtained. Use of $Os_3(CO)_{12}$ affords the identical dinuclear product and $Os_4(CO)_{12}[\mu_4\text{-}\eta^2\text{-}(C_6H_3)Ph]$, whose X-ray structure is shown in Fig. 3. C–H bond and not C–C bond activation is observed when $Os_3(CO)_{10}(MeCN)_2$ is thermolyzed with biphenylene. Here the major product was found to be $(\mu\text{-H})_2Os_3(CO)_9[\mu_3\text{-}\eta^2\text{-}C_6H_2(C_6H_4)]$ [47].

A high-yield route to ruthenaboranes has been published. Starting with $Ru_3(CO)_9(MeCN)_3$ and $[B_3H_8]^-$ allows for the synthesis of $HRu_3(CO)_9(B_2H_5)$, while the use of $BH_3{\cdot}THF$ furnishes the hexaruthenium cluster $HRu_6B(CO)_{17}$ [48]. The synthesis and characterization of $Cp^*_3Ru_3B_3H_8$ are reported. The Ru_3 cluster is obtained from the reaction between $[Cp^*RuCl_2]_n$ and $[BH_4]^-$. The molecular structure of the product exhibits a capped *nido* geometry where the polyhedral shape is driven by the ancillary hydrogen ligands [49]. The reaction of $Os_3(CO)_{10}(CNR)(MeCN)$ with HCl has been studied as a model for observing the fine-tuning of site-selective protonation in metal clusters. The site of protonation, which takes place at either the osmium center or the nitrogen atom of the isocyanide ligand, may be tuned by changing the nature of the isocyanide ligand, solvent polarity and acid strength. Included in this report are the X-ray structures of $(\mu_2\text{-Cl})Os_3(CO)_{10}(\mu_2\text{-C=NHCH}_2Ph)$ and $(\mu\text{-H})Os_3Cl(CO)_{10}(CNPr)$ [50]. Treatment of $Os_3(CO)_{10}(MeCN)_2$ with carboxylic acids gives clusters that contain a chelating μ,η^2-carboxylate ligand and a hydride bridge across one edge of the triangular frame. The course of these reactions, solution spectroscopic data and the X-ray data on $Os_3H(CO)_{10}[C_6H_4(OH)CO_2]$ and $Os_3H(CO)_{10}(C_6H_5COS)$ are dis-

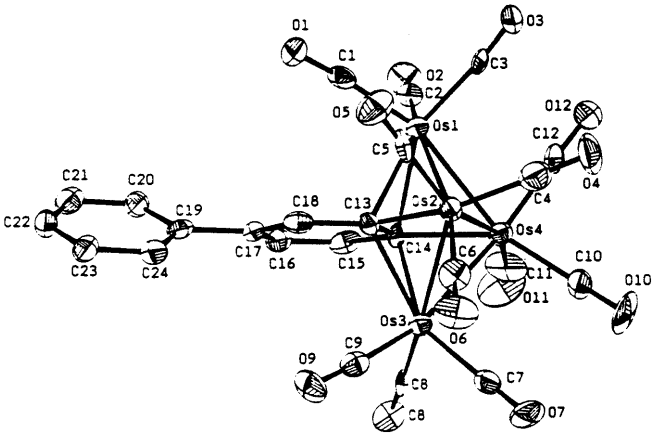

Fig. 3. X-ray structure of $Os_4(CO)_{12}[\mu_4\text{-}\eta^2\text{-}(C_6H_3)Ph]$. Reprinted with permission from Organometallics. Copyright 1998 American Chemical Society.

cussed [51]. The electrochemical behavior of $HRu_3(\mu_3\text{-}\eta^3\text{-}XCCRCR')(CO)_{9-n}(PPh_3)_n$ and the reactivity of these clusters with electrophiles have been studied. The observed dependence of the oxidation potential upon the degree of P-ligand substitution has been analyzed as an example of ligand additive ability in cluster systems. The stability and characterization of the thermally unstable radical cations are fully discussed [52]. The cyclic voltammetric data on $H_3Ru_3(\mu_3\text{-}CX)(CO)_{9-n}L_n$, $H_3Ru_3(\mu_3\text{-}COMe)(CO)_6(PPh_3)_2L$ and $H_3Os_3(\mu_3\text{-}CX)(CO)_7(PPh_3)_2$ reveal the presence of a quasi-reversible to reversible one-electron oxidation. The effect of the ligand (L) and substituent (X) upon the oxidation potential has been analyzed as an example of ligand additive ability in a cluster system. Selected radical cations were investigated by EPR spectroscopy, and the rate data for axial–equitorial ligand isomerization in the 47-electron clusters are contrasted with the isomerization reaction in the 48-electron clusters [53]. The new cluster compounds $Ru_3(CO)_9(\mu_3\text{-}NOMe)(\mu_3\text{-}\eta^2\text{-}RC_2Ph)$ (where R = H, Ph) have been prepared from $Ru_3(CO)_9(\mu_3\text{-}CO)(\mu_3\text{-}NOMe)$ with added alkyne. These new clusters exhibit an open triangular core of ruthenium atoms with the $\mu_3\text{-}\eta^2$-alkyne and μ_3-NOMe ligands on opposite faces of the metal triangle. Thermolysis of the phenylacetylene cluster gives $Ru_4(CO)_9(\mu\text{-}CO)_2(\mu_4\text{-}NOMe)(\mu_4\text{-}\eta^2\text{-}HC_2Ph)$, $Ru_4(CO)_9(\mu\text{-}CO)_2[\mu_4\text{-}NC(O)OMe](\mu_4\text{-}\eta^2\text{-}HC_2Ph)$ and $Ru_5(CO)_{13}(\mu\text{-}CO)(\mu_4\text{-}NH)(\mu_4\text{-}\eta^2\text{-}HC_2Ph)$, while the diphenylacetylene derivative yields clusters analogous to the former two products along with $Ru_4(CO)_9(\mu\text{-}CO)_2(\mu_4\text{-}NH)(\mu_4\text{-}\eta^2\text{-}PhC_2Ph)$ and $Ru_6(CO)_{13}(\mu\text{-}H)(\mu_5\text{-}N)(\mu_3\text{-}\eta^2\text{-}PhC_2Ph)_2$. Four X-ray structures are presented and the important structural features are discussed. The reactivity of these clusters in CO substitution reactions and with $[BH_4]^-$ was also investigated [54].

The C_{60}-substituted clusters $Os_3(CO)_{11}(\eta^2\text{-}C_{60})$, $Os_3(CO)_{10}(MeCN)(\eta^2\text{-}C_{60})$, $Os_3(CO)_{10}(PPh_3)(\eta^2\text{-}C_{60})$, $Os_3(CO)_9(PR_3)_2(\eta^2\text{-}C_{60})$ (where R = Me, Ph), $Os_3(CO)_9(\mu_3\text{-}\eta^2,\eta^2,\eta^2\text{-}C_{60})$ and $Os_3(CO)_8(PMe_3)(\mu_3\text{-}\eta^2,\eta^2,\eta^2\text{-}C_{60})$ have been synthesized and fully characterized in solution and by mass spectrometry. The X-ray structure of $Os_3(CO)_{11}(\eta^2\text{-}C_{60})$ is similar to that of $Os_3(CO)_{12}$ except for the presence of the equatorial C_{60} ligand. VT NMR data and reaction chemistry using Me_3NO are presented in Ref. [55]. A report on the synthesis, structure and electrochemical studies of $\mu_3\text{-}\eta^2,\eta^2,\eta^2\text{-}C_{60}$ triosmium complexes was published previously [56].

$[HSb\{Fe(CO)_4\}_3]^{2-}$ reacts with MeI and EtI to produce $[Sb(Me)I\{Fe(CO)_4\}_3]^-$ and $[ISb\{Fe(CO)_4\}_3]^{2-}$, respectively. The X-ray structure of the former cluster is included in this report, and data are presented that excludes a radical chain mechanism in the formation of both products [57]. The small anionic cluster $[TeFe_3(CO)_9]^{2-}$ has been used as a starting material in the synthesis of $[Te_{10}Fe_8(CO)_{20}]^{2-}$. Reaction of the Fe_8 cluster with $[Cu_2(dppm)_2(MeCN)_4]^{2+}$ affords the dppm-bridged cluster $Te_4Fe_4(CO)_{10}(dppm)$. The molecular structure of the double-cubic Fe_8 cluster was established by X-ray crystallography [58]. The alkylation of $[EFe_3(CO)_9]^{2-}$ (where E = S, Se, Te) with methyl triflate and MeI has been investigated. Methyl triflate reacts at the sulfur center to give $[Fe_3(CO)_9SMe]^-$, whereas alkylation occurs at the metal framework in the case of the other chalcogen-capped derivatives. The X-ray structure of $[MeFe_3(CO)_9Se]^-$ reveals the

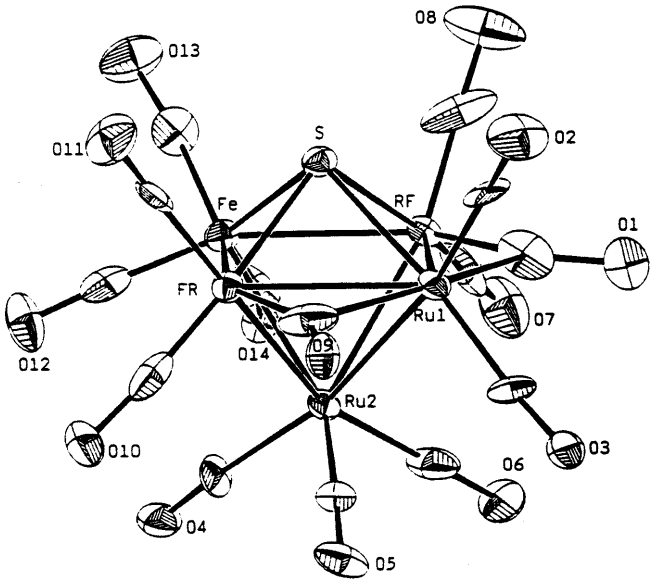

Fig. 4. X-ray structure of $[SFe_2Ru_3(CO)_{14}]^{2-}$. Reprinted with permission from Organometallics. Copyright 1998 American Chemical Society.

presence of a long Fe–Me bond. Changes in the electron density within these clusters were observed to be related to the ^{77}Se- and ^{125}Te-NMR chemical shifts [59]. A new synthesis for $[SFe_3(CO)_9]^{2-}$ and its reactivity towards electrophiles have been published. The reaction between Na_2SO_3 and $Fe(CO)_5$ in methanolic KOH gives the aforementioned cluster in good yield. Acidification furnishes $[SFe_3(\mu\text{-}H)(CO)_9]^-$ and $SFe_3(\mu\text{-}H)_2(CO)_9$, while alkylation using methyl triflate gives the sulfur-methylated cluster $[MeSFe_3(CO)_9]^-$. Treatment of the dianionic cluster with $Ru_3(CO)_{12}$ at elevated temperatures leads to the octahedral species $[SFe_2Ru_3(CO)_{14}]^-$, which may be alkylated at the sulfur center using methyl triflate. Four X-ray structures are presented, one of which is shown in Fig. 4 [60].

The use of the ligand dppf in the construction of polymetallic aggregates and oligomers has been published. Many examples involving Group 8–10 metals are presented [61]. The disorder in the X-ray structures of $Ru_3(CO)_{11}(CN^tBu)$ and $Ru_3(CO)_{11}(PMe_3)$ has been re-examined and found to reversibly disappear upon cooling. This behavior supports the contention that the disorder is dynamic in origin. The fact that the ancillary isocyanide and phosphine ligands move by ca. 0.8 Å suggests that the whole cluster does not rotate intact within the crystalline lattice, but rather the data point to an oscillation of the Ru_3 triangle with a relatively rigid ligand polyhedron. The X-ray structure and dynamic disorder in the metal framework of $Ru_3(CO)_9[P(OMe)_3]_3$ are also reported [62]. The reactivity of $M_3(CO)_{12-n}(Ph_2Py)_n$ (where $M = Ru$, $n = 3$; $M = Os$, $n = 1$) with different Lewis acids has been explored [63]. P–C bond cleavage and insertion of the but-2-yne ligand into the P≡C bond of an incoming phosphaalkyne have been observed in the reaction

between 2,2-dimethylpropylidynephosphine and $Os_3(CO)_{10}(\mu_3\text{-}\eta^1,\eta^2,\eta^1\text{-}C_2Me_2)$. The product cluster, $Os_3(CO)_8(\mu_2\text{-}PC^tBu)[\mu_3\text{-}PC(Me)C(Me)C(^tBu)]$, was isolated and characterized in solution and by X-ray crystallography. This 50-electron cluster exhibits an open triangular frame consistent with PSEP theory [64]. The X-ray structure of $Ru_3(CO)_9(\mu\text{-dppm})[P(OMe)_3]$ has been solved. Trends within the Ru–Ru bond distances as a function of the attached ligands are discussed [65].

The mono-substituted clusters $Os_3(CO)_{11}PR_3$ (where $R = p\text{-}C_6H_4F$, ^tBu) have been prepared from $Os_3(CO)_{11}(MeCN)$ and their X-ray structures determined. Two different forms of $Os_3(CO)_{11}P(p\text{-}C_6H_5F)_3$ are observed in the solid state (yellow and red), and the differences between these forms are discussed relative to the perturbation exerted on the cluster by the phosphine ligand [66]. P–C and Ru–Ru bond cleavage are observed when $Ru_3(CO)_{11}(Ph_2PC{\equiv}C\text{–}C{\equiv}CR)$ (where $R = ^tBu$, Ph, $SiMe_3$) is refluxed in THF. The following clusters have been isolated and characterized in solution: $Ru_4(CO)_9(\mu\text{-}PPh_2)_2[\mu_4\text{-}\eta^1,\eta^2,\eta^2,\eta^1\text{-}C{\equiv}C\text{–}C{=}C(^tBu)\text{–}C{\equiv}C\text{–}C{\equiv}C^tBu]$, $Ru_4(CO)_{10}(\mu\text{-}CO)(\mu_4\text{-}PPh)[\mu_4\text{-}\eta^1,\eta^1,\eta^2,\eta^2\text{-}(^tBuC{\equiv}C)\text{–}C{\equiv}CPh]$, $Ru_4(CO)_{10}(\mu_4\text{-}PPh)(\mu_4\text{-}\eta^1,\eta^1,\eta^3,\eta^3\text{-}PhC{\equiv}C\text{–}C{\equiv}C^tBu)$, $Ru_5(CO)_{11}(\mu\text{-}CO)(\mu\text{-}PPh_2)_2(\mu_3\text{-}\eta^1,\eta^1,\eta^1\text{-}C{\equiv}C\text{–}C{\equiv}C^tBu)(\mu_4\text{-}C)(\mu_2\text{-}\eta^1,\eta^1\text{-}C\text{–}C{\equiv}C^tBu)$ and $Ru_6(CO)_{13}(\mu\text{-}CO)_2(\mu\text{-}PPh_2)(\mu_5\text{-}C)(\mu_3\text{-}\eta^1,\eta^1,\eta^1\text{-}C\text{–}C{\equiv}CR)$. Reaction pathways are discussed and the results of extended Hückel MO calculations on the Ru_6 cluster suggest that the cluster is best viewed as a Ru_4C_2 octahedron that is bicapped by a phosphido-bridged Ru_2 unit, with the hydrocarbyl C–C–R fragment contributing a total of 7 valence electrons to the CVE [67]. The equilibrium between the two structural isomers of $(\mu\text{-}H)Os_3(CO)_9L(\mu\text{-}\eta^2\text{-}CH{=}CH_2)$ (where L = various phosphines) has been explored. The steric interactions between the phosphine ligand and the vinyl moiety are important in determining the stability of the two structural isomers. Isotope studies using selectively deuterated $(\mu\text{-}D)Os_3(CO)_9(PPh_3)(\mu\text{-}\eta^2\text{-}CH{=}CHD)$ help demonstrate the changes in the stereochemistry of the vinyl group that accompany the structural isomerization [68]. Bromination of $Os_3(CO)_{11}(EPh_3)$ (where E = P, Sb) affords the trimetallic chain clusters $Br_2Os(CO)_3Os(CO)_4Os(CO)_4(EPh_3)$ and $Br(CO)_4OsOs(CO)_4Os(CO)_3Br(EPh_3)$. The former clusters are shown to contain two donor–acceptor Os–Os bonds in tandem, as shown by the X-ray structure

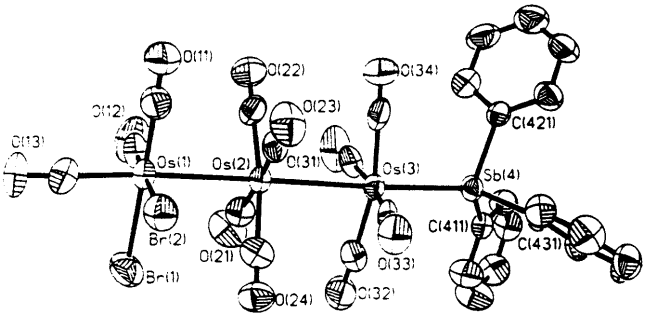

Fig. 5. X-ray structure of $Br_2Os(CO)_3Os(CO)_4Os(CO)_4(SbPh_3)$. Reprinted with permission from Organometallics. Copyright 1998 American Chemical Society.

of $Br_2Os(CO)_3Os(CO)_4Os(CO)_4(SbPh_3)$ (Fig. 5). VT ^{31}P-NMR studies provide evidence for a bromonium adduct that collapses with bromide ion to give both of the observed products [69].

$[Ru_3H(CO)_{11}]^-$ reacts with excess PCy_3 in methanol to give the trisubstituted clusters $Ru_3(CO)_9(PCy_3)_3$ (48e) and $Ru_3H_2(CO)_6(PCy_3)_3$ (46e), depending upon the reaction conditions. The identity of both clusters was ascertained by X-ray crystallography [70]. A report describing the molecular structures and solid-state packing of $[Ru_3(CO)_{11}]_2$(dppe) and $[Ru_3(CO)_{11}]_2$[1,4-bis(diphenylphosphino)benzene] has been published. Both molecules consist of centrosymmetric units where the ligating diphosphines are covered by the Ru_3 clusters. The packing motif in the solid state is dominated by interactions between sets of CO ligands similar to those exhibited by $Ru_3(CO)_{12}$ [71]. A low-temperature NMR study (^1H, ^{13}C, ^{31}P) on the addition of phosphines to $H_2Os_3(CO)_{10}$ provides evidence for the formation of four new isomeric derivatives of $H(\mu\text{-}H)Os_3(CO)_{10}(P)$. These kinetically formed isomers slowly transform into the thermodynamically stable isomer that contains the P-ligand *trans* to an Os–Os bond and *cis* to the bridging hydride. Rate measurements on the transformation to the thermodynamic isomer have allowed the activation energies to be calculated [72]. The reaction of the water-soluble phosphine ligand TPPTS with $Ru_3(CO)_{12}$, $Ru_6C(CO)_{17}$, $H_4Ru_4(CO)_{12}$ and $H_2Os_3(CO)_{10}$ furnishes TPPTS-substituted clusters that have been shown to function as catalyst precursors in the water–gas shift reaction. The use of electrospray mass spectrometry in characterizing these clusters in solution is discussed [73]. A kinetic study on the steric limitations in associative substitution reactions in $Os_3(CO)_9(\mu\text{-}C_4Ph_4)$ has been published. Small P-donor ligands (Tolman cone angle $\leq 143°$) react in an associative fashion to give an adduct that leads to the monosubstituted product $Os_3(CO)_8(P)(\mu\text{-}C_4Ph_4)$. P-ligands whose cone angles are greater than 145° react in a bimolecular fashion to furnish mono- and dinuclear osmium products. No evidence for monosubstituted Os_3 clusters was observed with large cone angle ligands. Two X-ray structures accompany this report [74].

The synthesis and spectral studies on the mixed-ligand clusters $Ru_3(CO)_9(\mu\text{-}Ph_2AsCH_2AsPh_2)L$ (where $L = PPh_3$, PCy_2Ph, $P(OMe)_3$) and $Ru_3(CO)_8(\mu\text{-}Ph_2AsCH_2AsPh_2)(\mu\text{-dppm})$ are described. The X-ray results on the latter cluster and the PCy_2Ph derivative reveal a planar Ru_3 frame, with differences in the Ru–Ru bond distances being discussed relative to the ancillary ligands [75]. Thermolysis of $Os_3(CO)_{10}(\mu\text{-dppm})$ with diphenylphosphine in toluene leads to $Os_3(CO)_9(\mu\text{-dppm})(PPh_2H)$ and the phosphido-bridged species $(\mu\text{-}H)Os_3H(CO)_7(\mu\text{-dppm})(\mu\text{-}PPh_2)$. This latter cluster exists in three isomeric forms in solution. The 46-electron cluster $Os_3(\mu\text{-}H)(CO)_8[Ph_2PCH_2P(Ph)(C_6H_4)]$ was allowed to react with excess Ph_2PH at room temperature to give $Os_3(\mu\text{-}H)(CO)_8[Ph_2PCH_2P(Ph)C_6H_4](Ph_2PH)$ and $Os_3(CO)_8(\mu\text{-dppm})(Ph_2PH)_2$. The thermolysis chemistry of these clusters has been explored, and all new clusters have been characterized in solution and by X-ray analysis in the case of four derivatives [76]. The coupling of 1,3-diynes on a triruthenium cluster has been demonstrated in the reaction between $Ru_3(\mu_3\text{-}PhC_2C{\equiv}CPh)(\mu\text{-dppm})(CO)_8$ and $Me_3SiC{\equiv}C{-}C{\equiv}CSiMe_3$. The compounds $Ru_2(\mu\text{-dppm})[\mu\text{-}C(C{\equiv}CPh){=}CPhC(SiMe_3){=}C(C{\equiv}CSiMe_3)](CO)_4$, $Ru_3[\mu_3\text{-}C(SiMe_3) = (C{\equiv}C\text{-}$

$SiMe_3$)(=CPh)C(=CPh)C(O)](μ-dppm)(μ-CO)$(CO)_7$ and $Ru_3(\mu_4$-$PhC_2C{\equiv}CPh)(\mu_4$-$Me_3SiC_2C{\equiv}CSiMe_3)$(μ-dppm)(μ-CO)$(CO)_8$ have been isolated from this reaction. A discussion on the insertion reaction and three X-ray structures are included in the report [77]. The reaction of $Ru_3(CO)_{10}$(dppm) with the ethyne-1,2-diyl compounds $[(\eta^5$-$C_5H_4R)Ru(CO)_2]_2(\mu$-$C{\equiv}C)$ (where R = H, Me) affords the medium nuclearity clusters $Ru_5(\mu_5$-$C{\equiv}C)(\eta^5$-$C_5H_4R)_2$(dppm)$(\mu_2$-$CO)_2(CO)_7$ in high yields. X-ray diffraction analysis on both derivatives reveals that the core of these clusters incorporates an open and accessible carbide ligand that is attached to a spiked butterfly Ru_5 framework [78].

PCy_2H reacts with $Ru_3(CO)_{12}$ in refluxing toluene to produce the cluster complexes $Ru_3(CO)_7(\mu$-$H)(\mu$-$PCy_2)_3$ and $Ru_3(CO)_6(\mu$-$H)(\mu$-$PCy_2)_3(PCy_2H)$. Both of these clusters react with CO to give the 52-electron cluster $Ru_3(CO)_9(\mu$-$H)(\mu$-$PCy_2)_3$. The X-ray structure of $Ru_3(CO)_7(\mu$-$H)(\mu$-$PCy_2)_3$ is presented [79]. The osmium–antimony cluster $Os_3(CO)_{10}(\mu$-$H)(\mu$-$SbPh_2)$ reacts with donor ligands by way of cleavage of the antimony-bridged and hydrido-bridged Os–Os bond to give the addition adducts $Os_3(CO)_{10}(H)(\mu$-$SbPh_2)L$ (where L = various ligands). The incoming ligand occupies an equatorial site on the Os_3Sb framework, as verified by X-ray analysis on the $AsPh_3$ and $SbPh_3$ complexes. Solution NMR studies confirm the presence of an isomeric mixture in each case, which presumably reflects different ligand arrangements relative to the antimony vertex [80]. The μ_3-benzyne cluster $Ru_3(CO)_7(\mu$-$PPh_2)_2(\mu_3$-$C_6H_4)$ reacts with donor ligands at room temperature to afford $Ru_3(CO)_6L_2(\mu$-$PPh_2)_2(\mu_3$-$C_6H_4CO)$ (where L = CO, $P(OMe)_3$, CN^tBu). Isotopic labeling studies with ^{13}CO confirm that the reaction involves a migratory insertion of CO into the benzyne–Ru σ bond. The larger phosphine ligands PPh_3 and $P(^iPr)_3$ react with the starting cluster at elevated temperature to produce $Ru_3(CO)_6(PR_3)(\mu$-$PPh_2)_2(\mu_3$-$C_6H_4)$, which may be subsequently carbonylated to furnish the corresponding μ_3-benzoyl species. Treatment of the heptacarbonyl μ_3-benzyne cluster with H_2 releases benzaldehyde. The mechanism associated with the carbonylation of the μ_3-benzyne ligand and implications relevant to metal surface chemistry are discussed [81]. The first example of an insertion into a cluster-bound hydrocarbon moiety has been reported in the reaction between $Ru_3(CO)_9(\mu$-$H)(C_{12}H_{17})$ and $AsPh_3$. The product of the reaction, $Ru_3(CO)_6(\mu_2$-$CO)(\mu_2$-$AsPh_2)(\mu$-$O{=}C$–$C_{12}H_{17})$, was characterized in solution and the solid-state structure determined by X-ray crystallography [82]. The reaction between $Ru_3(CO)_8(\mu$-$H)_2(\mu$-$P^tBu_2)_2$ and Cy_2PH leads to the three cluster compounds $Ru_3(CO)_7(\mu$-$H)(\mu$-$P^tBu_2)(\mu$-$PCy_2)_2$, $Ru_3(CO)_8(\mu$-$H)_2(\mu$-$P^tBu_2)(\mu$-$PCy_2)$ and $Ru_3(\mu$-$CO)(CO)_5(\mu$-$H)_2(\mu$-$P^tBu_2)(P^tBu_2H)$. The X-ray structures of the first and third clusters are reported [83]. The homogeneous hydrogenation of alkynes and 1,4-cyclohexadiene using the benzyne-substituted clusters $Ru_3(CO)_7(PPh_2)_2(C_6H_4)$ and $Ru_4(CO)_{11}(PPh)(C_6H_4)$ is described. Both of these clusters show the highest alkyne hydrogenation activity relative to other metal carbonyl clusters observed to date. The alkyne-substituted clusters $Ru_3(CO)_7(PPh_2)_2(HC_2Ph)$ and $Ru_4(CO)_{11}(PPh)$-(C_2Ph_2) have also been examined in comparable reactions. Despite the fact that intermediates could not be isolated or observed, direct and indirect evidence is presented that supports cluster catalysis [84].

The synthesis and photochemical properties of several $Os_3(CO)_{10}(\alpha\text{-diimine})$ clusters are reported. Resonance Raman spectra of the visible absorption band of these clusters reveal transitions consisting of Os-to-α-diimine charge transfer (MLCT) character. Irradiation into these transitions leads to the zwitterions $^{-}Os(CO)_4–Os(CO)_4–Os^{+}(S)(CO)_2(\alpha\text{-diimine})$ in coordinating solvents (S) and biradicals $^{\bullet}Os(CO)_4–Os(CO)_4–Os^{+}(S)(CO)_2(\alpha\text{-diimine}^{-\bullet})$ in non-coordinating solvents and THF. The lifetimes of these intermediates, quantum yield measurements, EPR trapping experiments and mechanistic pathways available to the zwitterionic and biradical species are discussed [85]. Treatment of $Os_3(CO)_{10}(MeCN)_2$ with pyz and dpp leads to the clusters $[Os_3(CO)_{10}(\mu\text{-H})]_2(pyz)$, $[Os_3(CO)_{10}]_2(dpp)$, $Os_3(CO)_{10}(\mu\text{-H})(pyz)$ and $Os_3(CO)_{10}(dpp)$ depending on the cluster/ligand stoichiometry. All four clusters were characterized in solution by IR and ^{1}H-NMR spectroscopy. Electrochemical data are presented that show strong evidence for electronic interaction between the metal cores of the diimine-bridged clusters [86]. Melamine reacts with $Ru_3(CO)_{12}$ to afford the monometallated cluster $Ru_3(CO)_9(\mu\text{-H})_2[\mu_3\text{-}\eta^2\text{-}NHC_3N_3(NH_2)_2]$ and the isomeric bimetallated species *cis*-$[Ru_3(CO)_9(\mu\text{-H})]_2[\mu_3\text{-}\eta^2\text{:}\mu_3\text{-}\eta^2\text{-}NHC_3N_3(NH_2)]$ and *trans*-$[Ru_3(CO)_9(\mu\text{-H})]_2[\mu_3\text{-}\eta^2\text{:}\mu_3\text{-}\eta^2\text{-}NHC_3N_3(NH_2)]$. The molecular structures of all three products have been determined by X-ray analysis [87]. The cluster compound $[PPN][Ru_8(CO)_{22}(\mu_8\text{-P})]$ has been isolated in fair yield from the reaction between $Ru_3(CO)_{10}(\mu\text{-H})(\mu\text{-}NC_5H_4)$ and Ph_2PCl in refluxing chlorobenzene. ^{31}P-NMR data reveal the presence of two isomers in solution, presumably due to differing carbonyl distributions. The X-ray structure confirms that the phosphorus atom occupies an interstitial square antiprismatic site defined by the eight ruthenium atoms. The multiple redox waves observed in the cyclic voltammogram of the Ru_8 cluster are discussed with respect to the electron deficiency predicted by Wade's rules [88]. Photolysis of $M_3(CO)_{12}$ (where M = Ru, Os) with pyrazole, 3,5-dimethylpyrazole and 3,5-diphenylpyrazole gives a variety of products. The X-ray structure of $HOs_3(CO)_{10}(C_3HMe_2N_2)$ has been solved [89]. The binuclear and tetranuclear complexes $Ru_2(CO)_6(\mu\text{-H})[\mu\text{-}\eta^3\text{-PhC=CHC(O)NRR}']$ and $Ru_4(CO)_{10}(\mu_3\text{-H})_2[\mu\text{-}\eta^3\text{-PhC=CHC(O)NRR}']$ have been obtained from the thermolysis of $Ru_3(CO)_{12}$ with *N*-substituted cinnamic acid amides PhCH=CHCONRR′. The X-ray structures of two derivatives and the thermally promoted transformations exhibited by these compounds are fully discussed [90].

Protonation of the phosphine-substituted clusters $Ru_3(CO)_8(\mu\text{-H})(\mu\text{-N=CPh}_2)(\mu\text{-dppm})$, $Ru_3(CO)_9(\mu\text{-H})(\mu\text{-N=CPh}_2)(PPh_3)$ and $Ru_3(CO)_8(\mu\text{-H})(\mu\text{-N=CPh}_2)(PPh_3)_2$ takes place at the ruthenium atoms to give the corresponding cationic dihydrido complexes. Extended Hückel MO calculations on the parent cluster $Ru_3(CO)_{10}(\mu\text{-H})(\mu\text{-N=CPh}_2)$ and the phosphine-substituted derivatives support the course of these reactions, as the highest occupied orbitals all show extensive metallic character [91]. A study on the reactivity of $Ru_3(CO)_{10}(\mu\text{-H})(\mu\text{-N=CPh}_2)$ with H_2, R_3SiH and R_3SnH has been published. H_2 reacts with the 1-azavinylidene cluster to give $H_4Ru_4(CO)_{12}$ and H_2NCHPh_2 as the end-products, with the imido and amido intermediates $Ru_3(CO)_9(\mu\text{-H})_2(\mu_3\text{-NCHPh}_2)$ and $Ru_3(CO)_{10}(\mu\text{-H})(\mu_3\text{-NHCHPh}_2)$, respectively, being observed during the reaction. While no reaction was observed

between the starting cluster and tertiary organosilanes, R_3SnH (where R = Ph, Bu) readily reacts to afford $Ru_3(CO)_9(\mu\text{-}H)_2(\mu\text{-}N{=}CPh_2)(SnR_3)$. These two organostannes were characterized in solution and by X-ray diffraction analysis in the case of the triphenylstannyl complex [92]. $Ru_3(CO)_{10}(\mu\text{-}H)(\mu\text{-}N{=}CPh_2)$ has been allowed to react with diphenylacetylene and 1-phenyl-1-propyne in refluxing 1,2-dichloroethane to give the metallacyclic derivatives $Ru_2(CO)_4(\mu\text{-}CO)[\mu\text{-}PhC{=}CR\text{-}CPh{=}CR\text{–}N{=}CPh(C_6H_4)]$. These reactions represent the first examples involving the insertion of weakly electrophilic alkynes into Ru–N bonds. At lower temperature these reactions proceed via cluster fragmentation and alkyne insertion into the Ru–H bond, giving the binuclear alkenyl complexes $Ru_2(CO)_6(\mu\text{-}RC{=}CHR')(\mu\text{-}N{=}CPh_2)$. Three X-ray structures and reaction schemes illustrating these transformation are presented [93].

$Os_3(CO)_{10}(MeCN)_2$ reacts with thiazole at ambient temperature to give the isomeric clusters $Os_3(CO)_{10}(\mu\text{-}H)(\mu\text{-}2,3\text{-}\eta^2\text{-}\overline{C{=}NCH{=}CHS})$ and $Os_3(CO)_{10}(\mu\text{-}H)(\mu\text{-}3,4\text{-}\eta^2\text{-}\overline{HC{=}NC{=}CHS})$ in 20 and 60% yields, respectively. PPh_3 and $P(OMe)_3$ react with the latter cluster at 110°C to afford the substitution products $Os_3(CO)_9P(\mu\text{-}H)(\mu\text{-}3,4\text{-}\eta^2\text{-}\overline{HC{=}NC{=}CHS})$, which exist as a mixture of two isomers in solution. The former $Os_3(CO)_{10}$ cluster reacts with PPh_3 under analogous conditions to give an isomeric mixture of $Os_3(CO)_{10}(PPh_3)(\mu\text{-}H)(\mu\text{-}2,3\text{-}\eta^2\text{-}\overline{C{=}NCH{=}CHS})$ in solution. The X-ray structure of this last cluster and the aforementioned $P(OMe)_3$ derivative accompany this paper [94]. A study dealing with the solution dynamics of adduct formation and electronic communication between a bridging quinoline ligand and an Os_3 core has been published. Ammonia and aliphatic amines have been allowed to react with the electron-deficient clusters $Os_3(CO)_9(\mu\text{-}H)(\mu_3\text{-}\eta^2\text{-}C_9H_6N)$ and $Os_3(CO)_9(\mu\text{-}H)(\mu_3\text{-}\eta^2\text{-}XC_9H_5N)$ (where X = 5-NH_2, 3-NH_2, 6-NH_2, 5-Br, 5-Me) to initially give addition adducts that isomerize to a mixture of two isomers whose ratio is dependent on the cluster, amine and solvent. The thermodynamic values $\Delta H°$ and $\Delta S°$ have been calculated for each isomer equilibrium via VTNMR studies. The major cause for the change in the isomer ratio stems come from the changes in $\Delta S°$ as a result of solvation effects. The protonation of several of these clusters with coordinating (TFA) and non-coordinating acids (HBF_4) yields cationic dihydrido clusters that have been explored by NMR techniques [95]. $Ru_3(CO)_{10}(\mu\text{-}dppm)$ has been allowed to react with quinolines to furnish $Ru_3(\mu\text{-}CO)(CO)_7(\mu_3\text{-}\eta^2\text{-}PPhCH_2PPh_2)[\mu\text{-}\eta^2\text{-}C_9H_5(R)N]$ (where R = 4-Me, H) as the major product and minor amounts of the known cluster $Ru_3(CO)_9[\mu_3\text{-}\eta^3\text{-}PPhCH_2PPh_2(C_6H_4)]$. The X-ray structure of the 4-Me derivative was determined. Use of 4-methylquinoline as a ligand in the reaction with $Ru_3(CO)_{10}(\mu\text{-dppm})$ leads to a quinoline-substituted cluster and the binuclear complexes $Ru_2(CO)_6[\mu\text{-}(C_6H_4)PPhCH_2PPh]$ and $Ru_2(CO)_6[\mu\text{-}CH_2PPh(C_6H_4)PPh]$ [96]. CO substitution in $Os_3(CO)_{10}(\mu\text{-}H)[\mu\text{-}1,2\text{-}\eta^2\text{-}C_9H_5(Me)N]$ by PPh_3 occurs at 110°C to give the mono- and bis-substituted clusters $Os_3(CO)_{10-n}(PPh_3)_n(\mu\text{-}H)[\mu\text{-}1,2\text{-}\eta^2\text{-}C_9H_5(Me)N]$ (where $n = 1, 2$). $P(OMe)_3$ reacts with the same starting cluster in an analogous fashion. The solution isomers of these P-substituted clusters have been examined by NMR spectroscopy and their compositions are discussed. Two X-ray structures accompany this report [97]. A paper outlining the functionalization of heterocycles by electron-deficient bonding

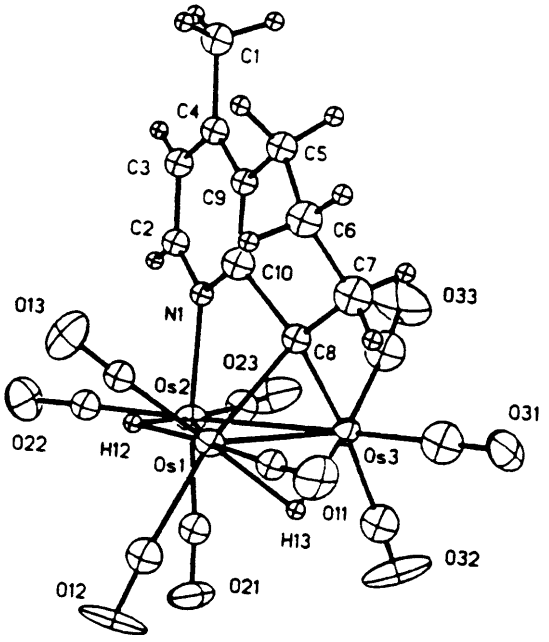

Fig. 6. X-ray structure of $Os_3(CO)_9(\mu\text{-}H)(\mu_3\text{-}\eta^3\text{-}C_9H_8N)$. Reprinted with permission from Organometallics. Copyright 1998 American Chemical Society.

to a triosmium cluster has appeared. The new methodology involves the addition of carbon-based nucleophiles to the carbocyclic ring of quinolines at the electronically deficient C(8) carbon [98]. Deuterium-labeling studies on the course of H^- and D^- attack on the electron-deficient clusters $Os_3(CO)_9(\mu\text{-}H)(\mu_3\text{-}\eta^2\text{-}C_9H_4NRR')$ indicate that the attack of hydride occurs at the 5-position of the quinoline ring. When this reaction is followed by protonation with H^+ (or D^+), reduction of the C(5)–C(6) bond is observed to give $Os_3(CO)_9(\mu\text{-}H)(\mu_3\text{-}\eta^3\text{-}C_9H_6NRR')$. The selectivity associated with ^{13}CO incorporation in these and related clusters, along with the results of cyclic voltammetric studies, are discussed. The molecular structures of $Os_3(CO)_9(\mu\text{-}H)(\mu_3\text{-}\eta^3\text{-}C_9H_8N)$ (Fig. 6), $Os_3(CO)_9(\mu\text{-}H)_2(\mu_3\text{-}\eta^2\text{-}C_9H_7N)$, $Os_3(CO)_9(\mu\text{-}H)(\mu_3\text{-}\eta^2\text{-}C_9H_8N)$ and $Os_3(CO)_9(\mu\text{-}H)[P(OEt)_3][\mu\text{-}\eta^2\text{-}(4\text{-}Me)C_9H_5N]$ have been determined by X-ray crystallography [99].

Tetramethylthiourea and H_2O react with $Os_3(CO)_{12}$ in a methanol solution of Me_3NO at 80°C to furnish the known cluster $Os_3(CO)_9(\mu\text{-}OH)(\mu\text{-}OMeCO)[\eta^1\text{-}SC(NMe_2)_2]$ and the new sulfido-capped cluster $Os_3(CO)_8(\mu\text{-}H)(\mu_3\text{-}S)(\mu\text{-}OMeCO)[\eta^1\text{-}SC(NMe_2)_2]$. Carrying out this reaction without tetramethylthiourea leads to the new cluster $Os_3(CO)_{10}(\mu\text{-}OH)(\mu\text{-}OMeCO)$ and the known complexes $Os_3(CO)_{10}(\mu\text{-}H)(\mu\text{-}OMe)$ and $Os_3(CO)_{10}(\mu\text{-}H)(\mu\text{-}OH)$. The reactivity of the monosubstituted derivatives under comparable conditions has been explored, and the solution isomers of $Os_3(CO)_8(\mu\text{-}H)(\mu_3\text{-}S)(\mu\text{-}OMeCO)(PPh_3)$ have been studied by spectroscopic methods. Two X-ray structures have been solved and the adopted

polyhedral shapes are discussed relative to other clusters [100]. Heating the indenyl complex (η^5-ind)Ru(SEt)(PPh_3) in toluene gives the triruthenium cluster [(η^5-ind)Ru(SEt)]$_3$, which contains bridging ethanethiolato and indenyl ligands. This cluster reacts with MeI at one of the ethanethiolate ligands to give [(η^5-ind)$_3$Ru$_3$(μ-SEt)$_2$(μ-SEtMe)][I] with high stereoselectivity via attack of the MeI on the axial SEt ligand from the equatorial side. Treatment of this anionic cluster with CO produces [(η^5-ind)$_2$Ru$_2$(μ-SEt)(CO)$_4$]$^+$. CO also reacts with the neutral Ru_3 cluster to give (η^5-ind)$_3$Ru$_3$(μ-SEt)$_3$(μ-CO)(CO) and [(η^5-ind)Ru(μ-SEt)(CO)]$_2$. Hapticity changes in the indenyl ligand are believed to play a crucial role in these transformations. Mechanistic schemes are fully discussed [101]. The spectroscopic detection of an intermediate having an agostic Os–H–S interaction in the addition of thiols to Os_3 clusters has been reported. The reaction between $Os_3(CO)_{11}$(MeCN) and *para*-thiocresol and other thiols proceeds via a two-step consecutive process, with each individual step being dissociative in nature. The first step of the reaction involves the generation of the labile and unsaturated cluster $Os_3(CO)_{11}$, which is then free to react with added thiol to give $Os_3(CO)_{11}$(RSH). CO loss from this species generates the sulfido derivative $Os_3(CO)_{10}$(μ-H)(μ-SR) [102]. A report describing the concept of a 'molecular-scale wire' linked to an Os_3 cluster was published. Attachment of (*p*,*p*)-HSC$_6$H$_4$C≡CC$_6$H$_4$C≡CC$_6$H$_5$ to $Os_3(CO)_{10}(MeCN)_2$ leads to the thiol-terminated cluster $Os_3(CO)_{10}$(μ-H)(μ-SC$_6$H$_4$C≡CC$_6$H$_4$C≡CC$_6$H$_5$). This cluster, with its pendant organic residue, serves as a model compound that has a molecular wire attached to a metallic surface. The X-ray structure confirms the bridging nature of the coordinated thiol to one edge of the triangular Os_3 frame [103]. $Ru_3(CO)_{12}$ reacts with thiazole (one equivalent) in the presence of sodium benzophenone ketyl to afford $Ru_3(CO)_{10}$(μ-H)(μ-2,3-η^2-C=NCH=CHS). Use of excess thiazole produces $Ru_3(CO)_8$(μ-H)(μ-2,3-η^2-$\overline{\text{C=NCH=CHS}}$)$_2$ and $Ru_3(CO)_9$(μ-H)(μ_5-η^5-H-$\overline{\text{C=NC=CHS}}$)Ru$_2(CO)_4$($\mu$-H)($\eta^1$-H$\overline{\text{C=NCH=CHS}}$)($\mu$-2,3-$\eta^2$-$\overline{\text{C=NCH=CHS}}$). The X-ray structure of this latter cluster contains a ring-opened thiazole that serves to bridge the Ru_3 and Ru_2 moieties [104]. The cleavage of C–S bonds in benzothiophene and dibenzothiophene by a Ru_3 cluster is reported. Treatment of $Cp^*_3Ru_3$(μ-H)$_3$(μ_3-H)$_2$ with benzothiophene at 50°C gives the μ_3-sulfido-μ_3-alkylidyne cluster (Cp*Ru)$_3$(μ-H)$_2$(μ_3-S)(μ_3-CCH$_2$C$_6$H$_5$) in quantitative yield. Definitive proof for the successive cleavage of two C–S bonds was ascertained by X-ray diffraction analysis of the product (Fig. 7). An intermediate thiaruthenacycle was isolated and shown to be a precursor to the end-product. The kinetics and activation parameters for this reaction are reported, and the large negative $\Delta S^{\neq}$ value is consistent with a reaction at a (Cp*Ru)$_3$ unit that requires an intimate fitting between the substrate and the Ru_3 reaction site [105].

Hydrogenolysis of the acetate group in Ru$_2$(CO)$_4$(OAc)$_2$(PR$_3$)$_2$ by H_2 has been investigated in the presence of Na_2CO_3 as a function of temperature. The products isolated at the end of the reaction are H$_4$Ru$_4$(CO)$_9$(PR$_3$)$_3$, H$_4$Ru$_4$(CO)$_8$(PR$_3$)$_4$ and H$_2$Ru$_2$(CO)$_2$(PR$_3$)$_2$. The tris-substituted cluster originates from H$_4$Ru$_4$(CO)$_8$(PR$_3$)$_4$ and CO, and the CO is produced from CO_2 by the reverse water–gas shift reaction, which is catalyzed by the ruthenium complexes. The CO_2 arises from the released AcOH and its reaction with Na_2CO_3 [106]. Aqueous phase hydrogenation of

cyclohexene has been achieved using $(\eta^6\text{-}C_6H_6)_2Ru_2Cl_4$ as a catalyst precursor. The catalyst solutions were shown to contain the tetraruthenium cations $[(\eta^6\text{-}C_6H_6)_4Ru_4H_4]^{2+}$ and $[(\eta^6\text{-}C_6H_6)_4Ru_4H_6]^{2+}$, both of which exhibit lower hydrogenation activity compared to the catalyst precursor. ^{1}H-NMR spectroscopy has detected a species under autogeneous catalysis that was identified as $[(\eta^6\text{-}C_6H_6)_3Ru_3(\mu_2\text{-}Cl)(\mu_3\text{-}O)(\mu_2\text{-}H)_2]^+$ [107]. The X-ray structures of [Crypt221-Na]$_2$[$H_2Ru_4(CO)_{12}$] and [Crypt222-K]$_2$[$Ru_4(CO)_{13}$] were solved and contrasted with the structures of other tetranuclear hydrido clusters of Group 8 and their conjugate bases. Both of these clusters exhibit a tetrahedral core of ruthenium atoms [108]. The ethynediyl complex $Cp^*(CO)_2Fe\text{–}C{\equiv}C\text{–}FeCp^*(CO)_2$ reacts with $Fe_2(CO)_9$ to afford the tetrairon dicarbide complex $(\mu_4\text{-}C_2)Fe_4Cp^*_2(CO)_9$, which reveals dynamic behavior in the form of reversible scission and recombination of the Fe–Fe bonds. The butadiyne diyl complex $Cp^*(CO)_2Fe\text{–}C{\equiv}C\text{–}C{\equiv}C\text{–}FeCp^*(CO)_2$ undergoes a similar reaction to give the corresponding tetrairon nona- and decacarbonyl complexes [109]. Thermolysis of $Cp_2Fe_2(CO)_4$ and PPh_3 in xylene yields as the major product $Cp_4Fe_4(CO)_4$, along with minor amounts of $(C_5H_4Ph)Cp_3Fe_4(CO)_4$ and $Cp_3Fe_3(CO)_3(PPh_2)$. It was found that $Cp_4Fe_4(CO)_4$ may be alkylated and arylated by using organolithium reagents to afford $(C_5H_4R)Cp_3Fe_4(CO)_4$. The functionalization reaction is in competition with reduction of the starting cluster by RLi. A higher yielding functionalization route free of the redox sequence involves the deprotonation of $Cp_4Fe_4(CO)_4$ using LDA, followed by treatment with elec-

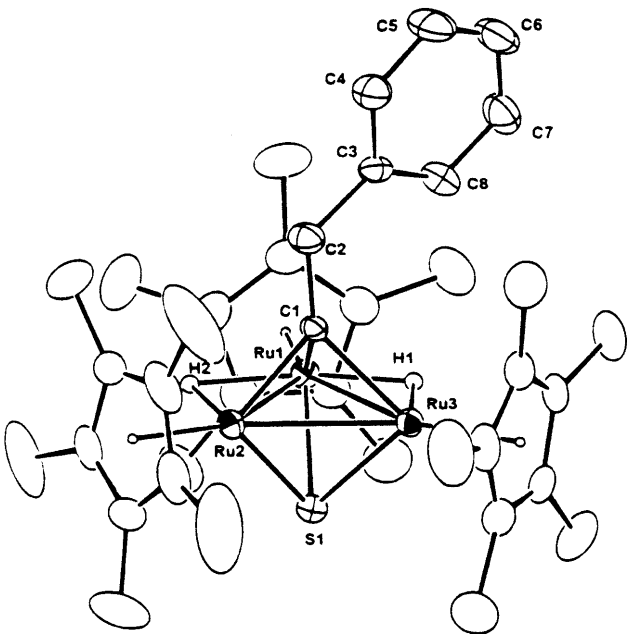

Fig. 7. X-ray structure of $(Cp^*Ru)_3(\mu\text{-}H)_2(\mu_3\text{-}S)(\mu_3\text{-}CCH_2C_6H_5)$. Reprinted with permission from Journal of American Chemical Society. Copyright 1998 American Chemical Society.

trophiles, to give the mono-substituted Cp cluster. Use of excess LDA allowed for the formation of bi- and trifunctionalized derivatives. The X-ray structures of $[(C_5H_4)Cp_3Fe_4(CO)_4]_2CHOH$ and $(C_3H_4PPh_2)Cp_3Fe_4(CO)_4RuCl_2$(cymene) have been solved [110]. The reductive coupling of the carbonyl ligands in the reaction between $Cp_4Fe_4(CO)_4$ and $LiAlH_4$ in THF is reported. The major product from this reaction is the nonsubstituted acetylene-coordinated cluster $Cp_4Fe_4(HC{\equiv}CH)_2$. X-ray structural analysis reveals an Fe_4 polyhedron consisting of a puckered rhombus, where the acetylene ligands are bound in a μ_4-η^2:η^2:η^2:η^2 fashion. Cyclic voltammetric data reveal the presence of three reversible or quasireversible one-electron oxidation waves and one irreversible one-electron reduction wave for the $+3/+2$, $+2/+1$, $+1/0$ and 0/-1 redox couples, respectively. $(MeCp)_4Fe_4(CO)_4$ reacts similarly to furnish the corresponding bis-acetylene cluster [111].

The monoanionic cluster $[HOs_3(CO)_{11}]^-$ has been allowed to react with the cationic complex $[CpRu(MeCN)_3]^+$ to produce the mixed-metal cluster $CpRuOs_3(CO)_{11}H$ in high yield. Deprotonation using DBU, followed by treatment with additional $[CpRu(MeCN)_3]^+$, gives the pentanuclear cluster $Cp_2Ru_2Os_3$-$(CO)_9(\mu_3\text{-}CO)_2$. Parallel reactions using the dianionic cluster $[Os_3(CO)_{11}]^{2-}$ also gave the same Ru_2Os_3 product. Both product clusters have been fully characterized in solution and by X-ray diffraction analysis. The solid-state structure of $Cp_2Ru_2Os_3(CO)_9(\mu_3\text{-}CO)_2$ shows a Ru_2Os_3 core that is based on a trigonal bipyramid, but this structure may also be viewed as an Os_3Ru tetrahedron with the second CpRu fragment capping an Os_2Ru triangular face [112]. The dinuclear compound $Ru_2(CO)_4(O_2CH)_2(PCy_2H)_2$ reacts with H_2 to give the tetranuclear clusters $H_4Ru_4(CO)_8(PCy_2)_4$ (64e) and $H_5Ru_4(CO)_8(PCy_2)_3$ (62e). Both clusters exhibit a square-planar arrangement of ruthenium atoms, as determined by X-ray analysis. The adopted polyhedral shapes are discussed with respect to PSEP theory and other structurally characterized clusters having similar electron counts [113]. The results of VT, MAS and wide-line solid-state NMR measurements are reported for $H_4Ru_4(CO)_{12}$ and $H_4Ru_4(CO)_{11}[P(OMe)_3]$. Both samples exhibit similar hydride motion, on the basis of spin-lattice relaxation times (T_1) and linewidths at $\Delta\nu_{1/2}$. The hydride motion is attributed to a 2-site H-flip about H-occupied Ru–Ru edges that preserves the site symmetry of the crystals [114]. The reaction between the clusters $H_4Ru_4(CO)_{12}$ and $HRuCo_3(CO)_{12}$ with added tris(2-thienyl)phosphine has been examined. The clusters $H_4Ru_4(CO)_{11}[P(thienyl)_3]$, $HRuCo_3(CO)_{11}[P(thienyl)_3]$ and $H_4Ru_4(CO)_{10}(S_2C_4H_8)$ were isolated and structurally characterized. Only the phosphorus atom was coordinated to a metal center in the former two examples [115]. The reversible triple CO addition to $Ru_4(CO)_9(\mu\text{-}PPh_2)[\mu\text{-}Ph_2PPCC$-(Ph)CC(Ph)] has been observed to give $Ru_4(CO)_{11}(\mu\text{-}PPh_2)[\mu_4\text{-}Ph_2PC(O)CC(Ph)$-CC(Ph)], whose X-ray structure is shown in Fig. 8. The starting Ru_4 cluster employed in the carbonylation reaction was isolated from the thermolysis reaction of $Ru_2(CO)_6(\mu\text{-}PPh_2)(\mu\text{-}\eta^1\text{:}\eta^2\text{-}C{\equiv}CPh)$ as the major product. The minor product was found to be $Ru_4(CO)_9(\mu\text{-}PPh_2)[\mu_4\text{-}Ph_2PC(Ph)CCC(Ph)]$. The X-ray structures of these two Ru_4 clusters confirm the head-to-tail and head-to-head coupling of the binuclear acetylides, respectively. The major product of the coupling reaction exhibits a spiked-triangular structure while the minor product shows an open-chain frame [116].

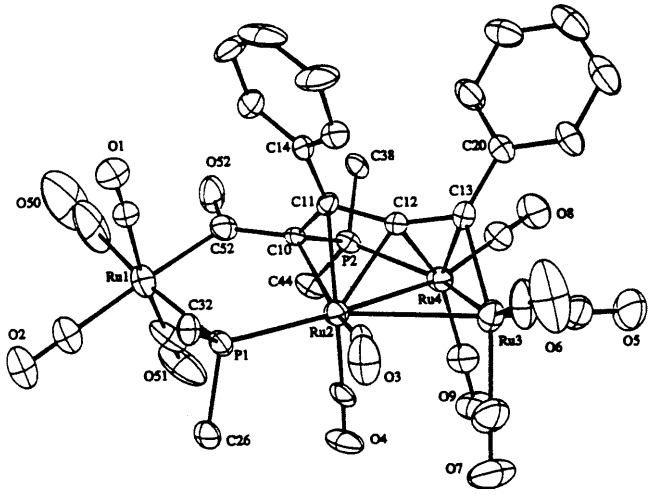

Fig. 8. X-ray structure of $Ru_4(CO)_{11}(\mu\text{-}PPh_2)[\mu_4\text{-}Ph_2PC(O)CC(Ph)CC(Ph)]$. Reprinted with permission from Organometallics. Copyright 1998 American Chemical Society.

Treatment of $[Ru_4(CO)_{12}(\mu_3\text{-}PPh)]^{2-}$ and $[Ru_4(CO)_{12}]^{4-}$ with $Cl_2PN^iPr_2$ yields $Ru_4(CO)_{10}(\mu\text{-}CO)(\mu_4\text{-}PPh)(\mu_4\text{-}PN^iPr_2)$ and $Ru_4(CO)_{12}(\mu_4\text{-}PN^iPr_2)_2$, respectively. The dianion was generated from the reduction of $Ru_4(CO)_{13}(\mu_4\text{-}PPh)$ by cobaltocene, and X-ray analysis of the dianion revealed relatively small structural changes as a result of electron accession. The two product clusters were structurally characterized and their molecular structures are discussed relative to the cluster electron count. In the case of $Ru_4(CO)_{12}(\mu_4\text{-}PN^iPr_2)_2$, the internuclear μ_4-P–μ_4-P distance of 3.152 Å is the longest value reported to date for a bisphosphinidene-capped M_4P_2 cluster [117]. The reaction between the three isomeric tertiary phosphines diphenyl-*n*-pyrrolylphosphine (where $n = 1, 2, 3$) and $Ru_3(CO)_{12}$ affords the isomeric clusters $Ru_4(CO)_{11}(\mu_4\text{-}PPh)(\mu_4\text{-}C_4H_3N)$, which possess diagonal C,C bonded and parallel C,N bonded pyrrolyne moieties. The formation of these Ru_4 clusters from a Ru_3 cluster with a metallated pyrrolyl ring is presented along with two X-ray structures [118]. The synthesis, X-ray structures and (spectro)electrochemical studies of $Ru_4(CO)_{10}(\mu\text{-}H)_4L$ (where L = bpym, dpp, bpy) have been published. VT ^{1}H-NMR measurements have been carried out in order to study the fluxional behavior associated with the hydride ligands of these three clusters. One-electron reduction of the bpym and dpp derivatives yields the corresponding radical anions, which have been characterized by IR, UV–vis and EPR spectroscopy. These data support a dominantly L(π^*)-localized LUMO. Use of the stronger σ-donor ligand bpy yields a radical anion complex that is only detectable on the sub-second time scale of cyclic voltammetry [119]. Tolylacetylene reacts with $Ru_3(CO)_9(\mu_3\text{-}CO)(\mu_3\text{-}NOMe)$ in refluxing octane to furnish the nitrene-substituted clusters $Ru_4(CO)_9(\mu\text{-}CO)_2(\mu_4\text{-}NH)(\mu_4\text{-}\eta^2\text{-}HC_2Tol)$ and $Ru_4(CO)_9(\mu\text{-}CO)_2[\mu_4\text{-}NC(O)OMe](\mu_4\text{-}\eta^2\text{-}HC_2Tol)$. The X-ray structures of both Ru_4 clusters reveal a slightly twisted square-base polyhedron [120].

The clusters $H_4Ru_4(CO)_{12}$ and $HRuCo_3(CO)_{12}$ have been allowed to react with 3-methyl-2-benzothiazolinethione [PhNMeC(S)S] to give the trinuclear clusters $Ru_3(CO)_8(\mu_3\text{-}S)(\eta^1\text{-}L)$ and $RuCo_2(CO)_8(\mu_3\text{-}S)(\eta^1\text{-}L)$. The molecular structure of each product was determined by X-ray crystallography [121]. The thermal reaction of $Fe_3(CO)_9Te_2$ with $Fe_2(CO)_9$ and photolysis of $Fe_3(CO)_9Te_2$ with $Fe(CO)_5$ lead to $Fe_4(CO)_{10}(\mu_2\text{-}CO)(\mu_4\text{-}Te)_2$. The planar array of iron atoms was ascertained by X-ray diffraction analysis. The Mössbauer data on the Fe_4Te_2 cluster show two doublets whose nearly equal intensities confirm the existence of two equipopulated crystallographic sites of iron [122]. The cubane-type Ru_4 sulfido cluster $(Cp^*Ru)_4(\mu_3\text{-}S)_4$ has been synthesized from the dinuclear complex $Cp^*RuCl(\mu_2\text{-}SH)_2RuClCp^*$ upon treatment with Et_3N. The new cluster $(Cp^*Ru)_2(\mu_3\text{-}S)_2(\mu_2\text{-}H)RuCl(PPh_3)_2$ has been isolated from the reaction between the thiol-bridged dimer and $RuH_2(PPh_3)_4$. The X-ray structure of this Ru_3 cluster (Fig. 9) exhibits a triangular metal core capped by two μ_3-S ligands. This same cluster reacts with $NaBH_4$ to give the corresponding dihydride cluster $(Cp^*Ru)_2(\mu_3\text{-}S)_2(\mu_2\text{-}H)RuH(PPh_3)_2$, which when treated with CO is converted into the dicarbonyl cluster $(Cp^*Ru)_2(\mu_3\text{-}S)_2Ru(CO)_2(PPh_3)_2$. The X-ray structures of these latter two Ru_3 clusters are included in this report [123].

An article describing the structural chemistry of penta- and hexanuclear ruthenium and osmium clusters that contain an ancillary arene (η^6-Ar) or cyclopentadienyl (η^5-Cp) ligand(s) has been published. The X-ray structural data are compared and contrasted with those of related binary carbonyl and carbonyl hydride clusters. The steric and electronic factors that determine the position of the M(η^6-Ar) or M(η^5-Cp) units within the polyhedral framework are discussed. The adopted metal

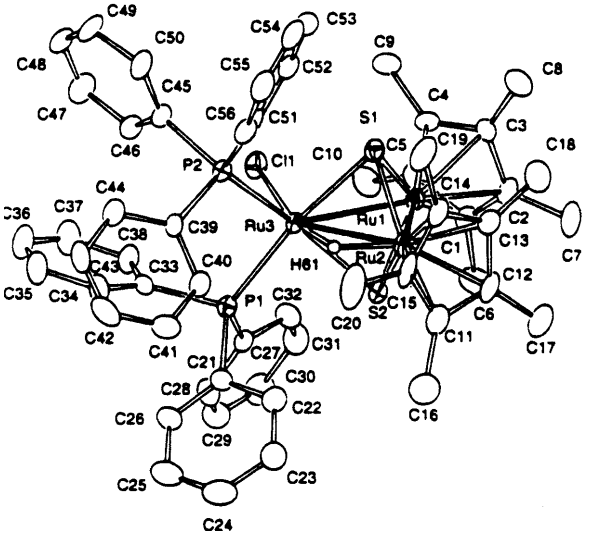

Fig. 9. X-ray structure of $(Cp^*Ru)_2(\mu_3\text{-}S)_2(\mu_2\text{-}H)RuCl(PPh_3)_2$. Reprinted with permission from Organometallics. Copyright 1998 American Chemical Society.

core geometries for these M_5 and M_6 clusters are also discussed [124]. Structural data on substituted Ru_5 carbido clusters have been published [125]. An example of a cluster containing a μ_4-PO ligand has been published. Treatment of $Ru_4(CO)_{13}(\mu_3\text{-}PNCy_2)$ with $Ru(CO)_5$ gives $Ru_5(CO)_{15}(\mu_4\text{-}PNCy_2)$ in high yield, which when treated with $HBF_4{\cdot}Et_2O$ yields $Ru_5(CO)_{15}(\mu_4\text{-}PF)$. This is the first example of a cluster having a capping μ_4-fluorophosphinidene ligand. If $Ru_5(CO)_{15}(\mu_4\text{-}PNCy_2)$ is treated with $HBF_4{\cdot}Et_2O$ in refluxing CH_2Cl_2, an extremely different course of reaction is observed, with the cluster $[Ru_5(CO)_{15}(\mu_4\text{-}P{=}O)][H_2NCy_2]$ being isolated as the major product. The X-ray structures of both μ_4-PX capped clusters consist of a square based pyramid of five ruthenium atoms, with the square face capped by either the μ_4-PF or μ_4-P=O groups [126]. The use of the open pentaruthenium cluster $Ru_5(\mu_5\text{-}C_2)(\mu\text{-}SMe)_2(\mu\text{-}PPh_2)_2(CO)_{11}$ as a template for the aggregation of additional iron and ruthenium carbonyls is discussed. The new metals add to the C_2 ligand to afford a series of higher nuclearity clusters. The X-ray structures of $MRu_5(\mu_6\text{-}C_2)(\mu\text{-}SMe)_2(\mu\text{-}PPh_2)_2(CO)_{14}$ and $M_2Ru_5(\mu_6\text{-}C_2)(\mu_3\text{-}SMe)_2(\mu\text{-}PPh_2)(\mu\text{-}CO)(CO)_{15}$ (where M = Fe, Ru) have been determined and the polyhedral shapes discussed. The cores of the MRu_5 clusters are constructed of two edge-sharing squares, which give rise to a permetallabicyclo[2.2.0]hexane skeleton. In the case of the M_2Ru_5 clusters, the additional M atom bridges an outer edge of one of the squares [127]. Carbonyl substitution chemistry at ruthenium clusters bearing a dicarbide ligand is described. The addition of CN^{t}Bu to $Ru_5(\mu_5\text{-}C_2)(\mu\text{-}SMe)_2(\mu\text{-}PPh_2)_2(CO)_{11}$ proceeds to yield $Ru_5(\mu_5\text{-}C_2)(\mu\text{-}SMe)_2(\mu\text{-}PPh_2)_2(CO)_{11}(CN^tBu)$, whose X-ray structure reveals a flattened Ru_5 pentagon and elongated Ru–Ru separations. The addition adduct loses CO upon heating to furnish the corresponding decacarbonyl species with a restored cluster geometry. The related hexaruthenium cluster $Ru_6(\mu_6\text{-}C_2)(\mu_3\text{-}SMe)_2(\mu\text{-}PPh_2)_2(CO)_{14}$ reacts with Me_3NO/MeCN to give the acetonitrile-substituted cluster, which undergoes reaction with added phosphines to give P-ligand substituted clusters. Whereas $BuNH_2$ reacts with the original Ru_5 cluster to produce $Ru_5(\mu_5\text{-}C_2)(\mu\text{-}SMe)_2(\mu\text{-}PPh_2)_2(CO)_{10}(NH_2Bu)$, the use of secondary and tertiary amines leads to the known cluster $Ru_5(\mu_5\text{-}CCH_2)(\mu\text{-}SMe)_2(\mu\text{-}PPh_2)_2(CO)_{10}$ [128]. New face-coordinated C_{60} complexes of pentaruthenium carbide clusters have been prepared and structurally characterized. Some of the clusters used in this study include $Ru_5C(CO)_{15}$, $Ru_5C(CO)_{14}(PPh_3)$, $Ru_5C(CO)_{13}$(P–P) (where P–P = dppe, dppf), $PtRu_5C(CO)_{16}$ and $PtRu_5C(CO)_{14}$(cod). Six X-ray structures were solved, and the robust nature of the C_{60}–Ru_5C and C_{60}–$PtRu_5C$ bonding in the fullerene-substituted clusters is discussed [129].

The synthesis, isolation and structural characterization of $[2_n]$cyclophane clusters have been published as a feature article. The use of alternating cyclophane and cluster subunits as precursors to novel organometallic polymer chains and networks is described [130]. The redox behavior of $Ru_6C(CO)_{17}$ and $[Ru_6C(CO)_{16}]^{2-}$ was investigated by cyclic voltammetry and in situ spectroelectrochemistry methods. In the absence of O_2, $Ru_6C(CO)_{17}$ is reduced to $[Ru_6C(CO)_{16}]^{2-}$. Carrying out the reduction in the presence of O_2 leads to 1.1–1.3 mol of CO_2 per mol of cluster, in addition to the dianion and some cluster fragmentation products. Electrochemical mechanisms are discussed, and the intervention of a peroxy-carbonate ligand as the

source of CO_2 is outlined [131]. The electrophilic reactivity of arene ligands coordinated to Ru_6 carbido clusters has been published. The addition of RLi (where R = Ph, Me) to $Ru_6C(CO)_{14}(\eta^6\text{-}C_6H_6)$ and $Ru_6C(CO)_{12}(\eta^6\text{-}C_6H_6)(\mu_2\text{-}\eta^2\text{:}\eta^2\text{-}C_6H_8)$, gives $Ru_6C(CO)_{14}(\eta^4\text{-}C_6H_6R_2)(AuPPh_3)_2$ and $Ru_6C(CO)_{12}(\eta^5\text{-}C_6H_6R)(\mu_2\text{-}\eta^2\text{:}\eta^2\text{-}C_6H_8)(AuPPh_3)$, respectively, after treatment with $AuCl(PPh_3)/TlPF_6$. The intermediate anions may be treated with [trityl][BF_4] to furnish the corresponding substituted arene clusters $Ru_6C(CO)_{14}(\eta^6\text{-}C_6H_4R_2)$ and $Ru_6C(CO)_{12}(\eta^6\text{-}C_6H_5R)(\mu_2\text{-}\eta^2\text{:}\eta^2\text{-}C_6H_8)$. The crystal and molecular structures of $Ru_6C(CO)_{14}(\eta^6\text{-}C_6H_4Ph_2)$ and the two polymorphs of $Ru_6C(CO)_{14}(\eta^6\text{-}C_6H_4Me_2)$ are reported [132]. Cluster build-up reactions using $Ru_3(CO)_{12}$ are presented. Broad-band UV photolysis of $Ru_3(CO)_{12}$ in the presence of ethylene furnishes $Ru_6C(CO)_{17}$. A scheme showing the course of the reaction is presented, and it is suggested that the carbide ligand originates from a coordinated CO group and not ethylene, which serves to stabilize the coordinatively unsaturated ruthenium intermediates formed in the reaction [133]. $Ru_6C(CO)_{17}$ reacts with cyclohepatriene to give several products that have been characterized in solution and by X-ray crystallography in the case of $Ru_6(CO)_{15}$(ethylenenorbornadiene), $Ru_6C(CO)_{14}(C_7H_8)$ and $Ru_6C(CO)_{11}(\eta^5\text{-}C_7H_9)(\mu_3\text{-}\eta^2\text{:}\eta^2\text{:}\eta^3\text{-}C_7H_7)$. These latter two clusters demonstrate the coordination variability of the carbocyclic rings based on the C_7 frame. The source of the two extra carbon atoms in the ethylenenorbornadiene ligand originates from C_7H_9 by an unknown process [134]. New Ru_6 and Ru_7 clusters have been obtained from the reaction between $Ru_3(CO)_{12}$ and 1,1-diphenylethylene. The three ruthenium clusters isolated were $Ru_6C(CO)_{14}(\eta^6\text{-}PhCHMePh)$, $Ru_6C(CO)_{14}(\eta^6\text{-}PhC{=}CH_2Ph)$ and $Ru_7C(CO)_{14}(\mu_3\text{-}\kappa\text{:}\eta^6\text{:}\eta^6\text{-}C_6H_4CH_2C_6H_4)$. The X-ray structure of the last cluster confirms it as the first example of a cluster chelated by a diphenyl ligand, in addition to it being a rare example of a Ru_7C 'spiked' cluster that shows a packing motif made up of interlocking snakes of molecules, which exhibit two dominant interactions that extend along the '*a*' axis [135]. The coupling of an alkyl cyanide with 7-azaindole has been achieved on a hexaosmium cluster. Treatment of $Os_6(CO)_{16}(NCR)_2$ (where R = Me, Et) with 7-azaindole leads to $Os_6(CO)_{14}(\mu\text{-}CO)(\mu\text{-}H)(\mu\text{-}\eta^1\text{:}\eta^2\text{-}C_8H_5N_3)(R)$. The coupling reaction was ascertained by the solution characterization of the two products and the X-ray structure of the acetonitrile-derived cluster $Os_6(CO)_{14}(\mu\text{-}CO)(\mu\text{-}H)(\mu\text{-}\eta^1\text{:}\eta^2\text{-}C_9H_8N_3)$, which exhibits a bicapped-tetrahedral metal core [136]. The octahedral cluster $H_2Ru_6(CO)_{18}$ undergoes spontaneous decarbonylation to give the bicapped tetrahedral cluster $H_2Ru_6(CO)_{17}$. Both of these clusters have nearly identical IR and ^{1}H-NMR spectra. $H_2Ru_6(CO)_{17}$ reacts with $BH_3{\cdot}SMe_2$ to give an improved synthesis of $H_2Ru_6(CO)_{17}B$, whose polyhedron consists of an octahedral core and an interstitial boron atom at the center of the Ru_6 core. This boride cluster fragments under high pressures of CO to furnish $HRu_4(CO)_{12}B$ and ruthenaboride clusters that were proposed to be $HRu_5(CO)_{15}B$ and $HRu_5(CO)_{16}B$ [137]. A *cis* and *trans* mixture of 3,7,11,-trimethyl-1,5,9-trithiacyclododecane ($Me_3$12S3) was allowed to react with $Ru_6(CO)_{17}(\mu_6\text{-}C)$ to yield the new cluster compounds $Ru_6(CO)_{13}[\mu\text{-}\eta^3\text{-}cis\text{-}SCH_2CHMe(CH_2SCH_2CHMe)_2CH_2](\mu_6\text{-}C)$ and two isomers of $Ru_6(CO)_{13}[\mu\text{-}\eta^3\text{-}cis\text{-}$

$SCH_2CHMe(CH_2SCH_2CHMe)_2CH_2](\mu_6\text{-}C)$. Two X-ray structures confirm that the macrocyclic ligands adopt a tridentate coordination mode [138].

CO substitution in the edge-shared bioctahedral cluster $[PPN]_2[Ru_{10}C_2(CO)_{24}]$ by nbd and PhC≡CPh has been studied. The substituted cluster $[Ru_{10}C_2(CO)_{22}(nbd)]^{2-}$ was synthesized in diglyme at 140°C and may be oxidized by $[Cp_2Fe][BF_4]$ to produce the neutral species $Ru_{10}C_2(CO)_{23}(nbd)$. This same cluster is also obtained by the direct oxidative substitution of $[Ru_{10}C_2(CO)_{24}]^{2-}$ with $[Cp_2Fe][BF_4]$ (two equivalents) in the presence of nbd. X-ray diffraction studies reveal that the nbd ligand occupies a chelating position on one of the exterior ruthenium atoms in the bifurcated $Ru_{10}C_2$ polyhedron. The analogous $[Ru_{10}C_2(CO)_{22}(Ph_2C_2)]^{2-}$ and $Ru_{10}C_2(CO)_{23}(Ph_2C_2)$ clusters were synthesized, and the alkyne was found in an 'inner' site bridging two apical ruthenium centers. These clusters were fully characterized in solution and by negative ion FAB mass spectrometry [139]. Allene reacts cleanly with $[Ru_{10}C_2(CO)_{24}]^{2-}$ in diglyme at 90°C to afford the monoallene cluster $[Ru_{10}C_2(CO)_{22}(\mu\text{-}\eta^2\text{:}\eta^2\text{-}C_3H_4)]^{2-}$. Reaction of either cluster with allene at 140°C gives the bis-allene species $[Ru_{10}C_2(CO)_{20}(\mu\text{-}\eta^2\text{:}\eta^2\text{-}C_3H_4)_2]^{2-}$ in high yield. The molecular structures of both allene-substituted clusters are based on edge-shared bioctahedra, with the allene ligand(s) serving to bridge apical positions. The solution structures and ligand dynamics of the mono- and bisallene clusters were explored by VT ^{13}C-NMR spectroscopy and ^{13}C-^{13}C COSY experiments [140]. The reversible transformation between a methylene and a methylidyne-hydride tautomer has been demonstrated in a $Ru_{10}C_2$ cluster. The oxidative substitution of $[Ru_{10}C_2(CO)_{22}(nbd)]^{2-}$ with $[Cp_2Fe][BF_4]$ in the presence of diazomethane yields the new cluster $Ru_{10}C_2(CO)_{22}(nbd)(\mu\text{-}CH_2)$. The methylene ligand symmetrically bridges two adjacent apical ruthenium centers, as confirmed by X-ray crystallography (Fig. 10). At 80°C the methylene derivative is transformed into the methylidyne tautomer, $Ru_{10}C_2(CO)_{22}(nbd)(\mu\text{-}CH)(H)$. This tautomer has been isolated and fully characterized in solution by IR and NMR spectroscopy. Thermolysis of pure $Ru_{10}C_2(CO)_{22}(nbd)(\mu\text{-}CH_2)$ or $Ru_{10}C_2(CO)_{22}(nbd)(\mu\text{-}CH)(H)$ yields a tautomeric mixture of both Ru_{10} clusters [141].

2.5. Group 9 clusters

Deprotonation of the double-bridging μ_2-methylene complex $[Cp^*_2Rh_2(\mu_2\text{-}CH_2)_2(\mu_2\text{-}SH)][BPh_4]$ with $[Cp^*_2Rh_2(\mu_2\text{-}OH)_3][BPh_4]$ leads to the sulfido-capped cluster $[Cp^*_3Rh_3(\mu_3\text{-}S)(\mu_3\text{-}\eta^2\text{-}\|\text{-}C_2H_2)][BPh_4]_2$. The acetylene forms by way of a unique C–C bond coupling and deprotonation of the μ_2-CH_2 ligands. X-ray diffraction analysis confirms the bonding mode adopted by the acetylene ligand, which represents the first example of acetylene formation from two μ_2-CH_2 ligands. The fluxional behavior of the acetylene complex in both solution and the solid state was examined by VT ^{1}H, ^{13}C and CP/MAS ^{13}C-NMR spectroscopy [142]. The coupling of two CO_2 molecules to generate oxalate ($C_2O_4^{2-}$) has been demonstrated by using the sulfido-bridged cluster $[Cp^*_3Ir_3(\mu_3\text{-}S)_2][BPh_4]_2$. Electrochemical reduction at −1.30 V (vs. Ag/AgCl) in CO_2-saturated MeCN affords oxalate and $[Cp^*_3Ir_3(CH_2CN)(\mu_3\text{-}S)_2]^+$, whose X-ray structure confirms the attachment of the

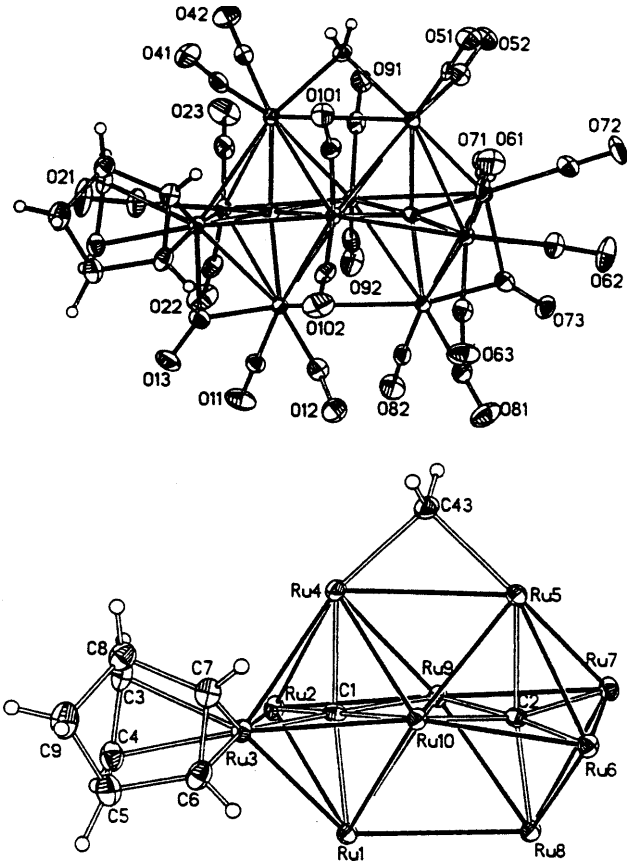

Fig. 10. X-ray structure of $Ru_{10}C_2(CO)_{22}(nbd)(\mu\text{-}CH_2)$. Reprinted with permission from Organometallics. Copyright 1998 American Chemical Society.

linear CH_2CN group to one of the Cp* rings. Here the CH_2CN unit is linked to the polyene in an *exo* fashion and the $C_5Me_5CH_2CN$ ligand is coordinated to an Ir center via an η^4-mode. The cyclic voltammetry of this novel complex under CO_2 shows a strong catalytic current due to the reduction of CO_2; the authors have proposed that this cluster functions as the active catalyst in the reduction of CO_2. A mechanism accounting for the electrochemical reduction of CO_2 is presented [143].

The face-capped arene clusters $(CpCo)_3(\mu_3\text{-}\eta^2\text{:}\eta^2\text{:}\eta^2\text{-arene})$ (where arene = various styrene derivatives and 2-phenylbut-2-ene) have been synthesized from $CpCo(ethylene)_2$ or $CpCo(C_6Me_6)$ and the appropriate arene precursor. The two X-ray structures accompany this report and the VT NMR data showing two clusters that exist as a mixture of exchanging diastereomers are presented and discussed [144]. The thermally unstable complexes isolated from the reaction between $Co_2(CO)_8$ and REER (where E = S, R = Ph, Et; E = Se, R = Ph) and assigned the structure $Co_3(CO)_9(\mu_3\text{-}ER)$ have been reformulated as $Co_3(CO)_8(R)(\mu_3\text{-}E)$, on the basis of

spectroscopic properties and their reactivity with alkynes and isocyanides. These clusters react with phenylacetylene to afford $Co_7(CO)_7[PhCCHC(O)R](\mu_3\text{-}E)$. The reaction is believed to take place by an initial R migration to produce an acyl group, which is then followed by alkyne insertion into the Co-acyl group bond. Coordination of the acyl oxygen then gives the observed five-membered metallacyclic ring. CN^{t}Bu is shown to react with these clusters in an analogous fashion. The X-ray structures of $Co_7(CO)_7[PhCCHC(O)Ph](\mu_3\text{-}S)$ and $Co_3(CO)_7(\mu\text{-}^t BuN{=}CPh)(\mu_3\text{-}S)$ have been solved, and mechanistic schemes that account for the observed alkyne and isocyanide insertion products are discussed [145]. The paramagnetic cluster $Co_3(CO)_9(\mu_3\text{-}S)$ reacts with organic compounds possessing S–H, S–S, or P–H bonds to produce the diamagnetic clusters $Co_3(CO)_7(\mu\text{-}X)(\mu_3\text{-}S)$. This oxidative substitution route represents the first successful and rational approach towards the synthesis of substituted $Co_3(CO)_9(\mu_3\text{-}S)$ clusters. The report also includes an new, high-yield synthesis of the starting cluster employing ethylene sulfide as a sulfur-transfer agent. The X-ray structures of $Co_3(CO)_7(\mu\text{-}S_2CSMe)(\mu_3\text{-}S)$ (Fig. 11) and four other new clusters have been determined [146].

In situ spectroelectrochemistry measurements have been made on $PhCCo_3(CO)_9$ in CH_2Cl_2, absolute MeOH, CO saturated MeOH and in the presence of the ligand TPPTS. The SNIFTIRS (substractively normalized interfacial FTIR spectroscopy) data have allowed for the observation of the cluster species $[PhCCo_3(CO)_9]^{-\bullet}$ (49e), $[PhCCo_3(CO)_9]^{2-}$ (50e), $[PhCCo_3(CO)_8]^{-}$ (47e) and $[PhCCo_3(CO)_8L]^{-\bullet}$ (49e). The assignment of the latter two clusters remains tentative. A scheme outlining the interrelationships between these species is presented, and it is speculated that adsorption of these clusters at the electrode surface may be responsible for the observed CO_2 formed, which is also related to the decomposition of $[Co(CO)_4]^{-}$ [147]. A report describing the use of $RCCo_3(CO)_9$ (where R = various groups) as a

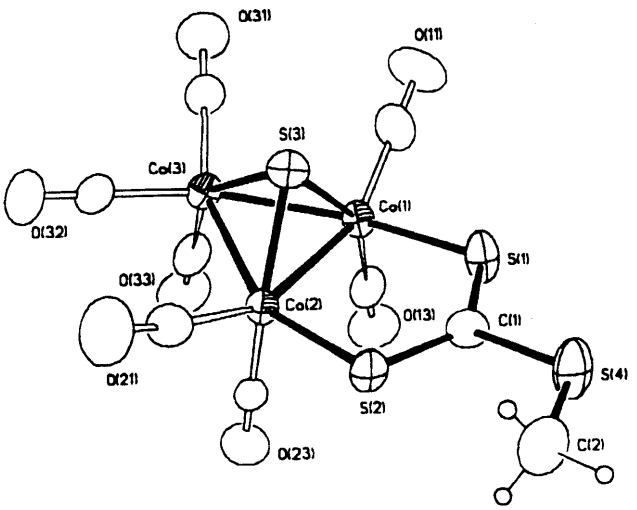

Fig. 11. X-ray structure of $Co_3(CO)_7(\mu\text{-}S_2CSMe)(\mu_3\text{-}S)$. Reprinted with permission from Organometallics. Copyright 1998 American Chemical Society.

catalyst in the Pauson–Khand reaction has appeared. The use of small capping substituents is favored for catalysis, whereas phenyl substituents were found to be detrimental to catalysis [148]. The cluster $Co_3(CO)_9[\mu_3\text{-}Si(OH)_3]$ has been employed as a single-source precursor for the construction of nanocomposite materials. Incorporation of this cluster into a silica xerogel matrix, followed by thermolysis under H_2, yields a material characterized as SiO_2 xerogel·Co_3Si [149].

A normal coordinate analysis on the bridging carbonyl groups in $M_4(CO)_{12}$ (where M = Co, Rh), $HCo_3Fe(CO)_{12}$ and $HCo_3Ru(CO)_{12}$ has been carried out, and excellent agreement between the calculated spectra and IR data collected under high resolution is observed. It is concluded that the bridging carbonyls may provide structural information about these and related clusters [150]. A report describing the application of the spherical harmonic model to the study of the terminal ν(CO) spectra of $Rh_4(CO)_{12}$ and 34 other metal carbonyl clusters has been published [151]. Experimental and theoretical studies on the site exchanges in $Rh_4(CO)_{12}$ and $IrRh_3(CO)_{12}$ are presented. The intramolecular scrambling of the ancillary CO groups proceeds by a merry-go-round process ($3\mu_2\text{-}CO \leftrightarrow 3\eta^1\text{-}CO$) about any triangular face of the cluster tetrahedron. Density functional calculations on the bridged and unbridged forms of these clusters have been performed at two levels of approximation [152]. New rhodium systems for the biphasic hydrogenation and hydroformylation of 1-hexene have been synthesized from several water-soluble phosphine ligands. One of the species observed in the reaction was assigned to the tetrarhodium species $Rh_4(CO)_{12-x}(P)_x$ [153]. Mechanisms related to the silylformylation of terminal alkynes catalyzed by $Rh_2Co_2(CO)_{12}$ have been investigated [154]. The monosubstituted cluster $Ir_4(CO)_{11}(Ph_2PCl)$ reacts on silica gel to give $HIr_4(CO)_{10}(\mu\text{-}PPh_2)$, $Ir_4(CO)_{11}(Ph_2POH)$ and $Ir_6(CO)_{12}(\mu\text{-}CO)(\mu\text{-}PPh_2)_2$. The yields of these products are dependent on the cluster loading and polarity of the eluent. The solid-state structure of the Ir_6 cluster was determined crystallographically and consists of an Ir_6 octahedron that is symmetrically bridged by the PPh_2 ligands across non-adjacent edges. Thermolysis of $HIr_4(CO)_{10}(\mu\text{-}PPh_2)$ in THF yields the same Ir_6 cluster, along with $Ir_7(CO)_{13}(\mu\text{-}CO)(\mu\text{-}PPh_2)(\mu_3\text{-}PPhC_6H_4)$ and $Ir_8(CO)_{14}(\mu\text{-}CO)_2(\eta^1\text{-}Ph)(\mu\text{-}PPh_2)(\mu_4\text{-}PPh)$. The X-ray structures of these latter two clusters are presented, and plausible mechanisms accounting for the formation of these high nuclearity clusters are discussed [155]. The surface-mediated synthesis of $Ir_4(CO)_{12}$, $[Ir_6(CO)_{15}]^{2-}$ and $[Ir_8(CO)_{22}]^{2-}$ by controlled reduction of silica-supported $IrCl_3$ and $[Ir(coe)_2(\mu\text{-}Cl)]_2$ is shown to proceed in high yield. These reactions are compared to the conventional synthetic methods in solution and to reactions on a MgO surface. A scheme outlining the possible pathway for the generation of the various iridium carbonyl clusters on SiO_2 is discussed [156]. [2.2.2]-*p*-Cyclophane reacts with $Co_4(CO)_{12}$ in refluxing benzene to give the new arene clusters $[Co_4(CO)_9]_n(C_{24}H_{24})$ (where $n = 1, 2, 3$). The molecular structures of the new mono- and bis-clusters were determined by X-ray crystallography. The tris-cluster complex was characterized in solution by IR and NMR spectroscopy [157].

$Co(PPh_3)_3Cl$ reacts with the dipotassium salt of 2,2-dicyano-1,1-ethylenedithiolate in MeCN to give $Co_5(\mu_3\text{-}S)_4[\mu\text{-}SC{=}C(CN)_2]_2(PPh_3)_4$ and an octanuclear cluster. The coordination of the thioalkene moiety to the Co_5 frame, which consists of a highly distorted trigonal bipyramid, was verified by X-ray crystallography [158].

A solid-state NMR study and quantum chemical investigation of ^{13}C and ^{17}O chemical shift tensors, ^{17}O-NQR tensors and bonding in transition-metal carbonyl clusters have been published. The cluster complex $Rh_6(CO)_{16}$ was explored, and good agreement between DFT predictions and the experimentally determined carbon and oxygen shielding tensors has been found [159]. Multinuclear NMR data (^{13}C, ^{31}P, $^{13}C\{^{31}P\}$, $^{13}C\{^{103}Rh\}$, $^{31}P\{^{103}Rh\}$) for several mono- and di-substituted $Rh_6(CO)_{16}$ clusters containing two-electron donor ligands are reported. Detailed ^{13}C-NMR assignments on the CO groups in $Rh_6(CO)_{15}(PPh_3)$ and $Rh_6(CO)_{14}$-(dppm) have been made on the basis of $^{13}C\{^{103}Rh\}$ and double resonance measurements, with the specific stereochemical features of the observed long-range couplings being fully discussed. The exchange pathways available to the fluxional CO groups in these clusters have been elucidated by VT NMR spectroscopy [160]. The kinetics for the displacement of the weakly bound ligands, L, in $Rh_6(CO)_{15}L$ (where L = DMSO, MeCN, coe, THF, EtOH) by $P(OPh)_3$ have been examined. These reactions proceed via a dissociative pathway with generation of the unsaturated intermediate $Rh_6(CO)_{15}$, which may be stabilized by the solvent or extra CO bridges [161]. The synthesis of cobalt-carbonyl complexes containing tellurium atoms has appeared. Treatment of $Co_2(CO)_8$ with Te_2O gives the known clusters $Co_4(CO)_{10}Te_2$ and $Co_4(CO)_{11}Te_2$ and the new clusters $Co_6C(CO)_{12}Te_2$ and $Co_6C(CO)_{10}Te_2(Te_3)$. The X-ray structure of the PPh_3 derivative of $Co_6C(CO)_{12}Te_2$ was solved in order to clarify the disordered structure of the parent cluster. A prismatic geometry of cobalt atoms was found, and an interstitial carbon atom and capping tellurium atoms complete the structure. The molecular structure of the other product cluster, which possesses 92 valence electrons, has a similar prismatic CCo_6 cage. The presence of two long Co–Co bond distances derives from two extra electrons that populate Co–Co antibonding orbitals [162]. PhTeTePh reacts with $[Ir_6(CO)_{15}]^{2-}$ and $Ir_6(CO)_{16}$ to yield $[Ir_6(CO)_{14}(\mu\text{-TePh})]^-$ and $Ir_6(CO)_{13}(\mu\text{-TePh})_2$, respectively. Use of diphenyldisulfide and diphenyldiselenide gave analogous iridium products. Electrochemical experiments verify the different reactivity of PhTeTePh and PhSSPh in these reactions. PhTeTePh is shown to add to the electrogenerated transient radical $[Ir_6(CO)_{15}]^{-\bullet}$ while PhSSPh adds to the neutral intermediate $Ir_6(CO)_{15}$. Both $[Ir_6(CO)_{14}(\mu\text{-TePh})]^-$ (Fig. 12) and $Ir_6(CO)_{13}(\mu\text{-TePh})_2$ exhibit octahedral cores, as established by X-ray crystallography [163].

The anionic carbide cluster $[Co_9(C_2)(CO)_{19}]^{2-}$ has been isolated from the pyrolysis reaction of $[Co_6C(CO)_{14}]^-$ in diglyme at 130°C. This paramagnetic cluster was characterized by X-ray diffraction analysis. The $Co_9(C_2)$ core consists of a D_{3h} tricapped trigonal prism of cobalt atoms with an interstitial carbide moiety [164]. The oxidation of $[Bi_{12}Co_4(CO)_{11}]$ by $Mo(CO)_3$(toluene) furnishes the clusters $[Bi_4Co_9(CO)_{16}]^{2-}$ and $[Bi_8Co_{14}(CO)_{20}]^{2-}$, whose molecular structures are shown to be based on tetragonally distorted tetracapped cubic metal arrays with interstitial metal atoms. Given the alternative bonding description of close-packed arrays based upon a cuboctahedron, extended Hückel MO calculations were carried out in order to explore these bonding possibilities [165]. The synthesis and X-ray structure (Fig. 13) of the nitrido cluster $[Co_{10}N_2(CO)_9(\mu\text{-}CO)_{10}]^{4-}$ have been published. The new cluster was prepared from $[Co_6N(CO)_{15}]^-$ in aqueous KOH. The 142 cluster

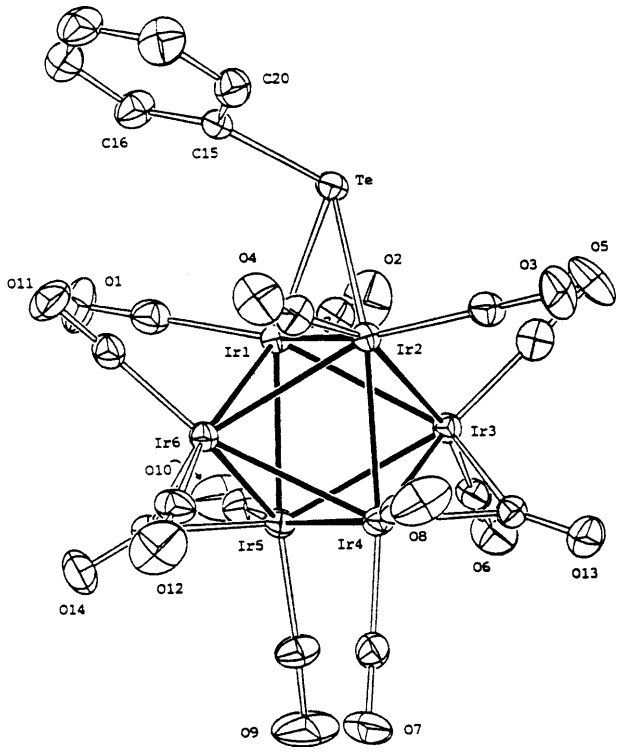

Fig. 12. X-ray structure of $[Ir_6(CO)_{14}(\mu\text{-TePh})]^-$. Reprinted with permission from Organometallics. Copyright 1998 American Chemical Society.

valence electrons in $[Co_{10}N_2(CO)_9(\mu\text{-}CO)_{10}]^{4-}$ are in agreement with the EAN rule, and the structure is composed of two trigonal prismatic moieties that share a common Co–Co edge. Each trigonal prismatic unit contains an interstitial nitrogen atom [166].

The electronic structure of the hydrido cluster $[H_2Rh_{13}(CO)_{24}]^{3-}$ was investigated by DFT calculations. The DFT calculations support an isomer with H atoms encapsulated in polyhedral cavities having the smallest number of bridging CO ligands, in agreement with the available X-ray structural data [167].

2.6. Group 10 clusters

The activated alkyne $MeO_2CC{\equiv}CCO_2Me$ reacts with the clusters $Pt_3(\mu\text{-}CO)_3(PCy_3)_3$ and $Pt_6(\mu\text{-}CO)_6(\mu\text{-dppm})_3$ at low temperature to give $Pt_3(CO)_3(PCy_3)_3$-$(MeO_2CC{\equiv}CCO_2Me)$ and $Pt_6(\mu\text{-}CO)_6(\mu\text{-dppm})_3(MeO_2CC{\equiv}CCO_2Me)$. These new clusters are thermally unstable and fragment upon warming to room temperature to afford binuclear complexes [168]. Thermolysis of $Pt(PPh_3)_2$(ethylene), $Pt(PPh_3)_3$ and various $Pt(PPh_3)_2$(alkyne) complexes in toluene yields the dinuclear complex

$(PPh_3)Pt[\mu\text{-}C_6H_4(PPh_2)\text{-}2](\mu\text{-}PPh_2)Pt(PPh_3)$ and the known cluster $Pt_3(\mu\text{-}PPh_2)_3(Ph)(PPh_3)_2$. The X-ray structure of the dinuclear Pt complex verifies the cleavage of the C–H and P–Ph bonds of the coordinated PPh_3 ligand [169]. The trinickel clusters $[Ni_3(\mu_2\text{-dppm})(\mu_3\text{-L})(\mu_3\text{-I})]^+$ (where L = various isocyanides and CO) undergo a one-electron reduction to afford the corresponding neutral radicals, $[Ni_3(\mu_2\text{-dppm})(\mu_3\text{-L})(\mu_3\text{-I})]^{\bullet}$. Infrared spectroelectrochemical measurements have been employed both in the characterization of these radical clusters and in the study of their reactions with added CO_2. Electrochemical kinetics reveal that the rates of the reaction are first order in [cluster] and $[CO_2]$. A mechanism for CO_2 reduction involving CO_2 activation on the isocyanide-capped face of the cluster is discussed [170].

A report describing the synthesis and X-ray structure of $[Me_3PtF]_4$ has been published, and structural comparisons to the known hydroxide complex $[Me_3PtOH]_4$ are discussed [171]. The X-ray structures of $[Me_3PtSMe]_4$ and $[Me_3PtI]_4{\cdot}CH_3I$ have been determined and their geometries discussed relative to other structurally characterized cubane systems [172]. $Pd_2(dba)_3$ reacts with $P'Bu_3$ in the presence of organic halides $RCCl_3$ (where R = H, F) to give the novel

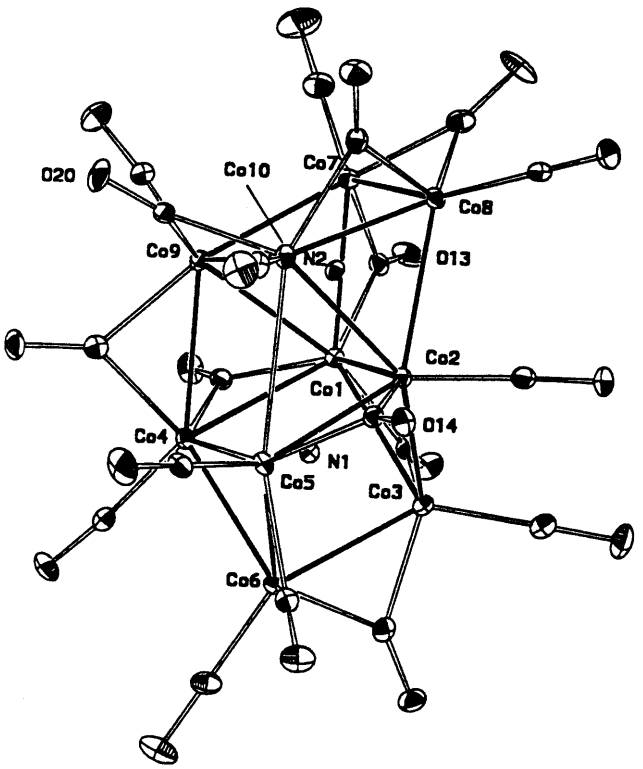

Fig. 13. X-ray structure of $[Co_{10}N_2(CO)_9(\mu\text{-}CO)_{10}]^{4-}$. Reprinted with permission from Inorganic Chemistry. Copyright 1998 American Chemical Society.

methylidyne clusters $Pd_4(\mu_3\text{-}CR)(\mu\text{-}Cl)_3(P^tBu_3)_4$. These are the first such examples of μ_3-alkylidyne palladium compounds. Substitution reactions with LiBr yield the clusters $Pd_4(\mu_3\text{-}CR)(\mu\text{-}Br)_3(P^tBu_3)_4$, while the reaction with H_2 leads to fragmentation and conversion of the capping μ_3-CF ligand to CFH_3. The heterometallic clusters $CoPd_3(\mu_3\text{-}X)(\mu\text{-}CO)_3(CO)_2(P^tBu_3)_3$ (where X = Cl, Br, I) are obtained upon treatment of the Pd_4 clusters with $Co_2(CO)_8$ [173]. The new 58-electron butterfly cluster $[Pt_4(\mu_2\text{-dpam})_3(\mu_2\text{-}CO)_3(\eta^1\text{-dpam})]^{2+}$ has been synthesized from Pt(dpam)$(CF_3CO_2)_2$ and CO in aqueous methanol. The X-ray structure consists of two edge sharing Pt_3 triangles, with a small '$Pt_3(\mu_2\text{-dpam})_3^{2+}$' unit and a larger '$Pt_3(\mu_2\text{-}CO)_3L_3$' (where L = arsine atom) unit. The structural peculiarities were analyzed by carrying out extended Hückel MO calculations. The fluxionality exhibited by this cluster was examined by VT ^{1}H-NMR spectroscopy, with the observed behavior discussed with respect to the existence of two isomers that have different steric requirements [174]. The reaction between Cp*Ga, prepared via reductive dehalogenation of Cp*GaI_2 with potassium and $Ni(CO)_4$ leads to the tetranickel cluster $Ni_4(\mu\text{-Cp*Ga})_4(CO)_6$. The intermediate species Ni(Cp*Ga)$(CO)_3$ has been spectroscopically characterized (IR and NMR) and shown to afford the Ni_4 end-product. The X-ray structure of this cluster consists of a Ni_4 tetrahedron, with the Cp*Ga moieties serving to bridge the nickel centers in both μ_2 and μ_3 modes [175].

The solution structures of $[Ni_6(CO)_{12}]^{2-}$ and $[Pt_6(CO)_{12}]^{2-}$ have been shown to adopt an overall staggered ditriangular structure of D_3 symmetry, as determined by liquid X-ray scattering measurements. Attempts to stabilize monotriangular carbonyl clusters of Ni and Pt were unsuccessful except for $[Pt_3(CO)_6]^{2-}$ [176]. Oxidation of $Pd_{10}(CO)_{10}(PBu_3)_6$ and $Pd_4(CO)_5(PBu_3)_4$ using Me_3NO yields the dodecanuclear cluster $Pd_{12}(CO)_{12}(PBu_3)_6$. The same product has been isolated from the reaction between $Pd_{10}(CO)_{10}(PBu_3)_6$ and $Pd_2(dba)_3$ under argon. X-ray diffraction analysis reveals the presence of two independent hexacapped distorted octahedra of Pd atoms in the unit cell [177]. A published report on the synthesis of $Pd_{59}(CO)_{32}(PMe_3)_{21}$ provides an example of a nanosized metal cluster possessing a trigonal D_3 Pd_{59} core with eleven interior palladium atoms. X-ray diffraction analysis has confirmed the polyhedral structure of this cluster, making it the largest crystallographically determined metal-atom frame with direct metal–metal bonding published to date [178].

2.7. Group 11 clusters

The reaction of $(Me_3SiCH_2Au)_2(\mu\text{-P–P})$ (where P–P = dppm, dppe) with $AgOClO_3$ or $AgOSO_2CF_3$ gives the trinuclear clusters $[Au_2Ag(CH_2SiMe_3)_2(\mu\text{-P–P})]^+$ and the pentanuclear cluster $[Au_4Ag(CH_2SiMe_3)_4(\mu\text{-dppm})]^+$. The presence of four Ag^1–Au^1 non-supported bonds in the Au_4Ag cluster was confirmed by X-ray crystallography [179]. The new metal sandwich compound $[Ag\{Au(\mu\text{-}N^3,C^2\text{-bzim})_3\}_2]^+$ has been isolated from the reaction between $[Au(\mu\text{-}N^3,C^2\text{-bzim})_3]_3$ and Ag^+. The X-ray structure shows that the naked silver ion coordinates to six gold atoms in the unit cell, forming a distorted, Ag^+ centered trigonal prism. The complex regenerates the starting material upon dissolution in coordinating solvents

[180]. The synthesis, luminescence behavior and electrochemical properties of mixed-capped trinuclear copper clusters have been published. The clusters examined in this study include $[Cu_3(\mu\text{-dppm})_3(\mu_3\text{-}\eta^1\text{-}C{\equiv}CC_6H_4OMe\text{-}p)(\mu_3\text{-}\eta^1\text{-}C{\equiv}CC_6H_4OEt\text{-}p)]^+$ and $[Cu_3(\mu\text{-dppm})_3(\mu_3\text{-}\eta^1\text{-}C{\equiv}CC_6H_4OMe\text{-}p)(\mu_2\text{-}\eta^1\text{-}C{\equiv}CC_6H_4NO_2\text{-}p)]^+$. The solid-state structures of these clusters were crystallographically determined [181].

New synthetic perspectives using acetylide starting materials have allowed for the preparation of $[Ag_5(C_2Ph)_6]^-$, $[Au_2Cu(C_2Ph)_4]^-$, $[Au_3M_2(C_2Ph)_6]^-$ (where M = Cu, Ag), $[Ag_6Cu_2(C_2Ph)_{14}]^-$ and $[AuAg_6Cu_6(C_2Ph)_{14}]^-$. An extension of these ethynylation reactions to neutral compounds has led to the isolation of the following clusters $Au_2Ag_2(C_2Ph)_4(PPh_3)_2$, $Ag_2Cu_2(C_2Ph)(PPh_3)_4$, $[AuAg(C_2Ph)_2]_n$, $[AuCu(C_2Ph)_2]_n$ and $[AgCu(C_2Ph)_2]_n$. The synthesis, structures and bonding in these clusters have been reviewed [182]. MP2 calculations on $CH(AuPH_3)_3$, $C(AuPH_3)_4$ and related species have been carried out, and two different ways to estimate the intramolecular gold–gold interaction energy from the total energy are proposed [183]. The synthesis and X-ray structure of $Ag_2C_2{\cdot}2AgClO_4$ are reported. A dumbbell-like structure is observed where the C_2^{2-} ligand is encapsulated inside an octahedral Ag_6 cage [184].

3. Heteronuclear clusters

3.1. Trinuclear clusters

The alkynechalcogenolate complex $Cp_2Ti(SC{\equiv}CPh)_2$ reacts with $Ni(cod)_2$ to give the linear Ti_2Ni cluster $[Cp_2Ti(SC{\equiv}CPh)_2]_2Ni$. The nickel atom links the two $Cp_2Ti(SC{\equiv}CPh)_2$ moieties via interactions with the thiolate sulfur bridges, as shown by X-ray crystallography. The short Ni–Ti bond distances and acute Ni–S–Ti bond angles support a dative bond between the d^{10} Ni and d^0 Ti centers [185]. Treatment of the heterobimetallic phosphido- and hydrido-bridged complexes $Cp_2TaH(\mu\text{-}H)(\mu\text{-}PMe_2)M(CO)_4$ (where M = Cr, Mo, W) with the diphosphine ligands dmpm or dmpe gives $Cp_2TaH_2(\mu\text{-}PMe_2)M(CO)_4(P{-}P)$. These complexes are able to bind the $Cr(CO)_5$ fragment using the pendant diphosphine ligand to produce the linear trinuclear complexes $Cp_2TaH_2(\mu\text{-}PMe_2)M(CO)_4(P{-}P)[Cr(CO)_5]$ [186].

The cluster $MoRu_2(\mu_2\text{-}CO)_3[\mu_3\text{-}C{\equiv}C\{Ru(CO)_2Cp\}](\eta\text{-}Cp)_3$ is produced as the major product in the reaction between $[Ru(CO)_2(\eta\text{-}Cp)]_2(\mu\text{-}C{\equiv}C)$ and $(\eta\text{-}Cp)_2Mo_2(CO)_4$. The carbide ligand is bound in a μ_3 fashion to the $MoRu_2$ triangle through one carbon and to a single ruthenium center in a monohapto fashion by the other carbon atom. An interesting feature of this cluster concerns the tetrahedral core, which is unsaturated by virtue of the 45 valence electron count [187]. Several new polynuclear clusters have been obtained from the reaction between $Cp_2Mo_2(CO)_4$ and the alkynyl complexes $CpM(CO)_2(CCR)$ (where M = Fe, Ru; R = Me, Ph). Four X-ray structures are presented, and the fluxional behavior observed by VT ^{1}H-NMR spectroscopy in $Cp_3Mo_2Ru(CO)_6(\mu_3\text{-}CMe)$ is discussed [188]. The mixed-metal sulfido clusters $M'(PPh_3)(\mu_2\text{-}S)_3[M(S_2CNEt_2)]_2(\mu_2\text{-}S)_2$ (where M = Mo, W; M′ = Pd, Pt) have been synthesized and structurally characterized in

the case of the PtW_2 derivative. Treating the $PdMo_2$ cluster with $Pd(PPh_3)_4$ affords the cubane-type cluster $[Pd(PPh_3)]_2[Mo(S_2CNEt_2)_2]_2(\mu_3\text{-}S)_4$, which may also be prepared from the reaction of $Mo_2S_2(\mu_2\text{-}S)_2(S_2CNEt_2)_2$ with two equivalents of $Pd(PPh_3)_4$ [189].

Bis(cyclopentadienyl) ligands have been employed in the synthesis of double $MCoC_2$ and MFeCoS (where M = Mo, W) tetrahedral clusters. Treatment of $FeCo_2(CO)_9(\mu_3\text{-}S)$ with $[NaM(CO)_3(\eta^5\text{-}C_5H_4)]_2Z$ (where $Z = p\text{-}C(O)C_6H_4C(O)\text{-}p$, $o\text{-}CH_2C_6H_4CH_2\text{-}o$) or $[LiMo(CO)_3(\eta^5\text{-}C_5H_4)]_2(Me_2SiOSiMe_2)$ yields the corresponding bridged double clusters. These new compounds have all been characterized in solution by IR and ^{1}H-NMR spectroscopy [190]. Chiral tetrahedrane clusters containing a functionally substituted cyclopentadienyl ligand have been synthesized and structurally characterized in the case of $(\eta^5\text{-}C_5H_4CHO)(\eta^5\text{-}C_5H_5)MoNiFeS(CO)_5$ [191]. The sulfido-capped cluster $RuCo_2(\mu_3\text{-}S)(CO)_9$ reacts with $[\{\eta^5\text{-}C_5H_4C(O)\}M(CO)_3]^-$ and $^-[M(CO)_3\{\eta^5\text{-}C_5H_4C(O)C_6H_4C(O)C_5H_4\}\text{-}M(CO)_3]^-$ (where M = Mo, W) to yield $MRuCo(CO)_8(\mu_3\text{-}S)[\eta^5\text{-}C_5H_4C(O)]$ and $[MRuCo(CO)_8(\mu_3\text{-}S)]_2[\eta^5\text{-}C_5H_4C(O)C_6H_4C(O)C_5H_4]$. The X-ray structures of the MoRuCo and $W_2Ru_2Co_2$ clusters have been solved and their structural features are discussed [192]. The synthesis and nonlinear optical properties of the chalcogen-bridged clusters $Cp_2Mo_2M(\mu_3\text{-}E)(CO)_7$ (where M = Fe, Ru, Os; E = S, Se) have been described. The large refractive third-order nonlinearity observed in these clusters indicates the potential for promising optical limiting applications [193]. Treatment of $RuCo_2(CO)_9(\mu_3\text{-}Se)$ with $[\{\eta^5\text{-}C_5H_4C(O)R\}Mo(CO)_3]^-$ (where R = various groups) proceeds to give the chiral clusters $RuCoMo(\mu_3\text{-}Se)(CO)_8[\eta^5\text{-}C_5H_4C(O)R]$ when benzophenone ketyl is employed as an initiator. Reduction of the carbonyl moiety on the cyclopentadienyl ring by $NaBH_4$ yields the corresponding secondary alcohol complex. Two X-ray structures accompany this report [194]. Thermolysis of $Co_2(\mu\text{-}PhC{\equiv}CH)(CO)_6$ with $Cp_2Mo_2(CO)_4$ in THF furnishes the μ_3-alkylidyne cluster $Co_2MoCp(\mu_3\text{-}CCH_2Ph)(CO)_8$ as the major product. Plausible routes leading to this cluster are discussed. Use of the complexes $Co_2(\mu\text{-}CF_3C{\equiv}CR)(CO)_6$ (where $R = CF_3$, H), which contain an alkyne ligand with at least one strongly electron-withdrawing substituent, does not afford any of the trinuclear cluster product but rather the dinuclear compounds $CpMo(CO)_2(\mu\text{-}CF_3C_2R)Co(CO)_3$. $CpCo(CO)_2$ reacts with $CpMo(CO)_2(\mu\text{-}CF_3C_2CF_3)Co(CO)_3$ to give the mixed-metal butterfly cluster $Co_2Mo_2(CO)_3(\mu\text{-}CO)Cp_3$. The reaction between $Co_2(\mu\text{-}CF_3C{\equiv}CCF_3)(CO)_6$ and the phosphido complex $Cp_2Mo_2(\mu\text{-}CO)(\mu\text{-}PPh_2)_2$ has also been studied and found to give a single product, $Mo_2Cp_2(\mu\text{-}PPh_2)[\mu\text{-}PPh_2Co_2(CF_3C_2CF_3)(CO)_5](CO)_2$. It is shown that the phenyl ring of the $Mo(\mu\text{-}PPh_2)$ moiety is π-bonded to one of the two cobalt atoms [195]. The metal exchange reagents $[CpM(CO)_3]^-$ (where M = Mo, W) react with the ferrocenylacetylene complex $\mu\text{-}FcCCHCo_2(CO)_6$ to afford the polynuclear complexes $\mu\text{-}FcCCHCo(CO)_3M(CO)_2Cp$, which upon further reaction with $Fe_2(CO)_9$ in the presence of dba give the μ_3-ferrocenylvinylidene clusters $\mu_3\text{-}FcCHCFeCo_2(CO)_9$ and $\mu_3\text{-}FcCHCFeCoM(CO)_8Cp$. The spectroscopic data are reported for these compounds and two X-ray structures are presented [196]. The synthesis of $(\eta^5\text{-}C_5H_4R)MoCoFe(CO)_8(\mu_3\text{-}Se)$ (where R = H, MeCO, MeO_2C) from $Co_2Fe(CO)_9(\mu_3\text{-}$

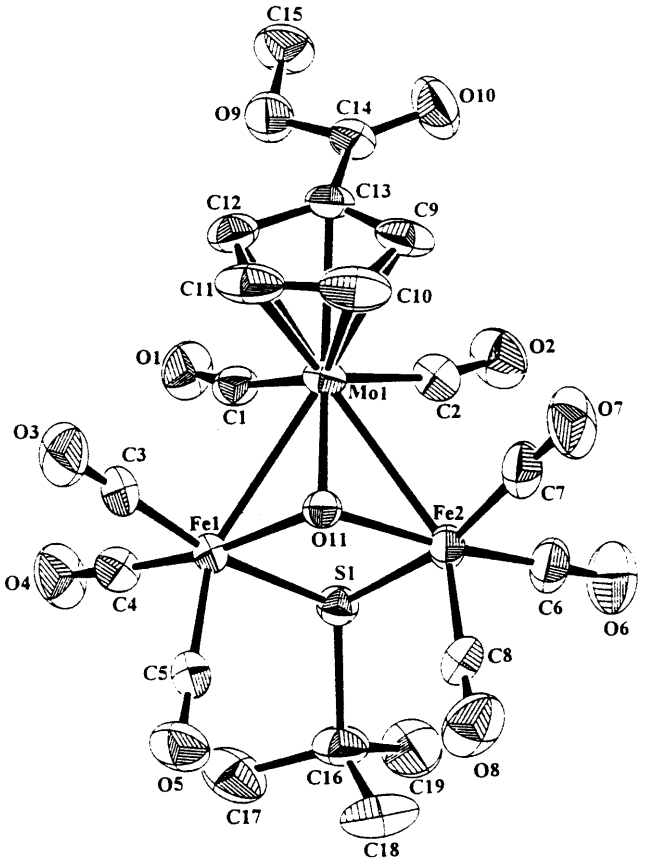

Fig. 14. X-ray structure of $(\eta^5\text{-}MeO_2CC_5H_4)(CO)_2MoFe_2(\mu_3\text{-}O)(\mu\text{-}S'Bu)(CO)_6$. Reprinted with permission from Organometallics. Copyright 1998 American Chemical Society.

Se) and $(\eta^5\text{-}C_5H_4R)_2Mo_2(CO)_4(\mu\text{-dppe})$ is reported. Included in this report is the X-ray structure of $[\eta^5\text{-}C_5H_4C(O)Me]MoCoFe(CO)_8(\mu_3\text{-Se})$ [197]. The novel oxo-capped clusters $(\eta^5\text{-}C_5H_4R')(CO)_2MoFe_2(\mu_3\text{-}O)(\mu\text{-SR})(CO)_6$ (where R and $R' =$ various groups) have been obtained from the reaction between $[(\mu\text{-SR})(\mu\text{-CO})\text{-}Fe_2(CO)_6]^-$ and $[(\eta^5\text{-}C_5H_4R')M(CO)_2]_2$ (where M = Mo, W) after exposure to air. The edge-opened square-pyramidal MFe_2SO polyhedron was confirmed by X-ray diffraction analysis on $(\eta^5\text{-}MeO_2CC_5H_4)(CO)_2MoFe_2(\mu_3\text{-}O)(\mu\text{-}S'Bu)(CO)_6$, whose structure is shown in Fig. 14 and $(\eta^5\text{-}EtO_2CC_5H_4)(CO)_2MoFe_2(\mu_3\text{-}O)(\mu\text{-SEt})(CO)_6$ [198].

Fenske–Hall molecular orbital (MO) calculations have been carried out on $Cp_2Cr_2B_4H_8Fe(CO)_3$, whose structure was based on the known Cp* derivative. The Cp_2Cr_2 fragment is shown to provide an additional low-energy (filled) or high-energy (unfilled) orbital to the cluster bonding frame with only small distortions to the Cr_2B_4 polyhedral core geometry [199]. Cluster expansion reactions utilizing Group

6 metallaboranes are reported. The complex $(Cp^*Cr)_2B_4H_8$ reacts with $Fe_2(CO)_9$ and $Co_2(CO)_8$ to yield the mixed-metal metallaboranes $(Cp^*Cr)_2B_4H_8Fe(CO)_3$ and $(Cp^*Cr)_2B_4H_7Co(CO)_3$, respectively, in good yields. Both of these clusters contain 6 SEP and exhibit bicapped bipyramidal geometries where the $M(CO)_3$ moiety occupies one of the capping positions. These clusters may also be viewed as complexes formed between the $M(CO)_3$ fragment and the four-electron $(Cp^*Cr)_2B_4H_8$ fragment (M = Fe) or the three-electron $(Cp^*Cr)_2B_4H_7$ fragment (M = Co). The fluxional behavior found in the Cr_2Fe cluster has been interpreted in terms of a motion involving the 'swinging' of the $Fe(CO)_3$ fragment between equivalent pairs of BH_2 groups. The molybdaborane complex $(Cp^*Mo)_2B_5H_9$ reacts with $Fe_2(CO)_9$ to give $(Cp^*Mo)_2B_5H_9Fe(CO)_3$, whose solid-state structure exhibits a bicapped octahedral geometry with the $Fe(CO)_3$ moiety occupying one of the high-connectivity polyhedral vertices, as opposed to a capping position. The structural changes observed during the addition of $Fe(CO)_3$ to the Mo_2B_5 complex are in keeping with delocalized bonding rules [200].

The synthesis of the bridging carbyne cluster $CpMnFeCo(CO)_7(\mu\text{-}CO)(\mu_3\text{-}CPh)$, which has been prepared from $CpMnCo(CO)_5(\mu\text{-}CPh)$ and $CpMnCo(CO)_5[\mu\text{-}C(CO)Ph]$ upon treatment with $Fe_2(CO)_9$, is reported. The corresponding ReFeCo trimetal cluster was prepared by using the analogous ReCo starting materials. The tetrahedral core present in these clusters was verified by X-ray diffraction analysis [201]. Refluxing $(CpCo)_2Fe(CO)_2(PPh_3)(\mu_3\text{-}S)(\mu_3\text{-}CS)$ in CS_2 leads to the new cluster $(CpCo)_2Fe(CO)(PPh_3)(\mu_3\text{-}S)[\mu_3\text{-}CSC(S)S]$, which is shown to contain a bridging C_2S_3 ligand that coordinates to the iron center with one of the sulfur atoms. The molecular structure was ascertained by X-ray crystallography [202]. The paramagnetic trinuclear clusters $(Cp^*M)_2(\mu_3\text{-}S)_2FeCl_2$ (where M = Rh, Ir) are synthesized from $Cp^*MCl(\mu_2\text{-}SH)_2MCp^*Cl$ and excess $FeCl_2{\cdot}4H_2O$ in THF. The iridium cluster transforms into the 78 electron pentanuclear bow-tie cluster $[(Cp^*Ir)_2(\mu_3\text{-}S)_2Fe(\mu_3\text{-}S)_2(IrCp^*)_2]^{2+}$ upon reaction with $NaBH_4$. Similarly, the dinuclear iridium starting material reacts with $CoCl_2$ and $NiCl_2{\cdot}6H_2O$ or Ni(cod) to afford the related 79 and 80 electron bow-tie clusters $[(Cp^*Ir)_2(\mu_3\text{-}S)_2M(\mu_3\text{-}S)_2(IrCp^*)_2]^{2+}$. The cyclic voltammetric behavior of these systems has been examined, and in the case of the bow-tie clusters the following trend in the reduction potential was observed Fe < Co < Ni. The X-ray structure of $(Cp^*Ir)_2(\mu_3\text{-}S)_2FeCl_2$ (Fig. 15) consists of a triangular 46 electron metal core, which is capped by the μ_3-S ligands. The X-ray structures of the other products have been solved, and the structural differences within the bow-tie series as a function of the central metal are discussed. The structural variations are interpreted by considering the total electron counts and the data obtained from extended Hückel MO calculations [203].

The 46 electron clusters $Pt_2M(\mu_3\text{-}\eta^1{:}\eta^1{:}\eta^2\text{-}PhC{\equiv}CC{\equiv}CPh)(CO)_5(PPh_3)_2$ (where M = Fe, Ru) are formed as the major products from the reaction between $Pt(\eta^2\text{-}PhC{\equiv}CC{\equiv}CPh)(PPh_3)_2$ and $Fe(CO)_5$ or $Ru_3(CO)_{12}$ in refluxing toluene. The Pt_2M clusters are isostructural. The X-ray structure of the Pt_2Fe cluster is composed of two $Pt(CO)(PPh_3)$ moieties and an $Fe(CO)_3$ group linked by two Pt–Fe bonds with the μ_3-diyne, which is coordinated by only one C≡C bond [204]. The heterometallic borole complex $(OC)_2[\eta^5\text{-}(1\text{-phenylborole})]Fe[Au(PPh_3)]_2$ was obtained from the

reaction between $[HFe\{\eta^5\text{-(1-phenylborole)}\}(CO)_2]^-$ and $AuCl(PPh_3)$ in CH_2Cl_2. This $FeAu_2$ cluster reacts with added $AuCl(PPh_3)/TlPF_6$ to produce the tetrahedral cationic cluster $[(OC)_2\{\eta^5\text{-(1-phenylborole)}\}Fe\{Au(PPh_3)\}_3]^+$. The solid-state structures were established by standard X-ray diffraction analysis ($FeAu_2$ cluster) and wide angle X-ray scattering (WAXS) measurements ($FeAu_3$ cluster). ^{13}C-NMR measurements support the contention that a three-center two electron bonding description for the $FeAu_2$ core is more important than the electron precise two-center three electron bonding description [205]. The anionic compounds $[Hg\{M(CO)_4\}_2]^{2-}$ (where M = Fe, Ru, Os) were synthesized from $K_2M(CO)_4$ and $HgCl_2$ employing a 2:1 molar ratio of reagents. Both the ruthenium and osmium complexes are thermally stable up to 170°C. The X-ray structures of $[PPN]_2[Hg\{Ru(CO)_4\}_2]$ and $[Ph_3PMe]_2[Hg\{Os(CO)_4\}_4]$ were determined and shown to consist of two trigonal-bipyramidal $M(CO)_4$ units that are joined at the apical sites by a mercury atom in a linear M–Hg–M array. Polymeric $[Hg\{M(CO)_4\}_2]_x$ complexes have been obtained from the reaction between $Na_2M(CO)_4$ and $HgCl_2$ (1:1 molar ratio of reagents). The polymers are air stable, but are insoluble in common organic solvents and water [206]. The reaction between $Cp_2Rh_2(CO)(\mu\text{-}\eta^1\text{:}\eta^1\text{-}CF_3C_2CF_3)(\eta^1\text{-dppe})$ and $CpPd(\eta^3\text{-}C_3H_5)$ gives the cluster $Cp_2Rh_2Pd(\mu_3\text{-}CO)(\mu\text{-}\eta^1\text{:}\eta^1\text{:}\eta^2\text{-}CF_3C_2CF_3)(\eta^2\text{-dppe})$, whose X-ray structure exhibits an open Rh_2Pd core with an unusual coordination mode for the alkyne ligand. The alkyne is σ-bonded to the central rhodium and sits across the nonbonding Rh···Pd edge of the cluster. The dppe ligand, which was initially attached to the rhodium, is chelated to the palladium center. The existence of solution isomers has been

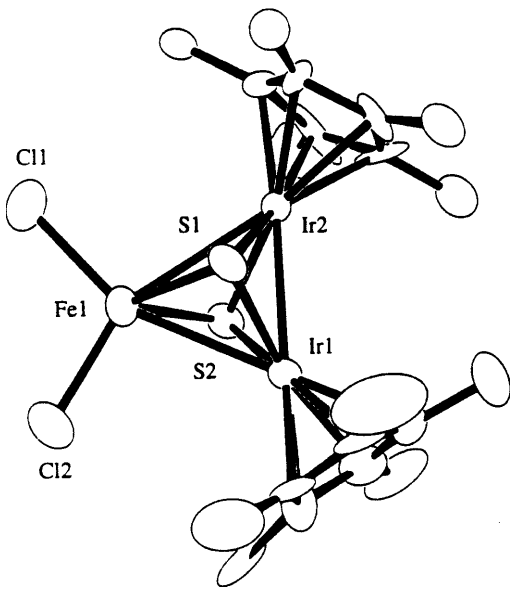

Fig. 15. X-ray structure of $(Cp^*Ir)_2(\mu_3\text{-}S)_2FeCl_2$. Reprinted with permission from Inorganic Chemistry. Copyright 1998 American Chemical Society.

investigated by VT-NMR spectroscopy [207]. A review article discussing the importance of mixed-metal palladium clusters in catalytic processes has been published [208].

3.2. Tetranuclear clusters

The tungsten tris-sulfide complex $[Cp^*WS_3]^-$ reacts with a variety of Cu(I) and Ag(I) complexes and $Pd(dppe)Cl_2$ to afford new heterometallic clusters. Both $[Cp^*WS_3Cu_3(PPh_3)_3(NO_3)]^+$ and $[(Cp^*WS_3)_2Ag_2(PPh_3)_3]^+$ have been isolated and fully characterized in solution. An incomplete WS_3Cu_3 cubic polyhedral geometry was found by X-ray diffraction analysis for the four metal centers. The structural data on the latter cluster reveals that it is best viewed as a composite of two subcluster units, $[Cp^*WS_3Ag(PPh_3)_2]^+$ and $Cp^*WS_3Ag(PPh_3)$, that are linked by Ag–S interactions [209]. CO substitution in $CpWIr_3(CO)_{11}$ by dppe and dppm yields $CpWIr_3(\mu\text{-P–P})(\mu\text{-CO})_3(CO)_6$. Use of monodentate phosphine ligands affords the clusters $CpWIr_3(\mu\text{-CO})_3(CO)_{8-n}P_n$. The fluxional behavior exhibited by these clusters was investigated by VT ^{31}P- and ^{13}C-NMR spectroscopy. Included in this report are the exchange pathways for CO scrambling and the X-ray structure of $CpWIr_3(\mu\text{-CO})_3(CO)_7(PMe_2Ph)$ [210]. Thermolysis of $Cp_2Mo_2Fe_2STe(CO)_7$ and PhSH in benzene gives $Cp_2Mo_2Fe_2(\mu_3\text{-S})(\mu_3\text{-Te})(\mu_2\text{-SPh})(\mu_3\text{-H})(CO)_5$, which exists in solution as an isomeric mixture. The X-ray structure of one of these isomers consists of a Mo_2Fe_2 tetrahedron that has face capping μ_3-Se and μ_3-Te ligands. The bridging thiol unit spans the Mo–Mo bond while the μ_3-H group caps one of the $MoFe_2$ polyhedral faces [211]. Decarbonylation of $CpWOs_3(CO)_{11}(\mu_3\text{-CTol})$ using Me_3NO/MeOH, followed by reaction with H_2S yields the sulfido-alkylidyne cluster $CpWOs_3(CO)_{10}(\mu_3\text{-CTol})(\mu_3\text{-S})$ as the major product. The cluster complexes $CpWOs_3(CO)_{10}(\mu\text{-CTol})(\mu_3\text{-S})(\mu\text{-H})$ and $CpWOs_3(CO)_9(\mu\text{-CTol})(\mu\text{-S})(\mu\text{-H})$ are also formed in the H_2S reaction in minor amounts. $CpWOs_3(CO)_{10}(\mu\text{-CTol})(\mu\text{-S})(\mu\text{-H})$ is decarbonylated with Me_3NO in CH_2Cl_2 to give the corresponding nonacarbonyl cluster. The molecular structures of these three clusters were established by X-ray crystallography. $CpWOs_3(CO)_{10}(\mu_3\text{-CTol})(\mu_3\text{-S})$ and $CpWOs_3(CO)_{10}(\mu\text{-CTol})(\mu_3\text{-S})(\mu\text{-H})$ both have 62 valence electrons and exhibit a butterfly WOs_3 core. The 60 valence electron cluster $CpWOs_3(CO)_9(\mu\text{-CTol})(\mu\text{-S})(\mu\text{-H})$ contains a tetrahedral core with the μ-sulfido and μ-alkylidene ligands bridging the W–Os(2) and W–Os(1) edges, respectively [212]. The phosphite-substituted clusters $CpWIr_3(\mu\text{-CO})_3(CO)_{8-n}L_n$ (where $L = P(OMe)_3$, $P(OPh)_3$; $n = 1-3$) have been prepared from $CpWIr_3(CO)_{11}$. The fluxional behavior exhibited by several of these clusters was investigated by VT ^{31}P-NMR spectroscopy, with the interconverting isomers resolvable at low temperature. The X-ray structure of $CpWIr_3(\mu\text{-CO})_3(CO)_6[P(OPh)_3]_2$ has been solved [213]. $Ru_3(\mu_3\text{-NPh})(CO)_9$ reacts with $Cp^*W(O)_2(CCR)$ (where $R = Ph$, $CMe{=}CH_2$) to afford the oxo clusters $Cp^*W(O)(\mu\text{-O})Ru_3(\mu_3\text{-NPh})(CCR)(CO)_8$, which contain both high- and low-valent metal fragments. Both clusters consist of an open triangular Ru_3 frame with the dioxo tungsten moiety coordinated to the central ruthenium by a $W{=}O \rightarrow Ru$ dative bond. Refluxing $Cp^*W(O)(\mu\text{-O})Ru_3(\mu_3\text{-NPh})(CCPh)(CO)_8$ with $Ru_3(CO)_{12}$ gives the pentametallic

cluster $Cp^*W(O)(\mu\text{-}O)Ru_4(\mu_3\text{-}NPh)(CCPh)(CO)_{10}$. The reactivity of the ancillary vinyl group and the dioxo tungsten moiety has been examined under a variety of conditions. Mechanisms accounting for the observed transformations and four X-ray structures are presented and discussed [214]. Alkyne–acetylide coupling has been reported in the reaction between $Cp^*WOs_3(\mu\text{-}O)_2(\mu\text{-}CCPh)(CO)_9$ and diphenylacetylene. The cluster compounds $Cp^*W(O)Os_3(\mu\text{-}O)(CCPh)(PhC_2Ph)(CO)_8$ and $Cp^*W(O)Os_3(\mu\text{-}O)(CCPhCPhCPh)(CO)_8$ have been isolated. The latter cluster demonstrates the cluster-assisted formation of C–C bonds between the acetylide and alkyne moieties. Use of phenylacetylene affords the coupled product $Cp^*W(O)Os_3(\mu\text{-}O)(CCPhCHCPh)(CO)_8$ and a small amount of the vinylidene cluster $Cp^*W(O)Os_3(\mu\text{-}O)(CCPhCCHPh)(CO)_8$. The interconversion of these clusters is documented, and mechanistic schemes outlining the observed transformations are fully discussed. The molecular structures of four clusters have been solved and their unique structural features discussed [215].

The bonding in cubane-type clusters possessing $Mo_3M'S_4$ cores has been examined by carrying out Fenske–Hall MO calculations. The data from Mo_3NiS_4 clusters suggest that cubane clusters may not serve as appropriate models for NiMoS hydrodesulfurization catalysts [216]. Terminal arylalkynes react with $Cp_2W_2Ir_2(CO)_{10}$ to afford the clusters $Cp_2W_2Ir_2(\mu_4\text{-}\eta^2\text{-}HC_2R)(\mu\text{-}CO)_4(CO)_4$ in good yield. X-ray diffraction analysis on the phenyl derivative confirms the site-selective alkyne insertion into the W–W bond of the starting cluster. This site reactivity is contrasted with the related cluster $CpWIr_3(CO)_{11}$, which shows a lack of reactivity towards terminal alkynes. The reaction of the buta-1,3-diynyl complex $Cp\text{-}W(CO)_3(C{\equiv}CC{\equiv}CH)$ with $Cp_2W_2Ir_2(CO)_{10}$ produces $Cp_2W_2Ir_2[\mu_4\text{-}\eta^2\text{-}HC_2C{\equiv}CW\text{-}(CO)_3Cp](\mu\text{-}CO)_4(CO)_4$. Solution spectroscopic measurements on the W_3Ir_2 cluster reveal that the diynyl moiety is attached to the cluster by the terminal C≡CH unit instead of the C≡W moiety [217]. The isomerization of an allyl moiety on a WOs_3 cluster and ring-methyl activation of a Cp* ligand have been reported. The tetranuclear carbido-benzofuryl cluster $Cp^*WOs_3(\mu_4\text{-}C)(\mu\text{-}H)(\mu\text{-}C_8H_6O)(CO)_9$ is converted to $Cp^*WOs_3(\mu_4\text{-}C)(\mu\text{-}H)(CO)_{11}$ under CO pressure. Decarbonylation using Me_3NO in the presence of diisopropyl acetylenedicarboxylate gives $Cp^*WOs_3(CO)_{10}[C_3H(CO_2^iPr)_2]$, whose X-ray structure (Fig. 16) has verified the formation of the allyl group by a hydride migration to the carbide group. The allyl group undergoes metathesis to yield an isomeric cluster having a different arrangement of the allyl C_3 backbone. Thermolysis of this metathesized allyl isomer gives the η^6-tetramethylfulvene cluster $[C_5Me_4(CH_2)]WOs_3(\mu\text{-}H)[C_3H(CO_2^iPr)_2](CO)_9$ and $Cp^*WOs_3(\mu_3\text{-}CH)(\mu_3\text{-}CCO_2^iPr)_2(CO)_9$. The carbyne-capped cluster results from the cleavage of two allyl C–C bonds. The molecular structures of four additional clusters have been solved and are discussed along with plausible mechanisms for all of the observed interconversions and transformations [218].

The synthesis and crystal structures of $HRuRh_3(CO)_9(SPh_2)_3$, $HRuRh_3\text{-}(CO)_9(SPhMe)_3$ and $[HRuRh_3(CO)_9]_2[SEt_2]_3$ are reported. All of the thioether ligands have replaced Rh-bound CO groups [219]. The unsaturated dihydride cluster $Os_3(CO)_{10}(H)_2$ reacts with Rh(cod)(L)(I) (where L = bpy, 1,10-phen, 4,4′-diphenylbpy) to furnish the hydrido clusters $Os_3Rh(\mu\text{-}H)_3(CO)_{10}(\eta^4\text{-cod})$, $Os_3Rh(\mu\text{-}$

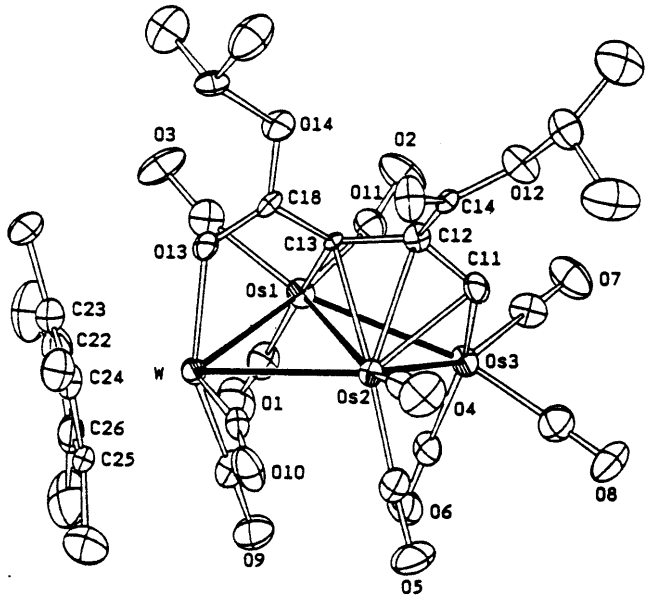

Fig. 16. X-ray structure of $Cp^*WOs_3(CO)_{10}[C_3H(CO_2^iPr)_2]$. Reprinted with permission from Organometallics. Copyright 1998 American Chemical Society.

$H)_2(CO)_8(\mu\text{-}CO)(\mu\text{-}I)(\eta^4\text{-cod})$, $Os_3Rh(\mu\text{-}H)_2(CO)_8(\mu\text{-}CO)(\mu\text{-}I)$(bpy), $Os_3Rh(\mu\text{-}H)_2$-$(CO)_8(\mu\text{-}CO)(\mu\text{-}I)$(1,10-phen) and $Os_3Rh(\mu\text{-}H)_2(CO)_8(\mu\text{-}CO)(\mu\text{-}I)(4,4'\text{-}Ph_2bpy)$. These clusters have been fully characterized by IR and NMR spectroscopy, mass spectrometry and X-ray crystallography in the case of the first three products [220]. Treatment of $Ru_3Pt(\mu\text{-}H)(\mu_4\text{-}C{\equiv}C'Bu)(CO)_9$(dppe) with excess $HC{\equiv}C'Bu$ yields the C–C bond coupled clusters $Ru_3Pt[\mu_4\text{-}C(^tBu)C(H)CC(^tBu)C(H)C(^tBu)][\mu\text{-}\sigma\text{-}\pi\text{-}C(H){=}CH(^tBu)](CO)_7$(dppe) and the inseparable mixture of *trans* and *gem* isomers of $Ru_3Pt[\mu_3\text{-}C(^tBu)CC(^tBu){\cdot}CH_2](CO)_8$(dppe). The X-ray structures of the former cluster and the *gem* isomer of the latter clusters have been solved [221]. The anionic clusters $[Ru_3Rh(CO)_{13}]^-$ and $[RuRh_3(CO)_{12}]^-$ have been synthesized from the reaction of $[Rh(CO)_4]^-$ with $Ru_3(CO)_{12}$ and by the oxidative degradation of $[RuRh_4(CO)_{12}]^{2-}$, respectively. X-ray diffraction studies on both products confirm the presence of a tetrahedral metal core (Fig. 17). PPh_3 reacts with $[Ru_3Rh(CO)_{13}]^-$ to give $[Ru_3Rh(CO)_{12}(PPh_3)]^-$, where the PPh_3 is attached to the rhodium center. VT ^{13}C-NMR spectroscopy provides evidence for the complete scrambling of the CO groups about the cluster polyhedron over the temperature range 170–295 K [222].

The synthesis of $[AuCo(CO)_4]_2$(dppf) from $(AuCl)_2(\mu\text{-dppf})$ and $LiCo_3(CO)_{10}$ in THF at room temperature has been published. X-ray diffraction analysis shows the existence of a P–Au–Co–CO(axial) skeleton that makes a pair in a head-to-tail manner with neighboring molecules. The 5.6220(8) Å Au–Au separation is in excess

of the normal aurophilic interaction [223]. Addition of $[Ir(CO)_4]^-$ to $[Pt_3(\mu_3\text{-}CO)(\mu\text{-}dppm)_3]^{2+}$ gives $[Pt_3(\mu_3\text{-}CO)(\mu\text{-}dppm)_3\{Ir(CO)_4\}]^+$ at low temperature. This adduct loses CO upon warming to give the butterfly cluster $[Pt_3\{Ir(CO)(\mu\text{-}CO)_2\}(\mu\text{-}CO)(\mu\text{-}dppm)_3]^+$. CO substitution at the iridium center by $P(OPh)_3$ gives the corresponding $P(OPh)_3$-substituted cluster, where the iridium center occupies a wing-tip position in the butterfly polyhedron. $[Pt_3\{Ir(CO)(\mu\text{-}CO)_2\}(\mu\text{-}CO)(\mu\text{-}dppm)_3]^+$ is thermally unstable and is shown to rearrange in solution to give the isomeric butterfly cluster $[Pt_2Ir\{Pt(CO)(\mu\text{-}CO)_2\}(\mu\text{-}CO)(\mu\text{-}dppm)_3]^+$. ^{31}P- and ^{13}C-NMR data reveal that the iridium atom occupies a hinge position within the cluster, in addition to providing evidence for the migration of two PPh_2 groups from the platinum to iridium center [224]. The new platinum(II) oxo complexes $[(cod)Pt(\mu_3\text{-}O)AuL]_2[BF_4]_2$ (where L = various phosphine ligands), $[(cod)Pt\{\mu_3\text{-}O(AuL)_2\}_2]^{2+}$ and $[(cod)_4Pt_4(\mu_3\text{-}O)_2Cl_2]^{2+}$ have been prepared and fully characterized in solution. The X-ray structures of four clusters have been determined and their structural features discussed [225].

3.3. Pentanuclear clusters

The phosphinidene-capped clusters $Ru_4(CO)_{10}(\mu_4\text{-}PPh)(CCPh)[WCp(CO)]$ (where Cp = Cp, Cp*) were prepared from $Ru_4(CO)_{13}(\mu_3\text{-}PPh)$ and the tungsten–acetylide complexes $CpW(CO)_3(CCPh)$. The Ru_4W clusters exist as a mixture of interconvertible isomers at elevated temperatures. Both Cp* isomers have been isolated in pure form and their molecular structures determined by X-ray crystallography, which reveals the presence of a novel WRu_4P octahedral core in each case. Possible

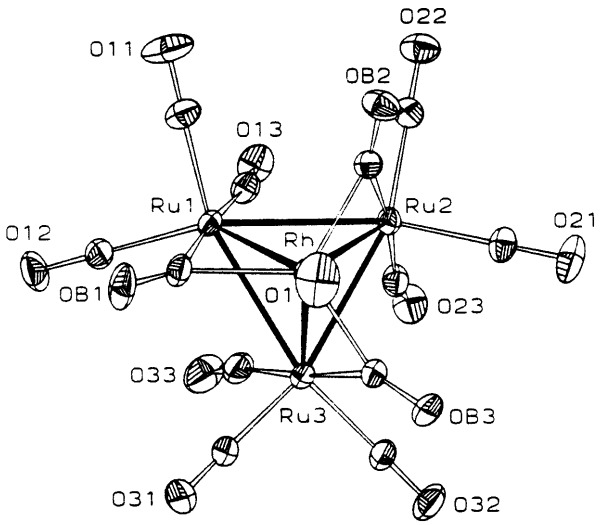

Fig. 17. X-ray structure of $[Ru_3Rh(CO)_{13}]^-$. Reprinted with permission from Inorganic Chemistry. Copyright 1998 American Chemical Society.

mechanisms for the skeletal isomerization are presented [226]. The synthesis and X-ray diffraction results of η^5-Cp*W(μ-O)Ru$_4$(CO)$_9$(μ-CO)[μ_3-η^2-OPN(^{i}Pr)$_2$](μ_4-η^2-CCPh) and η^5-Cp*W(O)$_2$Ru$_4$(CO)$_{10}$[μ_3-PN(^{i}Pr)$_2$](μ_5-η^2-CCPh) are reported. These clusters were prepared from Ru$_4$(CO)$_{12\text{-}13}$[PN(^{i}Pr)$_2$] and Cp*W(O)$_2$(CCPh) [227]. The reaction of $[Fe_5C(CO)_{14}]^{2-}$ with ClHgM (where M = Mo(CO)$_3$Cp, W(CO)$_3$Cp, Mn(CO)$_5$, Co(CO)$_4$, Fe(CO)$_2$Cp) furnishes the new heptametallic clusters $[Fe_5C(CO)_{14}\{\mu\text{-HgM}\}]^-$. Use of $Hg(NO_3)_2$ affords the spiro cluster [μ_4-Hg{Fe$_5$C(CO)$_{14}$}]$^{2-}$. ^{57}Fe-Mössbauer spectroscopy on the different iron clusters has established the number of unique iron sites present in each case. The X-ray structures of $[Fe_5C(CO)_{14}\{\mu\text{-HgW(CO)}_3\text{Cp}\}]^-$ and the spiro cluster are presented, and structural comparisons with related iron–gold derivatives are discussed [228].

The complex (*E*,*Z*)-Ru[C≡CCH=CH(μ_2-η^2-C≡CPh)]Co$_2$(CO)$_6$(η^5-ind)(PPh$_3$)$_2$ reacts with Co$_4$(CO)$_{12}$ to give an unprecedented tetracobalt ruthenium(II) vinylidene cluster. The use of this tetracobalt ruthenium(II) vinylidene cluster as a catalyst in the intramolecular Pauson–Khand reaction is discussed [229]. Treatment of Ru$_3$(μ-H)$_3$(μ_3-COMe)(CO)$_9$ with Au$_2$[μ-Ph$_2$P(CH$_2$)$_n$PPh$_2$]Me$_2$ (where $n = 1$ or 5) yields the mixed-metal clusters Au$_2$Ru$_3$(μ-H)(μ_3-COMe)[μ-Ph$_2$P(CH$_2$)$_n$PPh$_2$](CO)$_9$ in 30–40% yield. Both clusters exhibit distorted square-based pyramidal polyhedra, with two gold and two ruthenium atoms defining the basal plane. The metal skeletons are fluxional at high temperature in solution, and a process involving the migration of the diphosphine–digold moiety around three possible edge-bridging sites on the trigonal-planar Ru$_3$ unit, with concerted hydride movement, is postulated. Band-shape analysis as a function of temperature has allowed for the calculation of the values of $\Delta G^{\neq}$ for the proposed metal-core rearrangements. The free energies of activation are compared with values previously reported for skeletal rearrangements in other gold–ruthenium cluster complexes [230]. A report describing the chiroptical properties of heterometallic wing-tip butterfly clusters has appeared. $[HFe_2Ru_2C(CO)_{12}]^-$ reacts with [Pd(η^3-β-C$_{10}$H$_{15}$)Cl]$_2$ (where β-C$_{10}$H$_{15}$ = β-pinenyl) to yield HFe$_2$Ru$_2$PdC(CO)$_{12}$(η^3-β-C$_{10}$H$_{15}$), whose X-ray structure was determined by X-ray crystallography [231]. Hydrometalation of P ≡ C^{t}Bu and P–C bond activation by an Ir$_4$Pt cluster is reported. The reaction between HIr$_4$(CO)$_{10}$(μ-PPh$_2$) and Pt(dppe)(η^2-P ≡ C^{t}Bu) affords the four Ir$_4$Pt clusters Ir$_4$Pt(dppe)(CO)$_n$[μ-PC(H)^{t}Bu](μ-PPh$_2$) (where $n = 9$ or 10), HIr$_4$Pt(dppe)(μ-CO)(CO)$_7$[μ-PCH$^t_2$Bu](μ-PPh$_2$) and Ir$_4$Pt(dppe)(μ-CO)(CO)$_8$(μ_5-P)(μ-PPh$_2$). The identity of the first two clusters (nona- and decacarbonyl) was proposed on the basis of multinuclear NMR data and mass spectrometry. These two clusters provide the first examples of clusters containing a phosphido fragment that originates via the hydrometalation of a phosphaalkyne ligand. The X-ray structure of the 74 electron cluster HIr$_4$Pt(dppe)(μ-CO)(CO)$_7$[μ-PCH$^t_2$Bu](μ-PPh$_2$) (Fig. 18) is composed of a square-based pyramidal polyhedron with one Ir$_3$Pt face capped by the phosphinidene ligand. The last product cluster exhibits a butterfly metallic core with a semi-interstitial phosphide ligand [232].

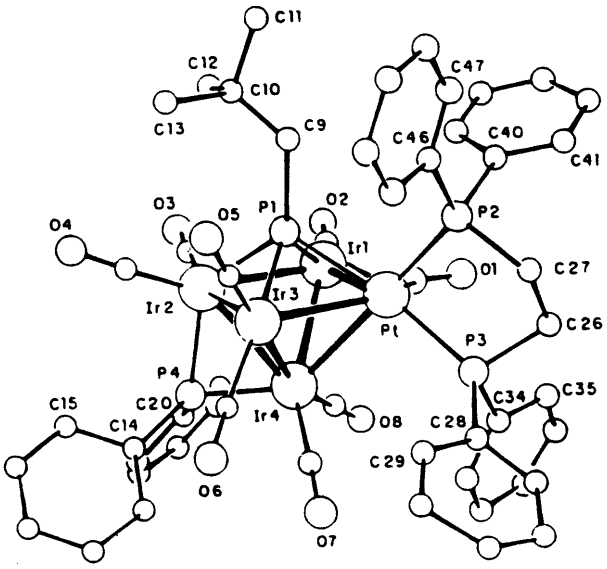

Fig. 18. X-ray structure of $HIr_4Pt(dppe)(\mu\text{-}CO)(CO)_7[\mu\text{-}PCH_2^tBu](\mu\text{-}PPh_2)$. Reprinted with permission from Organometallics. Copyright 1998 American Chemical Society.

3.4. Hexanuclear clusters

The early-late oxosulfide cluster $(CpTi)_2(\mu_4\text{-}O)(\mu_3\text{-}S)_3[Rh_4(CO)_6]$ has been prepared from $Cp_2Ti(SH)_2$ and $[Rh(\mu\text{-}OMe)(cod)]_2$ under CO pressure in the presence of a trace amount of water. Two CO groups may be replaced by P-ligands to produce $(CpTi)_2(\mu_4\text{-}O)(\mu_3\text{-}S)_3[Rh_4(CO)_4(PR_3)_2]$ [where $PR_3 = PPh_3$, $P(OMe)_3$, $P(OPh)_3$]. These clusters possess an incomplete double cubane-type core, as determined by X-ray diffraction analysis on the $P(OPh)_3$ derivative [233]. CO substitution in $[Rh_2Ru_4(CO)_{16}B]^-$ by PPh_3, followed by treatment with $AuCl(PPh_3)$, gives $Rh_2Ru_4(CO)_{15}(PPh_3)B(AuPPh_3)$ and $Rh_2Ru_4(CO)_{14}(PPh_3)_2B(AuPPh_3)$. ^{31}P-NMR data confirm the site of PPh_3 substitution at the rhodium center(s). X-ray diffraction analysis on the bisphosphine cluster shows that the rhodium atoms occupy *cis*-sites in the octahedral Rh_2Ru_4 core. Hydride clusters are isolated from the same reaction when the intermediate anionic clusters are protonated with TFA. When $P(OMe)_3$ is used as ligand P–O bond cleavage is observed, resulting in the formation of $Rh_2Ru_4(CO)_{14}[P(OMe)_3][\mu\text{-}P(OMe)_2]B$ and $Rh_2Ru_4(CO)_{13}[P(OMe)_3]_2$-$[\mu\text{-}P(OMe)_2]B$ [234]. The synthesis, characterization and redox studies of $[Fe_2(\mu$-$CO)(CO)_6(\mu\text{-}PPh_2)Au]_2(P\text{–}P)$ (where P–P = dppm, dppip, dppe, dppp) are reported. [235] $Ru_6C(CO)_{17}$ has been allowed to react with dppf to give the clusters $Ru_6C(CO)_{16}$(dppf) and $Ru_6C(CO)_{15}(\mu$-dppf). Under more forceful conditions these clusters give $Ru_5C(CO)_{13}(\mu$-dppf) as the major reaction product. A redox study on these clusters and $Ru_6C(CO)_{15}(\mu$-dppm) reveals a significant degree of communication between the redox-active sites in the $Ru_6C(CO)_{15}$ and

$Ru_5C(CO)_{13}$ derivatives. The synthesis of $Ru_6C(CO)_{15}(\mu\text{-dppe})$ was attempted but was unsuccessful owing to unfavorable redox chemistry. Two X-ray structures accompany this report [236]. The use of $PtRu_5(CO)_{16}$ in the construction of Pt/Ru nanoparticles is described. The bimetallic nanoparticles were characterized by extended X-ray absorption fine structure (EXAFS) spectroscopy, temperature-programmed desorption measurements and scanning transmission electron microscopy [237].

3.5. Higher nuclearity clusters

Iron–gold carbide clusters having Fe_5Au_2 or Fe_5Au polyhedral cores have been synthesized from $[Fe_5C(CO)_{14}]^{2-}$ and $(AuCl)_2(P\text{–}P)$ (where P–P = dppm, dppe, dppp). X-ray structural analysis of $Fe_5Au_2C(CO)_{14}(dppm)$ reveals a square-based pyramid of iron atoms and a bipyramid consisting of two iron atoms and one gold atom at the vertices of the base [238]. The synthesis and CO substitution reactivity of $Ru_6(CO)_{17}B(AuPPh_3)$ are reported. The cluster $Ru_6(CO)_{16}[P(OMe)_3]B(AuPPh_3)$ was structurally characterized by X-ray diffraction analysis. The gold(I) phosphine ligand bridges a Ru–Ru edge which leads to significant elongation of the Ru–Ru bond [239]. Reduction of $[CpRu(CO)_2]_2$ with Na/Hg, followed by treatment with the triplatinum cluster $[Pt_3(dppm)_3(CO)]^{2+}$, gives the heterometallic cluster $[Pt_3(dppm)_3\{(\mu_4\text{-Hg})RuCp(CO)_2\}_2]^{2+}$ in 40% yield. X-ray crystallographic data confirms the capping of the Pt_3 triangle above and below by Hg atoms that also bond to the $CpRu(CO)_2$ fragments [240]. Reversible coordination of the high-oxidation state dioxo-acetylene fragment $Cp^*W(O)_2(CCPh)$ to $Ru_6C(CO)_{17}$ has been demonstrated. Activation of the carbide cluster by Me_3NO, followed by reaction with $Cp^*W(O)_2(CCPh)$, affords the heptanuclear cluster $Cp^*W(O)_2(CCPh)$-$Ru_6C(CO)_{14}$. The $Cp^*W(O)_2(CCPh)$ fragment functions as a six-electron donor ligand and fills three adjacent coordination sites on a Ru_3 face. Thermolysis of this WRu_6 cluster in toluene yields $Cp^*W(O)_2(CCPh)Ru_6C(CO)_{11}$(toluene). X-ray analysis of $Cp^*W(O)_2(CCPh)Ru_6C(CO)_{14}$ shows evidence for hydrogen bonding between the terminal oxo group and the methanol solvate present in the unit cell [241]. Reaction of the 84-electron cluster $Pt_6(\mu\text{-CO})_6(\mu\text{-dppm})_3$ with either the zero-electron metalloligands LM^+ (where L = phosphine; M = Cu, Ag, Au) or InX_3 (where X = Cl, Br) or the two-electron metalloligands Tl^+ and Hg furnishes the 84-electron clusters $[Pt_6(\mu_3\text{-ML})_2(\mu\text{-CO})_6(\mu\text{-dppm})_3]^{2+}$ or $Pt_6(\mu_3\text{-InX}_3)_2(\mu\text{-CO})_6(\mu\text{-dppm})_3$ or the 88-electron clusters $[Pt_6(\mu_3\text{-Tl})_2(\mu\text{-CO})_6(\mu\text{-dppm})_3]^{2+}$ and $[Pt_6(\mu_3\text{-Hg})_2(\mu\text{-CO})_6(\mu\text{-dppm})_3]$, respectively. Oxidation of the mercury-capped cluster by CH_2I_2 gives the known 86-electron cluster $[Pt_6(\mu_3\text{-Hg})_2(\mu\text{-CO})_6(\mu\text{-dppm})_3]^{2+}$. Treatment of the starting 84-electron Pt_6 cluster with $[Ir(CO)_4]^-$ yields the 98-electron anionic cluster $[Pt_6\{\mu_3\text{-Ir}(CO)_2\}(\mu\text{-CO})_6(\mu\text{-dppm})_3]^-$, which may be further functionalized with $[Au(PPh_3)]^+$ to give $Pt_6\{\mu_3\text{-Ir}(CO)_2\}(\mu_3\text{-AuPPh}_3)(\mu\text{-CO})_6(\mu\text{-dppm})_3$. All new complexes were characterized by IR and NMR spectroscopic methods and by X-ray crystallography in the case of $[Pt_6(\mu_3\text{-AuP}^i\text{Pr}_3)_2(\mu\text{-CO})_6(\mu\text{-dppm})_3]^{2+}$. This series of clusters represents the most complete set of trigonal prismatic and capped-trigonal prismatic clusters reported to date [242].

The gold-capped cluster $[HRe_6C(CO)_{18}(AuPPh_3)]^{2-}$ was obtained from $[HRe_6C(CO)_{18}]^{3-}$ and $Au(PPh_3)Cl$. VT ^{13}C-NMR spectroscopy confirms the fluxional nature of the ancillary CO groups, with the slow exchange limit being observed at $-100°C$. The X-ray structure reveals the presence of an octahedral Re core with one face capped by the $Au(PPh_3)$ fragment. Deprotonation of $[H_2Re_6C(CO)_{18}]^{2-}$ by DBU, followed by reaction with $Au(PPh_3)Cl$, gives the corresponding bis-gold derivative $[Re_6C(CO)_{18}(AuPPh_3)_2]^{2-}$. X-ray analysis of this cluster shows that the $Au(PPh_3)$ moieties cap the *trans*-(1,4) faces of the Re_6 octahedron [243]. Loss of a $[Re(CO)_3]^+$ capping unit from $[Re_5Ir(\mu_6\text{-}C)(CO)_{17}\{\mu_3\text{-}Re(CO)_3\}_2]^{2-}$ occurs in refluxing acetonitrile to produce the heptanuclear cluster $[Re_5Ir(\mu_6\text{-}C)(CO)_{17}\{\mu_3\text{-}Re(CO)_3\}]^{3-}$. The trianionic cluster has been capped with a $[AuPPh_3]^+$ group(s) to yield the mono- and digold species $[Re_6IrC(CO)_{20}(AuPPh_3)]^{2-}$ and $[Re_6IrC(CO)_{20}(AuPPh_3)_2]^-$, respectively. The structures of these new clusters were formulated on the basis of IR and NMR data, FAB mass spectrometry and X-ray crystallography in the case of $[Re_6IrC(CO)_{20}(AuPPh_3)_2]^-$, whose structure is shown in Fig. 19. The dynamic behavior of the CO groups in this Re_6IrAu_2 cluster has been explored by ^{13}C-NMR spectroscopy, and the results are discussed relative to the observed X-ray structure [244].

The hydroxo group in $[Re_7C(CO)_{21}HgOH]^{2-}$ is easily transformed to an arylthiolate moiety. Treatment of the hydroxo-substituted cluster with various arylthiols affords $[Re_7C(CO)_{21}HgSAr]^{2-}$ in good yield. These clusters display a 1,4-bicapped octahedral core with capping $Re(CO)_3$ and HgSAr groups, as verified by the X-ray

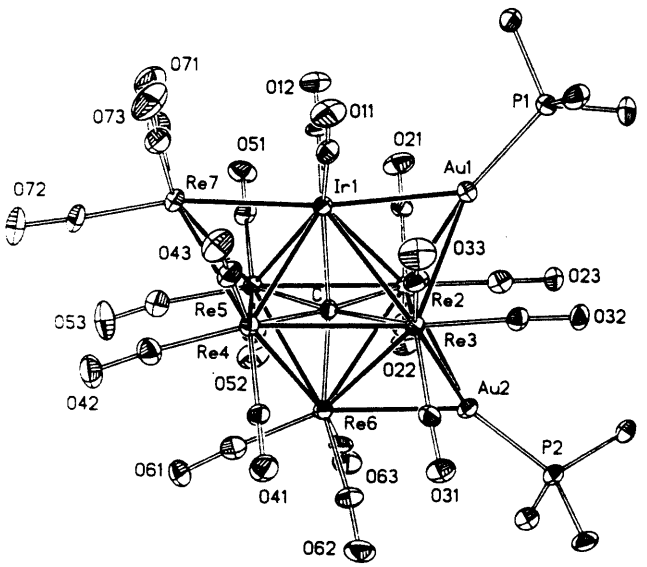

Fig. 19. X-ray structure of $[Re_6IrC(CO)_{20}(AuPPh_3)_2]^-$. Reprinted with permission from Inorganic Chemistry. Copyright 1998 American Chemical Society.

structure of $[Re_7C(CO)_{21}HgSH]^{2-}$. This particular cluster represents the first structurally characterized mercury cluster that possesses a terminal hydrogensulfide ligand [245].

The octanuclear cluster $Co_2Ru_6(\mu_7\text{-}C_2)(\mu_3\text{-}SMe)_2(\mu\text{-}PPh_2)_2(\mu\text{-}CO)_4(CO)_{13}$ and the nonanuclear cluster $Co_4Ru_5(\mu_8\text{-}C_2)(\mu_3\text{-}SMe)_2(\mu\text{-}PPh_2)_2(\mu\text{-}CO)_7(CO)_{11}$ were obtained as the major products in the reaction between $Co_2(CO)_8$ and $Ru_5(\mu_5\text{-}C_2)(\mu\text{-}SMe)_2(\mu\text{-}PPh_2)_2(CO)_{11}$. Both products were characterized by X-ray crystallography. The core of the Co_2Ru_6 cluster consists of a Co_2Ru_3 square pyramid that shares a basal edge with a $CoRu_3$ square. The seventh Ru atom bridges the outer edge of the square pyramid. Despite the observed disorder (M = Co/Ru = 1:1) in the Co_4Ru_5 cluster, the molecular structure has been shown to consist of two square pyramids (Co_2MRu_2 and Co_2M_2Ru) that share a non-bonded edge, with the ninth ruthenium atom bridging an outer edge [246]. The synthesis of the amphiphilic clusters $(\eta^6\text{-}p\text{-}MeC_6H_4^iPr)_4Ru_4Mo_4O_{16}$ and $(\eta^6\text{-}p\text{-}MeC_6H_4^iPr)_4Ru_4V_6O_{19}$ from *p*-cymene ruthenium dichloride and sodium molybdate or sodium vanadate, respectively, has been published. The molecular structure of each cluster was ascertained by X-ray crystallography and ^{17}O-NMR spectroscopy. Partial charge calculations on the oxygen atoms in the Ru_4Mo_4 cluster confirmed the existence of three different types of oxygen atoms [247]. The reactivity of $[Ru_6(CO)_{17}B]^-$ with different gold species has been explored, with the products observed to have the following composition $[Ru_6(CO)_{17}B]_2[\mu\text{-}Au(P\text{–}P)Au]$, $[Ru_6(CO)_{17}B][Au(P\text{–}P)Cl]$ and $[\{Ru_6(CO)_{17}B\}_2Au]^-$ (where P–P = various diphosphines) [248]. Aggregation of three WS_3Cu_2 clusters is promoted by Li_2S_2. The isolated product was found to be $[(Cp^*WS_3Cu_2)_3(\mu_3\text{-}S)_2]^-$, whose identity was confirmed by X-ray diffraction analysis [249]. Metal-core rearrangements are reported to occur in the reactions of $[Os_9(CO)_{24}]^{2-}$ with the electrophilic gold reagents $[AuPR_3]^+$ and $[Au_2(P\text{–}P)]^{2+}$ (where R = Ph, Cy; P–P = dppm, dppe). Detailed descriptions of the X-ray structures of $Os_9(CO)_{24}[Au(PCy_3)]_2$ and $Os_9(CO)_{23}[Au_2(dppe)]$ are included in this report [250]. The hydrosilation of diphenylacetylene using the layer-segregated platinum–ruthenium cluster $Pt_3Ru_6(CO)_{20}(\mu_3\text{-}PhC_2Ph)(\mu_3\text{-}H)(\mu\text{-}H)$ has been investigated. Turnover frequency numbers and the activation parameters are reported. The reaction is first order in the cluster and silane but zero order in alkyne concentration. On the basis of CO inhibition studies and a negligible effect by added mercury, a homogeneous catalytic cycle that takes place at a ruthenium triangle is presented. Mercury inhibition of the catalyst $[Pt_3Ru_6(CO)_{20}(\mu_3\text{-}PhC_2Ph)(\mu\text{-}H)]^-$ supports a system that reacts by a heterogeneous pathway [251]. $Pt_3Ru_6(CO)_{20}(\mu_3\text{-}PhC_2Ph)(\mu_3\text{-}H)(\mu\text{-}H)$ reacts with SMe_2 to give $Pt_3Ru_6(CO)_{19}(SMe_2)(\mu_3\text{-}PhC_2Ph)(\mu_3\text{-}H)(\mu\text{-}H)$, which contains a ruthenium-bound SMe_2 ligand. The coordinated SMe_2 ligand is labile and readily exchanges with free SMe_2 in solution, as demonstrated by EXSYS 2D ^1H-NMR spectroscopy. The catalytic behavior of the SMe_2-substituted cluster in the hydrogenation of diphenylacetylene to (*Z*)-stilbene has been studied in detail. The greater activity of this cluster relative to the parent cluster is attributed to a promotional effect that involves the relief of unsaturation at the ruthenium center by electron donation from adjacent platinum sites. The solid-state structure of the SMe_2 derivative was unequivocally established by X-ray crystallography (Fig. 20) [252].

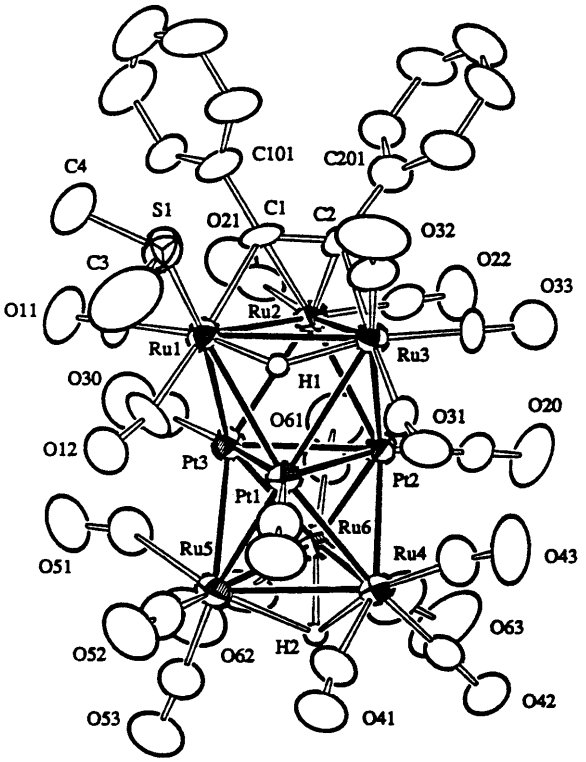

Fig. 20. X-ray structure of $Pt_3Ru_6(CO)_{19}(SMe_2)(\mu_3\text{-}PhC_2Ph)(\mu_3\text{-}H)(\mu\text{-}H)$. Reprinted with permission from Organometallics. Copyright 1998 American Chemical Society.

The high-nuclearity osmium–palladium clusters $Os_5Pd_6(CO)_{13}(\mu\text{-}CO)_5(\mu\text{-}H)_2(\mu\text{-}dppm)_2$, $Os_5Pd_6(CO)_{13}(\mu\text{-}CO)_6(\mu\text{-}dppm)$ and $Os_4Pd_6(CO)_8(\mu\text{-}CO)_8(\mu\text{-}dppm)_2$ have been synthesized in low yields from $Os_3(CO)_{10}(\mu\text{-}H)_2$ and $Pd_2(\mu\text{-}dppm)_2Cl_2$. Use of the osmium carbide cluster $Os_5(\mu_5\text{-}C)(CO)_{15}$ in place of $Os_3(CO)_{10}(\mu\text{-}H)_2$ yields the clusters $Os_5Pd_4(\mu_6\text{-}C)(CO)_{12}(\mu\text{-}CO)_3(\mu\text{-}dppm)_2$ and $Os_5(\mu_5\text{-}C)(CO)_{13}(\mu\text{-}dppm)$. The molecular structures of the Os_4Pd_6 and Os_5Pd_4 clusters were solved and polyhedral features discussed [253]. Condensation of $[M_2(P\text{–}P)]^{2+}$ (where M = Ag, Au; P–P = dppm, dppe) with $[Ag_4\{Fe(CO)_4\}_4]^{4-}$ produces the complexes $Ag_8[Fe(CO)_4]_4(dppm)_2$ and $Ag_4Au_4[Fe(CO)_4]_4(P\text{–}P)_2$. The solid-state structures of two of these clusters were crystallographically determined [254]. A review article discussing the use of tricobalt alkylidyne clusters as ligands in the construction of large assemblies of transition metal clusters has appeared. A discussion dealing with these cluster arrays as catalyst precursors is included in this review [255].

Appendix. Abreviations

ampy	2-amino-6-methylpyridinate
bpy	2,2′-bipyridine
bpym	2,2′-bipyrimidine
bzim	1-benzylimidazole
coe	cyclooctene
cod	1,5-cyclooctadiene
Cp	cyclopentadienyl
Cp*	pentamethylcyclopentadienyl
Cy	cyclohexyl
dba	dibenzylideneacetone
dmpm	bis(dimethylphosphino)methane
dpam	$Ph_2AsCH_2AsPh_2$
dpmp	$(Ph_2PCH_2)_2PPh$
dpp	2,3-bis(2-pyridyl)pyrazine
dppa	1,2-bis(diphenylphosphino)acetylene
dppb	1,4-bis(diphenylphosphino)butane
dppc	1,1′-bis(diphenylphosphino)cobaltocene
dppe	1,2-bis(diphenylphosphino)ethane
dppf	1,1′-bis(diphenylphosphino)ferrocene
dppip	1,1-bis(diphenylphosphino)isopropane
dppm	bis(diphenylphosphino)methane
dppp	1,3-bis(diphenylphosphino)propane
Fc	ferrocenyl
ind	indenyl
MAS	magic angle spinning
MeCp	methylcyclopentadienyl
nbd	norbornadiene
PPN	bis(triphenylphosphine)iminium
py	pyridine
pyz	pyrazine
pz	pyrazole
Tol	tolyl

References

[1] T.-Y. Lee, Diss. Abstr. B 58 (1998) 4213 [DA9805692].
[2] O.M. Kekia, Diss. Abstr. B 58 (1998) 4792 [DA9810874].
[3] K.E. Dungey, Diss. Abstr. B 59 (1998) 654 [DA9825207].
[4] M.S. Nashner, Diss. Abstr. B 58 (1998) 5392 [DA9812718].
[5] J. Hao, Diss. Abstr. B 59 (1998) 2746 [DANQ27945].
[6] D.S. Kolwaite, Diss. Abstr. B 59 (1998) 1108 [DA9828150].
[7] M.R. Jordan, Diss. Abstr. B 58 (1998) 4211 [DA9803619].

[8] H.-F. Hsu, Diss. Abstr. B 58 (1998) 5388 [DA12628].
[9] K. Lee, Diss. Abstr. B 58 (1998) 5389 [DA9812675].
[10] S.C.K. Cheng, Diss. Abstr. B 59 (1998) 1105 [DA9826823].
[11] T.S. Barnard, Diss. Abstr. B 58 (1998) 5951 [9815479].
[12] M.H. Drabnis, Diss. Abstr. B 59 (1998) 2192 [DA9835165].
[13] D.M. Somerville, Diss. Abstr. B 58 (1998) 5393 [DA9812778].
[14] C.D. Abernethy, F. Bottomley, A. Decken, D.A. Summers, R.C. Thompson, Organometallics 17 (1998) 1248.
[15] B. Zhuang, P. Yu, L. He, L. Huang, G. Pan, Polyhedron 17 (1998) 4393.
[16] A.S. Weller, M. Shang, T.P. Fehlner, J. Am. Chem. Soc. 120 (1998) 8283.
[17] K.M. Hillary, A.K. Hughes, K.L. Peat, K. Wade, Polyhedron 17 (1998) 2803.
[18] M. Bergamo, T. Beringhelli, G. D'Alfonso, P. Mercandelli, M. Moret, A. Sironi, Angew. Chem. Int. Ed. Engl. 37 (1998) 2128.
[19] C. Jiang, Y.-S. Wen, L.-K. Liu, T.S.A. Hor, Y.K. Yan, Organometallics 17 (1998) 173.
[20] K.A. Azam, M.A. Hossain, M.B. Hursthouse, S.E. Kabir, K.M.A. Malik, H. Vahrenkamp, J. Organomet. Chem. 555 (1998) 285.
[21] M. Bergamo, T. Beringhelli, G. D'Alfonso, P. Mercandelli, M. Moret, A. Sironi, J. Am. Chem. Soc. 120 (1998) 2971.
[22] J. Cabeza, A. Llamazares, V. Riera, R. Trivedi, F. Grepioni, Organometallics 17 (1998) 5580.
[23] T. Beringhelli, G. D'Alfonso, M. Panigati, F. Porta, P. Mercandelli, M. Moret, A. Sironi, Organometallics 17 (1998) 3282.
[24] U. Englert, F. Podewils, I. Schiffers, A. Salzer, Angew. Chem. Int. Ed. Engl. 37 (1998) 2134.
[25] E. Cariati, P. Recanati, D. Roberto, R. Ugo, Organometallics 17 (1998) 1266.
[26] H. Saito, K. Inoue, K. Matsumoto, M. Tadokoro, Y. Nakamura, J. Clust. Sci. 9 (1998) 145.
[27] E. Alonso, J. Ruiz, D. Astruc, J. Clust. Sci. 9 (1998) 271.
[28] P.J. Low, G.D. Enright, A.J. Carty, J. Organomet. Chem. 565 (1998) 279.
[29] N. Chatani, T. Morimoto, Y. Fukumoto, S. Murai, J. Am. Chem. Soc. 120 (1998) 5335.
[30] T. Fukuyama, N. Chatain, J. Tatsumi, F. Kakiuchi, S. Murai, J. Am. Chem. Soc. 120 (1998) 11522.
[31] N. Suzuki, T. Kondo, T. Mitsudo, Organometallics 17 (1998) 766.
[32] C.-H. Jun, D.-C. Hwang, S.-J. Na, J. Chem. Soc. Chem. Commun. (1998) 1405.
[33] G. Gervasio, R. Gobetto, P.J. King, D. Marabello, E. Sappa, Polyhedron 17 (1998) 2937.
[34] C.S.-W. Lau, W.-T. Wong, J. Chem. Soc. Dalton Trans. (1998) 3391.
[35] M.I. Bruce, H.-K. Fun, B.K. Nicholson, O.B. Shawkataly, R.A. Thomson, J. Chem. Soc. Dalton Trans. (1998) 751.
[36] L. Wesemann, Y. Ramjoie, M. Trinkaus, T.P. Spaniol, Eur. J. Inorg. Chem. (1998) 1263.
[37] W.-T. Wong, J. Chem. Soc. Dalton Trans. (1998) 1253.
[38] P. Mathur, I.J. Mavunkal, S.B. Umbarkar, J. Clust. Sci. 9 (1998) 393.
[39] K.O. Kallinen, T.T. Pakkanen, T.A. Pakkanen, J. Mol. Catal. A 135 (1998) 233.
[40] D. Campagnola, R. Giordano, E. Sappa, J. Clust. Sci. 9 (1998) 487.
[41] D. Campagnola, S. Deabate, R. Giordano, E. Sappa, J. Clust. Sci. 9 (1998) 205.
[42] M.I. Bruce, B.W. Skelton, A.H. White, N.N. Zaitseva, Inorg. Chem. Commun. 1 (1998) 134.
[43] M.J. Liddell, J. Organomet. Chem. 565 (1998) 271.
[44] R. Calderón, H. Vahrenkamp, J. Organomet. Chem. 555 (1998) 113.
[45] S. Aime, W. Dastrù, R. Gobetto, A. Viale, Organometallics 17 (1998) 5353.
[46] S. Aime, W. Dastrù, R. Gobetto, A. Viale, Organometallics 17 (1998) 3182.
[47] W.-Y. Yeh, S.C.N. Hsu, S.-M. Peng, G.-H. Lee, Organometallics 17 (1998) 2477.
[48] N.E. Leadbeater, Organometallics 17 (1998) 5913.
[49] X. Lei, M. Shang, T.P. Fehlner, Inorg. Chem. 37 (1998) 3900.
[50] M.-L. Chung, F.-Y. Lee, L.-C. Lin, C.-J. Su, M.-Y. Chen, Y.-S. Wen, H.-M. Gau, K.-L. Lu, J. Clust. Sci. 9 (1998) 445.
[51] E.W. Ainscough, A.M. Brodie, R.K. Coll, B.A. Coombridge, J.M. Waters, J. Organomet. Chem. 556 (1998) 197.

[52] H. Yao, R.D. McCarger, R.D. Allendoerfer, J.B. Keister, A.A. Low, J. Organomet. Chem. 568 (1998) 63.
[53] W.G. Feighery, H. Yao, A.F. Hollenkamp, R.D. Allendoerfer, J.B. Keister, Organometallics 17 (1998) 872.
[54] E.N.-M. Ho, W.-T. Wong, J. Chem. Soc. Dalton Trans. (1998) 4215.
[55] J.T. Park, H. Song, J.-J. Cho, M.-K. Chung, J.-H. Lee, I.-H. Suh, Organometallics 17 (1998) 227.
[56] H. Song, K. Lee, J.T. Park, M.-G. Choi, Organometallics 17 (1998) 4477.
[57] J.W. van Hal, J.L. Stark, K.H. Whitmire, J. Organomet. Chem. 557 (1998) 163.
[58] K.-C. Huang, M.-H. Shieh, R.-J. Jang, S.-M. Peng, G.-H. Lee, M. Shieh, Organometallics 17 (1998) 5202.
[59] J.W. van Hal, K.H. Whitmire, Organometallics 17 (1998) 5197.
[60] J.-J. Cherng, Y.-C. Tsai, C.-H. Ueng, G.-H. Lee, S.-M. Peng, M. Shieh, Organometallics 17 (1998) 255.
[61] S.-W.A. Fong, T.S.A. Hor, J. Clust. Sci. 9 (1998) 351.
[62] L.J. Farrugia, C. Rosenhahn, S. Whitworth, J. Clust. Sci. 9 (1998) 505.
[63] S.-M. Kuang, F. Xue, Z.-Y. Zhang, T.C.W. Mak, Z.-Z. Zhang, J. Organomet. Chem. 559 (1998) 31.
[64] M. Nowotny, B.F.G. Johnson, J.F. Nixon, S. Parsons, J. Chem. Soc. Chem. Commun. (1998) 2223.
[65] O.B. Shawkataly, K. Ramalingam, D.M. Ashari, H.-K. Fun, I.A. Razak, Acta. Crystallogr. C 54 (1998) 329.
[66] V.M. Hansen, A.K. Ma, K. Biradha, R.K. Pomeroy, M.J. Zaworotko, Organometallics 17 (1998) 5267.
[67] P. Blenkiron, G.D. Enright, P.J. Low, J.F. Corrigan, N.J. Taylor, Y. Chi, J.-Y. Saillard, A.J. Carty, Organometallics 17 (1998) 2447.
[68] D.H. Hamilton, J.R. Shapley, Organometallics 17 (1998) 3087.
[69] Y. Liu, W.K. Leong, R.K. Pomeroy, Organometallics 17 (1998) 3387.
[70] G. Süss-Fink, I. Godefroy, V. Ferrand, A. Neels, H. Stoeckli-Evans, J. Chem. Soc. Dalton Trans. (1998) 515.
[71] P.M.V. Calcar, M.O. Olmstead, A.L. Balch, Inorg. Chim. Acta 270 (1998) 28.
[72] S. Aime, R. Gobetto, E. Valls, Inorg. Chim. Acta 275-276 (1998) 521.
[73] D.J.F. Bryce, P.J. Dyson, B.K. Nicholson, D.G. Parker, Polyhedron 17 (1998) 2899.
[74] A.J. Poë, D.H. Farrar, R. Ramachandran, C. Moreno, Inorg. Chim. Acta 274 (1998) 82.
[75] O.B. Shawkataly, K. Ramalingam, S.T. Lee, M. Parameswary, H.K. Fun, K. Sivakumar, Polyhedron 17 (1998) 1211.
[76] K.A. Azam, M.B. Hursthouse, Md.R. Islam, S.E. Kabir, K.M.A. Malik, R. Miah, C. Sudbrake, H. Vahrenkamp, J. Chem. Soc. Dalton Trans. (1998) 1097.
[77] M.I. Bruce, B.W. Skelton, A.H. White, N.N. Zaitseva, J. Organomet. Chem. 558 (1998) 197.
[78] L.T. Byrne, C.S. Griffith, J.P. Hos, G.A. Koutsantonis, B.W. Skelton, A.H. White, J. Organomet. Chem. 565 (1998) 259.
[79] H.-C. Böttcher, M. Graf, K. Merzweiler, C. Bruhn, Polyhedron 17 (1998) 3433.
[80] G. Chen, W.K. Leong, J. Chem. Soc. Dalton Trans. (1998) 2489.
[81] J.P.H. Charmant, H.A.A. Dickson, N.J. Grist, S.A.R. Knox, A.G. Orpen, K. Saynor, J.M. Viňas, J. Organomet. Chem. 565 (1998) 141.
[82] O.B. Shawkataly, K. Puvanesvary, H.K. Fun, K. Sivakumar, J. Organomet. Chem. 565 (1998) 267.
[83] M. Graf, K. Merzweiler, C. Bruhn, H.-C. Böttcher, J. Organomet. Chem. 553 (1998) 371.
[84] M. Castiglioni, S. Deabate, R. Giordano, P.J. King, S.A.R. Knox, E. Sappa, J. Organomet. Chem. 571 (1998) 251.
[85] J. Nijhoff, M.J. Bakker, F. Hartl, D.J. Stufkens, W.-F. Fu, R. van Eldik, Inorg. Chem. 37 (1998) 661.
[86] R.M. de Souza, F. Martins, E. Stein, J. Organomet. Chem. 559 (1998) 37.
[87] R. Dorta, H. Stoeckli-Evans, G. Süss-Fink, J. Organomet. Chem. 553 (1998) 307.

[88] M.P. Cifuentes, S.M. Waterman, M.G. Humphrey, G.A. Heath, B.W. Skelton, A.H. White, M.P.S. Perera, M.L. Williams, J. Organomet. Chem. 565 (1998) 193.
[89] N.E. Leadbeater, J. Lewis, P.R. Raithby, G.P. Ward, Eur. J. Inorg. Chem. (1998) 1479.
[90] M.I. Rybinskaya, N.A. Stelzer, L.V. Rybin, F.M. Dolgushin, A.I. Yanovsky, Y.T. Struchkov, P.V. Petrovskii, Inorg. Chim. Acta 280 (1998) 243.
[91] J.A. Cabeza, I. del Río, V. Riera, D. Ardura, J. Organomet. Chem. 554 (1998) 117.
[92] C. Bois, J.A. Cabeza, R.J. Franco, V. Riera, E. Saborit, J. Organomet. Chem. 564 (1998) 201.
[93] J.A. Cabeza, I. del Río, M. Moreno, V. Riera, F. Grepioni, Organometallics 17 (1998) 3027.
[94] K.A. Azam, M.B. Hursthouse, S.A. Hussain, S.E. Kabir, K.M.A. Malik, M.M. Rahman, E. Rosenberg, J. Organomet. Chem. 559 (1998) 81.
[95] A.B. Din, B. Bergman, E. Rosenberg, R. Smith, W. Dastrú, R. Gobetto, L. Milone, A. Viale, Polyhedron 17 (1998) 2975.
[96] S.E. Kabir, T.A. Siddiquee, E. Rosenberg, R. Smith, M.B. Hursthouse, K.M.A. Malik, K.I. Hardcastle, M. Visi, J. Clust. Sci. 9 (1998) 185.
[97] M.B. Hursthouse, S.E. Kabir, K.M.A. Malik, M. Tesmer, H. Vahrenkamp, J. Organomet. Chem. 568 (1998) 133.
[98] B. Bergman, R. Holmquist, R. Smith, E. Rosenberg, J. Ciurash, K. Hardcastle, M. Visi, J. Am. Chem. Soc. 120 (1998) 12818.
[99] E. Arcia, D.S. Kolwaite, E. Rosenberg, K. Hardcastle, J. Ciurash, R. Duque, R. Gobetto, L. Milone, D. Osella, M. Botta, W. Dastrú, A. Viale, Organometallics 17 (1998) 415.
[100] S.M.T. Abedin, K.A. Azam, M.B. Hursthouse, S.E. Kabir, K.M.A. Malik, R. Miah, H. Vahrenkamp, J. Organomet. Chem. 564 (1998) 133.
[101] T. Sato, M. Nishio, Y. Ishii, H. Yamazaki, M. Hidai, J. Organomet. Chem. 569 (1998) 99.
[102] K. Kiriakidou, M.R. Plutino, F. Prestopino, M. Monari, M. Johansson, L.I. Elding, E. Valls, R. Gobetto, S. Aime, E. Nordlander, J. Chem. Soc. Chem. Commun. (1998) 2721.
[103] R.D. Adams, T. Barnard, A. Rawlett, J.M. Tour, Eur. J. Inorg. Chem. (1998) 429.
[104] K.A. Azam, M.B. Hursthouse, S.E. Kabir, K.M.A. Malik, M. Tesmer, H. Vahrenkamp, Inorg. Chem. Commun. 1 (1998) 402.
[105] K. Matsubara, R. Okamura, M. Tanaka, H. Suzuki, J. Am. Chem. Soc. 120 (1998) 1108.
[106] P. Frediani, C. Faggi, A. Salvini, M. Bianchi, F. Piacenti, Inorg. Chim. Acta 272 (1998) 141.
[107] E.G. Fidalgo, L. Plasseraud, G. Süss-Fink, J. Mol. Catal. A 132 (1998) 5.
[108] R. Suter, A.A. Bhattacharyya, L.-Y. Hsu, J.A.K. Bauer, S.G. Shore, Polyhedron 17 (1998) 2889.
[109] M. Akita, M.-C. Chung, M. Terada, M. Miyauti, M. Tanaka, Y. Moro-oka, J. Organomet. Chem. 565 (1998) 49.
[110] M.D. Westmeyer, M.A. Massa, T.B. Rauchfuss, S.R. Wilson, J. Am. Chem. Soc. 120 (1998) 114.
[111] M. Okazaki, T. Ohtani, S. Inomata, N. Tagaki, H. Ogino, J. Am. Chem. Soc. 120 (1998) 9135.
[112] R. Buntem, J. Lewis, C.A. Morewood, P.R. Raithby, M.C.R. de Arellano, G.P. Shields, J. Chem. Soc. Dalton Trans. (1998) 1091.
[113] G. Süss-Fink, I. Godefroy, A. Béguin, G. Rheinwald, A. Neels, H. Stoeckli-Evans, J. Chem. Soc. Dalton Trans. (1998) 2211.
[114] R.A. Harding, H. Nakayama, T. Eguchi, N. Nakamura, B.T. Heaton, A.K. Smith, Polyhedron 17 (1998) 2857.
[115] T.M. Räsänen, S. Jääskeläinen, T.A. Pakkanen, J. Organomet. Chem. 553 (1998) 453.
[116] E. Delgado, Y. Chi, W. Wang, G. Hogarth, P.J. Low, G.D. Enright, S.-M. Peng, G.-H. Lee, A.J. Carty, Organometallics 17 (1998) 2936.
[117] W. Wang, J.F. Corrigan, G.D. Enright, N.J. Taylor, A.J. Carty, Organometallics 17 (1998) 427.
[118] A.J. Arce, A.J. Deeming, Y.D. Sanctis, S.K. Johal, C.M. Martin, M. Shinhmar, D.M. Speel, A. Vassos, J. Chem. Soc. Chem. Commun. (1998) 233.
[119] J. Nijhoff, M.J. Bakker, F. Hartl, G. Freeman, S.L. Ingham, B.F.G. Johnson, J. Chem. Soc. Dalton Trans. (1998) 2625.
[120] E.N.-M. Ho, W.-T. Wong, J. Chem. Soc. Dalton Trans. (1998) 513.
[121] T.M. Räsänen, S. Jääskeläinen, T.A. Pakkanen, J. Organomet. Chem. 554 (1998) 129.
[122] T.F. Fässler, T. Vögl, P.B. Fabritchnyi, M.I. Afanasov, J. Organomet. Chem. 561 (1998) 221.
[123] S. Kuwata, M. Andou, K. Hashizume, Y. Mizobe, M. Hidai, Organometallics 17 (1998) 3429.

[124] P.R. Raithby, G.P. Shields, Polyhedron 17 (1998) 2829.
[125] R.A. Burrow, D.H. Farrar, J. Hao, A. Lough, O. Mourad, A.J. Pöe, Y. Zheng, Polyhedron 17 (1998) 2907.
[126] J.H. Yamamoto, K.A. Udachin, G.D. Enright, A.J. Carty, J. Chem. Soc. Chem. Commun. (1998) 2259.
[127] C.J. Adams, M.I. Bruce, B.W. Skelton, A.H. White, J. Organomet. Chem. 551 (1998) 235.
[128] C.J. Adams, M.I. Bruce, B.W. Skelton, A.H. White, J. Organomet. Chem. 561 (1998) 97.
[129] K. Lee, J.R. Shapley, Organometallics 17 (1998) 3020.
[130] B.F.G. Johnson, C.M. Martin, P. Schooler, J. Chem. Soc. Chem. Commun. (1998) 1239.
[131] R.J.H. Clark, P.J. Dyson, D.G. Humphrey, B.F.G. Johnson, Polyhedron 17 (1998) 2985.
[132] T. Borchert, J. Lewis, P.R. Raithby, G.P. Shields, H. Wadepohl, Inorg. Chim. Acta 274 (1998) 201.
[133] N.E. Leadbeater, Inorg. Chim. Acta 278 (1998) 250.
[134] D. Braga, F. Grepioni, L. Scaccianoce, B.F.G. Johnson, J. Chem. Soc. Dalton Trans. (1998) 1321.
[135] B.F.G. Johnson, D.S. Shephard, D. Braga, F. Grepioni, S. Parsons, J. Chem. Soc. Dalton Trans. (1998) 311.
[136] K.S.-Y. Leung, W.-T. Wong, J. Chem. Soc. Dalton Trans. (1998) 1939.
[137] D.A. McCarthy, J.K. Bauer, F.-E. Hong, J.R. Oh, H. Deng, J. Liu, S.G. Shore, J. Organomet. Chem. 550 (1998) 309.
[138] R.D. Adams, K.T. McBride, J. Clust. Sci. 9 (1998) 93.
[139] K. Lee, J.R. Shapley, Organometallics 17 (1998) 4368.
[140] K. Lee, J.R. Shapley, Organometallics 17 (1998) 4030.
[141] K. Lee, S.R. Wilson, J.R. Shapley, Organometallics 17 (1998) 4113.
[142] T. Nishioka, K. Isobe, I. Kinoshita, Y. Ozawa, A.V. de Miguel, T. Nakai, S. Miyajima, Organometallics 17 (1998) 1637.
[143] K. Tanaka, Y. Kushi, K. Tsuge, K. Toyohara, T. Nishioka, K. Isobe, Inorg. Chem. 37 (1998) 120.
[144] H. Wadepohl, K. Büchner, M. Herrmann, A. Metz, H. Pritzkow, J. Organomet. Chem. 571 (1998) 267.
[145] J.E. Davies, M.J. Mays, P.R. Raithby, V. Sarveswaran, G.P. Shields, J. Chem. Soc. Dalton Trans. (1998) 775.
[146] S. Vastag, G. Gervasio, D. Marabello, G. Szalontai, L. Markó, Organometallics 17 (1998) 4218.
[147] P.A. Brooksby, N.W. Duffy, A.J. McQuillan, B.H. Robinson, J. Simpson, J. Chem. Soc. Dalton Trans. (1998) 2855.
[148] T. Sugihara, M. Yamaguchi, J. Am. Chem. Soc. 120 (1998) 10782.
[149] J.P. Carpenter, C.M. Lukehart, S.B. Milne, S.R. Stock, J.E. Wittig, B.D. Jones, R. Glosser, J.G. Zhu, J. Organomet. Chem. 557 (1998) 121.
[150] G. Bor, F.H. Oldani, S.F.A. Kettle, J. Clust. Sci. 9 (1998) 259.
[151] S.F.A. Kettle, E. Diana, R. Rossetti, P.L. Stanghellini, Inorg. Chem. 37 (1998) 6502.
[152] K. Besancon, G. Laurenczy, T. Lumini, R. Roulet, R. Bruyndonckx, C. Daul, Inorg. Chem. 37 (1998) 5634.
[153] E. Mieczyńska, A.M. Trzeciak, R. Grzybek, J.J. Ziólkowski, J. Mol. Catal. A 132 (1998) 203.
[154] I. Ojima, Z. Li, R.J. Donovan, P. Ingallina, Inorg. Chim. Acta 270 (1998) 279.
[155] M.H. de Araujo, M.D. Vargas, D. Braga, F. Grepioni, Polyhedron 17 (1998) 2865.
[156] E. Cariati, D. Roberto, R. Ugo, J. Clust. Sci. 9 (1998) 329.
[157] P. Schooler, B.F.G. Johnson, C.M. Martin, P.J. Dyson, S. Parsons, J. Chem. Soc. Chem. Commun. (1998) 795.
[158] M. Hong, W. Su, R. Cao, F. Jaing, H. Liu, J. Lu, Inorg. Chim. Acta 274 (1998) 229.
[159] R. Salzmann, M. Kaupp, M.T. McMahon, E. Oldfield, J. Am. Chem. Soc. 120 (1998) 4771.
[160] S.P. Tunik, I.S. Podkorytov, B.T. Heaton, J.A. Iggo, J. Sampanthar, J. Organomet. Chem. 550 (1998) 221.
[161] A.J. Pöe, S.P. Tunik, Inorg. Chim. Acta 268 (1998) 189.
[162] E. Diana, G. Gervasio, D. Marabello, R. Rossetti, J. Clust. Sci. 9 (1998) 223.
[163] R.D. Pergola, A. Ceriotti, A. Cinquantini, F.F. de Biani, L. Garlaschelli, M. Manassero, R. Piacentini, M. Sansoni, P. Zanello, Organometallics 17 (1998) 802.

[164] S. Martinengo, L. Noziglia, A. Fumagalli, V.G. Albano, D. Braga, F. Grepioni, J. Chem. Soc. Dalton Trans. (1998) 2493.
[165] B. Zouchoune, F. Ogliaro, J.-F. Halet, J.-Y. Saillard, J.R. Eveland, K.H. Whitmire, Inorg. Chem. 37 (1998) 865.
[166] A. Fumagalli, S. Martinengo, M. Tasselli, G. Ciani, P. Macchi, A. Sironi, Inorg. Chem. 37 (1998) 2826.
[167] R. Gautier, J.-F. Halet, J. Organomet. Chem. 565 (1998) 217.
[168] G.J. Spivak, R.J. Puddephatt, J. Organomet. Chem. 551 (1998) 383.
[169] M.A. Bennett, D.E. Berry, T. Dirnberger, D.C.R. Hockless, E. Wenger, J. Chem. Soc. Dalton Trans. (1998) 2367.
[170] R.E. Wittrig, G.M. Ferrence, J. Washington, C.P. Kuiak, Inorg. Chim. Acta 270 (1998) 111.
[171] H. Donath, E.V. Avtomonov, I. Sarraje, K.-H. von Dahlen, M. El-Essawi, J. Lorberth, B.-S. Seo, J. Organomet. Chem. 559 (1998) 191.
[172] K.H. Ebert, W. Massa, H. Donath, J. Lorberth, B.-S. Seo, E. Herdtweck, J. Organomet. Chem. 559 (1998) 203.
[173] D.M.P. Mingos, R. Vilar, J. Organomet. Chem. 557 (1998) 131.
[174] T. Zhang, M. Drouin, P.D. Harvey, J. Clust. Sci. 9 (1998) 165.
[175] P. Jutzi, B. Neumann, G. Reumann, H.-G. Stammler, Organometallics 17 (1998) 1305.
[176] L. Bengtsson-Kloo, C.M. Iapalucci, G. Longoni, S. Ulvenlund, Inorg. Chem. 37 (1998) 4325.
[177] E.G. Mednikov, Y.T. Struchkov, Y.L. Slovokhotov, J. Organomet. Chem. 566 (1998) 15.
[178] N.T. Tran, M. Kawano, D.R. Powell, L.F. Dahl, J. Am. Chem. Soc. 120 (1998) 10986.
[179] M. Contel, J. Garrido, M.C. Gimeno, M. Laguna, J. Chem. Soc. Dalton Trans. (1998) 1083.
[180] A. Burini, J.P. Fackler, Jr., R. Galassi, B.R. Pietroni, R.J. Staples, J. Chem. Soc. Chem. Commun. (1998) 95.
[181] V.W.-W. Yam, W.K.-M. Fung, K.-K. Cheung, Organometallics 17 (1998) 3293.
[182] O.M. Abu-Salah, J. Organomet. Chem. 565 (1998) 211.
[183] P. Pyykkö, T. Tamm, Organometallics 17 (1998) 4842.
[184] G.-C. Guo, Q.-G. Wang, G.-D. Zhou, T.C.W. Mak, J. Chem. Soc. Chem. Commun. (1998) 339.
[185] H. Sugiyama, Y. Hayashi, H. Kawaguchi, K. Tatsumi, Inorg. Chem. 37 (1998) 6773.
[186] G. Boni, C. Moise, Polyhedron 17 (1998) 261.
[187] C.S. Griffith, G.A. Koutsantonis, B.W. Skelton, A.H. White, J. Chem. Soc. Chem. Commun. (1998) 1805.
[188] L.T. Byrne, C.S. Griffith, G.A. Koutsantonis, B.W. Skelton, A.H. White, J. Chem. Soc. Dalton Trans. (1998) 1575.
[189] T. Ikada, S. Kuwata, Y. Mizobe, M. Hidai, Inorg. Chem. 37 (1998) 5793.
[190] L.-C. Song, J.-Y. Shen, X.-Y. Wu, Q.-M. Hu, Polyhedron 17 (1998) 35.
[191] L.-C. Song, Y.-B. Dong, Q.-M. Hu, Y.-K. Li, J. Sun, Polyhedron 17 (1998) 1579.
[192] E.-R. Ding, S.-L. Wu, C.-G. Xia, Y.-Q. Yin, J. Organomet. Chem. 568 (1998) 157.
[193] P. Mathur, S. Ghose, M.M. Hossain, C.V.V. Satyanarayana, R.K. Chadha, S. Banerjee, G.R. Kumar, J. Organomet. Chem. 568 (1998) 197.
[194] E.-R. Ding, Y.-Q. Yin, J. Sun, J. Organomet. Chem. 559 (1998) 157.
[195] R. Rumin, P. Abiven, F.Y. Pétillon, K.W. Muir, J. Organomet. Chem. 555 (1998) 89.
[196] S.-L. Wu, E.-R. Ding, Y.-Q. Yin, J. Sun, J. Organomet. Chem. 570 (1998) 71.
[197] L.-C. Song, Y.-B. Dong, Q.-M. Hu, J. Sun, Polyhedron 17 (1998) 4339.
[198] L.-C. Song, H.-T. Fan, Q.-M. Hu, X.-D. Qin, W.-F. Zhu, Y. Chen, J. Sun, Organometallics 17 (1998) 3454.
[199] T.P. Fehlner, J. Organomet. Chem. 550 (1998) 21.
[200] S. Aldridge, H. Hashimoto, K. Kawamura, M. Shang, T.P. Fehlner, Inorg. Chem. 37 (1998) 928.
[201] Y. Tang, J. Sun, J. Chen, Organometallics 17 (1998) 2945.
[202] A.R. Manning, A.J. Palmer, J. McAdam, B.H. Robinson, J. Simpson, J. Chem. Soc. Chem. Commun. (1998) 1577.
[203] Z. Tang, Y. Nomura, S. Kuwata, Y. Ishii, Y. Mizobe, M. Hidai, Inorg. Chem. 37 (1998) 4909.
[204] S. Yamazaki, A.J. Deeming, D.M. Speel, Organometallics 17 (1998) 775.

[205] P. Braunstein, G.E. Herberich, M. Neuschütz, M.U. Schmidt, U. Englert, P. Lecante, A. Mosset, Organometallics 17 (1998) 2177.
[206] S.-H. Chun, E.A. Meyers, F.-C. Liu, S. Lim, S.G. Shore, J. Organomet. Chem. 563 (1998) 23.
[207] G.R. County, R.S. Dickson, G.D. Fallon, J. Organomet. Chem. 565 (1998) 11.
[208] S.-M. Lee, W.-T. Wong, J. Clust. Sci. 9 (1998) 417.
[209] J.-P. Lang, H. Kawaguchi, K. Tatsumi, J. Organomet. Chem. 569 (1998) 109.
[210] S.M. Waterman, M.G. Humphrey, D.C.R. Hockless, J. Organomet. Chem. 565 (1998) 81.
[211] P. Mathur, S. Ghose, M.M. Hossain, C.V.V. Satyanarayana, J.E. Drake, J. Organomet. Chem. 557 (1998) 221.
[212] J.-H. Chung, H. Song, J.T. Park, J.-H. Lee, I.-H. Suh, J. Organomet. Chem. 558 (1998) 71.
[213] S.M. Waterman, M.G. Humphrey, D.C.R. Hockless, J. Organomet. Chem. 555 (1998) 25.
[214] C.-W. Pin, Y. Chi, C. Chung, A.J. Carty, S.-M. Peng, G.-H. Lee, Organometallics 17 (1998) 4146.
[215] C.-W. Shiu, Y. Chi, C. Chung, S.-M. Peng, G.-H. Lee, Organometallics 17 (1998) 2970.
[216] C.S. Bahn, A. Tan, S. Harris, Inorg. Chem. 37 (1998) 2770.
[217] S.M. Waterman, M.G. Humphrey, V.-A. Tolhurst, M.I. Bruce, P.J. Low, D.C.R. Hockless, Organometallics 17 (1998) 5789.
[218] C. Chung, W.-C. Tseng, Y. Chi, S.-M. Peng, G.-H. Lee, Organometallics 17 (1998) 2207.
[219] T.M. Räsänen, S. Jääskeläinen, T.A. Pakkanen, J. Organomet. Chem. 552 (1998) 9.
[220] S.Y.-W. Hung, W.-T. Wong, J. Organomet. Chem. 566 (1998) 237.
[221] L.J. Farrugia, N. MacDonald, R.D. Peacock, Polyhedron 17 (1998) 2877.
[222] A. Fumagalli, M. Bianchi, M.C. Malatesta, G. Ciani, M. Moret, A. Sironi, Inorg. Chem. 37 (1998) 1324.
[223] S. Onaka, Y. Katsukawa, M. Yasashita, J. Organomet. Chem. 564 (1998) 249.
[224] B.T. Sterenberg, G.P. Spivak, G.P.A. Yap, R.J. Puddephatt, Organometallics 17 (1998) 2433.
[225] H. Shan, A. James, P.R. Sharp, Inorg. Chem. 37 (1998) 5727.
[226] W.-C. Tseng, Y. Chi, C.-J. Su, A.J. Carty, S.-M. Peng, G.-H. Lee, J. Chem. Soc. Dalton Trans. (1998) 1053.
[227] J.H. Yamamoto, G.D. Enright, A.J. Carty, Polyhedron 17 (1998) 2971.
[228] R. Reina, O. Riba, O. Rossell, M. Seco, P. Gómez-Sal, A. Martin, D. de Montauzon, A. Mari, Organometallics 17 (1998) 4127.
[229] V. Cadierno, M.P. Gamasa, J. Gimeno, J.M. Moretó, S. Ricart, A. Roig, E. Molins, Organometallics 17 (1998) 697.
[230] C.A. Collins, I.D. Salter, V. Sik, S.A. Williams, T. Adatia, J. Chem. Soc. Dalton Trans. (1998) 1107.
[231] S.P. Gubin, A.P. Klyagina, I.F. Galuzina, O.A. Belyakova, Y.V. Zubavichus, Y.L. Slovokhotov, Inorg. Chim. Acta 280 (1998) 275.
[232] M.H. Araujo, A.G. Avent, P.B. Hitchcock, J.F. Nixon, M.D. Vargas, Organometallics 17 (1998) 5460.
[233] M.A. Casado, M.A. Ciriano, A.J. Edwards, F.J. Lahoz, J.J. Pérez-Torrente, L.A. Oro, Organometallics 17 (1998) 3414.
[234] A.D. Hattersley, C.E. Housecroft, L.M. Liable-Sands, A.L. Rheingold, A. Waller, Polyhedron 17 (1998) 2957.
[235] M. Ferrar, A. Julià, R. Reina, O. Rossell, M. Seco, D. de Montauzon, J. Organomet. Chem. 560 (1998) 147.
[236] D.S. Shephard, B.F.G. Johnson, A. Harrison, S. Parsons, S.P. Smidt, L.J. Yellowlees, D. Reed, J. Organomet. Chem. 563 (1998) 113.
[237] M.S. Nashner, A.I. Frenkel, D. Somerville, C.W. Hills, J.R. Shapley, R.G. Nuzzo, J. Am. Chem. Soc. 120 (1998) 8093.
[238] O. Rossell, M. Seco, G. Segalés, M.A. Pellinghelli, A. Tiripicchio, J. Organomet. Chem. 571 (1998) 123.
[239] C.E. Housecroft, A.L. Rheingold, A. Waller, G.P.A. Yap, Polyhedron 17 (1998) 2921.
[240] W.D. King, C.M. Lukehart, J. Clust. Sci. 9 (1998) 107.
[241] W.-J. Chao, Y. Chi, C. Chung, A.J. Carty, E. Delgado, S.-M. Peng, G.-H. Lee, J. Organomet. Chem. 565 (1998) 3.

[242] G.J. Spivak, J.J. Vittal, R.J. Puddephatt, Inorg. Chem. 37 (1998) 5474.
[243] J.L. Latten, G. Hsu, T.J. Henly, S.R. Wilson, J.R. Shapley, Inorg. Chem. 37 (1998) 2520.
[244] L. Ma, U. Brand, J.R. Shapley, Inorg. Chem. 37 (1998) 3060.
[245] U. Brand, J.R. Shapley, Inorg. Chem. 37 (1998) 5697.
[246] C.J. Adams, M.I. Bruce, B.W. Skelton, A.H. White, Polyhedron 17 (1998) 2795.
[247] G. Süss-Fink, L. Plasseraud, V. Ferrand, S. Stanislas, A. Neels, H. Stoeckli-Evans, M. Henry, G. Laurenczy, R. Roulet, Polyhedron 17 (1998) 2817.
[248] C.E. Housecroft, A.L. Rheingold, A. Waller, G.P.A. Yap, J. Organomet. Chem. 565 (1998) 105.
[249] J.-P. Lang, K. Tatsumi, Inorg. Chem. 37 (1998) 160.
[250] Z. Akhter, S.L. Ingham, J. Lewis, P.R. Raithby, J. Organomet. Chem. 550 (1998) 131.
[251] R.D. Adams, T.S. Barnard, Organometallics 17 (1998) 2567.
[252] R.D. Adams, T.S. Barnard, Organometallics 17 (1998) 2885.
[253] J.W.-S. Hui, W.-T. Wong, J. Chem. Soc. Dalton Trans. (1998) 2065.
[254] V.G. Albano, M.C. Iapalucci, G. Longoni, M. Monari, A. Paselli, S. Zacchini, Organometallics 17 (1998) 4438.
[255] X. Lei, E.E. Wolf, T.P. Fehlner, Eur. J. Inorg. Chem. (1998) 1835.